Mitacs Accelerate Project
Final Report
Application Ref.: IT08015

Comprehensive Evaluation of NH_3 Production and Utilization Options for Clean Energy Applications

Period:
September 2016 - March 2017

Submission Date:
March 25, 2017

Principal Investigator:
Prof. Dr. Ibrahim Dincer

Intern:
Yusuf Bicer

Partner Organization:
Hydrofuel®TM Inc.

TABLE OF CONTENTS

LIST OF FIGURES

LIST OF TABLES

ACKNOWLEDGEMENT

The principal investigator and intern acknowledge the financial support provided by the Mitacs and Hydrofuel Inc.

NOMENCLATURE

e	Charge of an electron ($1.60217657 \times 10^{19}$ C)
F	Faraday constant (C/mol)
h	Enthalpy (kJ/kg)
I	Irradiance (W/m^2)
i	Current density (A/m^2)
$\dot{m}$	Mass flow rate (g/s)
M	Molarity (M)
$\dot{n}$	Mol flow rate (mol/s)
R	Resistance (ohm)
t	Time (s)
V	Volume (L)
$\dot{W}$	Work rate (W)

Greek Letters

η	Efficiency
δ	Nernst diffusion layer thickness (cm)

Acronyms

ADF	Abiotic Depletion Factor
ASTM	American Section of the International Association for Testing Materials
AOI	Angle of incidence
AR	Anti-reflective
CFC	Chlorofluorocarbon
CML	Center of Environmental Science of Leiden University
CCS	Carbon Capture Storage
CFC	Chlorofluorocarbon
CNG	Compressed Natural Gas
CPV	Concentrated photovoltaic
DB	Dichlorobenzene
DWT	Dead Weight Tonnage
DWT	Dead Weight Tonnage
DC	Direct current
EV	Electric Vehicle
EIS	Electrochemical impendence spectroscopy
GHG	Greenhouse Gas
GREET	Greenhouse Gases, Regulated Emissions, and Energy Use in Transportation
GWP	Global Warming Potential
HEV	Hybrid Electric Vehicle
IATA	The International Air Transport Association
IAM	Integrated Assessment
ICE	Internal Combustion Engine
IPCC	Intergovernmental Panel on Climate Change
IR	Infrared
ISO	International Organization for Standards
KN	Knot

LCA	Life Cycle Assessment
LDI	Lean Direct Injection
LPG	Liquefied Petroleum Gas
LNG	Liquefied Natural Gas
LHV	Lower heating value
MSWI	Municipal Waste Incineration Plant
NMI	Nautical Mile
NM	Non-Methane
NAAQS	National Ambient Air Quality Standards
NIR	Near infrared
NOCT	Nominal operating cell temperature
PAH	Polycyclic aromatic hydrocarbon
PTH	Pump to Haul
PM	Particulate Matter
PTWa	Pump to Wake
PV	Photovoltaic
PEC	Photoelectrochemical
PtB	Platinum black
PV	Photovoltaic
RSZ	Reduced Speed Zones
RER	Europe
RMS	Root mean square
SSPC	Solid-state proton conductors
SMR	Steam Methane Reforming
TKM	Tonne-kilometer
UCG	Underground Coal Gasification
UCTE	Union for the Co-ordination of Transmission of Electricity
UV	Ultraviolet
VOC	Volatile Organic Compounds
WTP	Wheel to Pump
WTH	Well to Haul

SUMMARY

Ammonia is not only a fertilizer but also an alternative fuel for transportation and power generation. It can easily be adapted to fuel both diesel generators and larger utility power plants. The ability of being produced from renewable energy sources allows on-site ammonia production where it is needed. The high hydroelectric, wind, and solar energy source potential of Canada make the energy storage attractive using ammonia. Ontario, with decreasing electricity prices, has potentials for on-site ammonia production from hydropower. Solar energy, as the most abundant source of energy in the world, can be directly utilized for ammonia synthesis via various routes such as electrochemical and thermochemical cycles.

Canada have significant potential of renewable resources such as hydropower and wind power. Ammonia can be transported via ocean tankers or pipelines. Besides being a zero emission fuel in the utilization process, about 30% greenhouse gas reduction is possible using renewable energy such as wind in the ammonia production when compared to conventional unleaded gasoline. Compared to propane, greenhouse gas production decreases about 18%. Hence in the overall life cycle, ammonia has significant environmental advantages. Even if ammonia is produced from hydrocarbons, it has similar greenhouse gas emissions with solar energy based route. It is important to emphasize that an ammonia driven passenger vehicle releases less greenhouse gas emissions than compressed natural gas (CNG), liquefied petroleum gas (LPG), diesel, and even hybrid electric vehicles. Considering vehicle and fuel production together, emissions from an ammonia-fueled passenger car is very close to electric vehicles per km traveled as even lower in a few routes. An ammonia-fueled vehicle can save 100 g of greenhouse gas per km compared to gasoline when the complete vehicle and fuel life cycle is considered. Depletion of abiotic resources is moderately lower for conventional ammonia production, which is originated from natural gas, than liquefied natural gas, diesel, petrol and propane fuels.

In this report, detailed background information about production and utilization of ammonia is presented in Chapter 1. In Chapter 2, an alternative ammonia synthesis method is experimentally realized and tested. The selected route is molten salt electrolyte based electrochemical ammonia production. In Chapter 3, the required hydrogen for ammonia synthesis is produced using photoelectrochemical route and integrated to ammonia synthesis. The experimental results are presented under different conditions. Chapter 4 explains ammonia production from hydrocarbon sources such as natural gas. The comparative results for liquefied natural gas (LNG) and ammonia are given for production and transport phases. Chapter 5 investigates the usage of ammonia in maritime applications and performs a life cycle assessment. In Chapter 6, ammonia is evaluated as a potential fuel for aviation industry and the performances of alternative fuels are comparatively presented. Chapter 7 performs a life cycle assessment for ammonia usage in road vehicles whereas in Chapter 8, ammonia is produced using different routes and decomposed on-board for hydrogen driven vehicles. On-board ammonia electrolysis is also analyzed and presented. Chapter 9 investigates the cost of photoelectrochemical hydrogen and ammonia using exergoeconomic approach and the system is scaled-up in Chapter 10 to find the total cost of hydrogen and ammonia.

CHAPTER 1:QUICK FACTS ABOUT AMMONIA

Currently about 4.8 million metric tonnes of ammonia are produced yearly in Canada. 95.4% of produced ammonia originates from natural gas via steam methane reforming technique. 2.3% is produced by coal gasification, and 2.3% is from petroleum-coke in Canada [1]. On the other hand, the U.S. yearly produces about 12 million metric tonnes of ammonia. China is the largest ammonia producer in the world with a capacity of 55 million metric tonnes [1]. Global ammonia production corresponds to about 200 million metric tonnes. Only 4% of ammonia is used directly whereas the remaining is either used as a fertilizer or as a chemical in other industrial applications [1]. 80 million metric tonnes of ammonia is converted to urea for fertilizer uses. 1 L of gasoline costs about 0.65 USD in the U.S. This corresponds to 0.84 USD per kg gasoline. In comparison, 1 kg of ammonia sells for about 0.35 USD in the U.S [2]. Hence, ammonia is a lower cost fuel in mass basis.

The United States, Mexico and Canada have now set to declare that 50% of North America's electricity will come from clean power sources by year 2025 at the Three Amigos Summit in Ottawa [3]. It is now more obvious that the importance of alternative fuels and storage mediums increases day by day. In this regard, renewable ammonia (NH_3), which is a carbon-free fuel, refrigerant and working fluid, appears to be a unique solution to overcome local and global issues. It will help achieve carbon-free economy. The most unique part of ammonia is that it can be used for multi-purpose applications, including fuel, refrigerant, working fluid, and storage media of hydrogen. The other clear advantage is that it can serve almost all sectors, ranging from transportation to residential, industrial to commercial, public to utility, and agricultural to chemical.

Ammonia as a potential fuel candidate for vehicles can also be produced using conventional hydrocarbons in a cleaner manner by implying current technologies and developments even with lower costs. Hydrogen can be produced by dissociation of hydrocarbons, which can be then converted to ammonia using nitrogen supply from air [4]. Dissociation of hydrocarbons such as methane and oil sand bitumen is a promising option especially for Canada [5,6]. Although decomposition of heavy fractions such as oil sand bitumen can bring some challenges because of various metal and sulfur contents, purification is always possible and applicable. This technology can be promising for oil sand reserves in Alberta and stranded natural gas reserves in Newfoundland and Labrador. Ammonia is an excellent fuel candidate with the ability to secure off peak power at negative or very low prices. We can convert excess electricity to ammonia, and then we can burn it in generators, internal combustion engines, fuel cells and use as fertilizer. Where and when needed, it can be transported via pipelines, trucks, and ocean tankers.

Using appropriate renewable resources and cleaner hydrocarbon utilization paths, ammonia production can be cost-effective and environmentally friendly. On-site production and utilization of ammonia brings additional significant cost and efficiency advantages.

Ammonia (NH_3):

- consists of one nitrogen atom from air separation and three hydrogen atoms from any conventional or renewable resources.
- is the second largest synthesized industrial chemical in the world.
- is a significant hydrogen carrier and transportation fuel that does not contain any carbon atoms and has a high hydrogen ratio.
- contains about 48% more hydrogen by volume than liquefied hydrogen.
- does not emit direct greenhouse gas emission during utilization

- can be used as solid and/or liquid for many purposes.
- can be stored and transported under relatively lower pressures.
- can be produced from various type of resources ranging from oil sands to renewables.
- is a suitable fuel to be transferred using steel pipelines with minor modifications which are currently used for natural gas and oil.
- can be used in all types of combustion engines, gas turbines, burners as a sustainable fuel with only small modifications and directly in fuel cells which is a very important advantage compared to other type of fuels.
- brings a non-centralized power generation via fuel cells, stationary generators, furnaces/boilers and enables smart grid applications.
- can be used as a refrigerant for cooling in the car.

1. What are the uses of ammonia?

Ammonia is considered a possible working fluid for thermodynamic cycles, working for refrigeration, heating, power or any mixture of those can be coupled with internal combustion engines, and using exhaust gasses to drive automotive absorption refrigeration system.

Ammonia has been recognized and employed as a leading refrigerant in the industrial sector due to its outstanding thermal properties, zero ozone depletion and global warming potential (GWP). Ammonia has the highest refrigerating effect per unit mass compared to all the refrigerants being used including the halocarbons. The remarkable advantages of ammonia over R-134a could be lower overall operating costs of ammonia systems, the flexibility in meeting complex and several refrigeration needs, and lower initial costs for numerous applications. Ammonia has better heat transfer properties than most of chemical refrigerants and consequently allow for the use of equipment with a smaller heat transfer area. Thereby plant construction cost will be lower. But as these properties also benefit the thermodynamic efficiency in the system, it also reduces the operating costs of the system. In many countries the cost of ammonia per mass is considerably lower than the cost of HFCs. This kind of advantage is even multiplied by the fact that ammonia has a lower density in liquid phase. Modern ammonia systems are fully contained closed-loop systems with fully integrated controls, which regulate pressures throughout the system. Ammonia is used as refrigerant highly in the refrigeration structures of food industry like dairies, ice creams plants, frozen food production plants, cold storage warehouses, processors of fish, poultry and meat and a number of other uses.

It is also stimulating to note that NH_3 is a reduction agent for the NOx typically current in combustion releases. The reaction of NOx with ammonia over catalysts produces only steam and nitrogen. An average car needs only approximately 30 mL of NH_3 per 100 km to neutralize any NOx emissions. If the vehicles run with NH_3 as fuel, this amount is unimportant with respect to the fuel tank volume.

Ammonia is used as fertilizer in the agriculture. It is also converted into urea by reacting with CO_2. The majority of growth in ammonia usage is expected to be for industrial uses and the production of fertilizer products.

It is also worth to examine the option to cool the engine with ammonia that can act as a refrigerant while it is heated to the temperature at which it is fed to the power producer (ICE or fuel cell). Optionally, the cooling outcome of ammonia, i.e., its high latent heat of evaporation, may be used to harvest some air conditioning onboard.

2. Is ammonia really a fuel?

Ammonia as a sustainable fuel can be used in all types of combustion engines, gas turbines, and burners with only small modifications and directly in fuel cells. Ammonia was initially used as a fuel for buses in Belgium in 1940s [7]. Many studies have already been performed and many applications have been implemented so far. A prototype unit for combustion which enabled liquid kerosene and gaseous ammonia to be fed, and ammonia was combusted in a gas-turbine unit. Further studies have been performed by various researchers which have proven the practicality of using ammonia as fuel [8–14]. Numerical studies of combustion characteristics of ammonia as a renewable fuel have been conducted. Ammonia can also be used a fuel blending option for current gasoline and diesel engines. Combustion and emissions characteristics of compression-ignition engine using dual ammonia-diesel fuel have been performed. Performance enhancement of ammonia-fueled engine by using dissociation catalyst has been studied. These are just a few examples to show the current progress in the ammonia utilization options in transportation applications.

3. Is ammonia a suitable fuel for transportation sector?

The storage and delivery infrastructure of ammonia is similar to liquefied petroleum gas (LPG) process. Under medium pressures (5-15 bar), both of the substances are in liquid form which brings the significant advantage because of storage benefits. Today, vehicles running with propane are mostly accepted and used by the public since their on-board storage is possible and it is a good example for ammonia fueled vehicle opportunities since the storage and risk characteristics of both substances are similar to each other. An ammonia pipeline from the Gulf of Mexico to Minnesota and with divisions to Ohio and Texas has served the ammonia industry for many years. It indicates that there is a working ammonia pipeline transportation which can be spread overall the world. The potential of ammonia usage in many applications will be dependent on the availability of ammonia in the cities. Ammonia is a suitable substance to be transferred using steel pipelines with minor modifications which are currently used for natural gas and oil. In this way, the problem of availability of ammonia can be eliminated.

4. How can ammonia be used in transportation?

Ammonia has significant potential as an alternative fuel to further the sustainable development of transportation sector. A few of the following alternatives are shown in Fig. 1 for direct ammonia usage in transportation applications.

Currently, the majority of the locomotive fleet is made up of diesel-electric locomotives, operating with either two-stroke or four-stroke prime mover diesel engines that is coupled to an electric generator. Application of ammonia fuel for internal combustion engine (ICE) with the alternative locomotive configurations direct feed, or a combination of direct feed and decomposition subcategory options will bring more sustainable solutions. Additionally, fuel cell driven vehicles and locomotives may contribute to solve the associated matters of urban air superiority and national energy security influencing the rail and transportation sector.

5. Is ammonia a clean fuel?

Compared to gasoline vehicles, ammonia-fueled vehicles do not produce direct CO_2 emission during operation. Since ammonia produces mainly water and nitrogen on combustion, replacing a part of conventional fuel with ammonia will have a large effect in reducing carbon dioxide emissions.

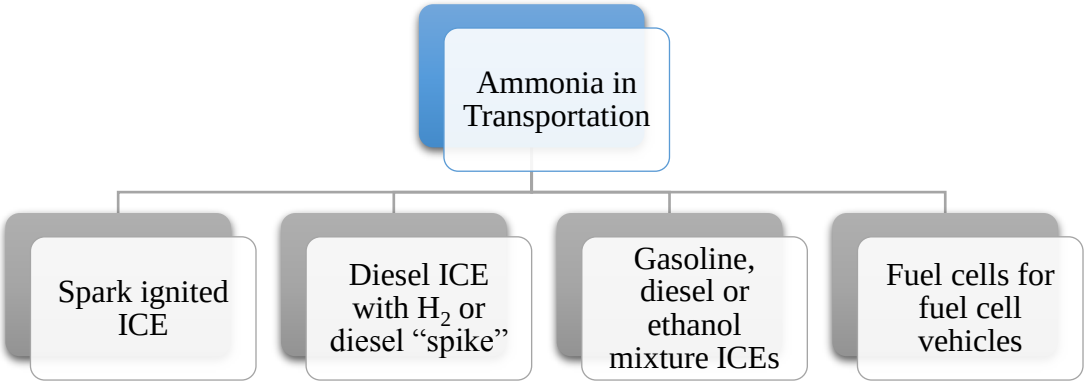

Figure 1 Ammonia utilization options in transportation sector

6. How much greenhouse gas can I save if I drive an ammonia car?

Considering a complete life cycle counting the production, transport and usage of the fuel, a diesel driven car can emit greenhouse gas emissions of about 220 g per km. Ammonia driven car can decrease this number down to about 70 g per km if it is produced from solar energy and about 150 g per km if it is produced from hydrocarbon cracking.

7. Is ammonia a cost effective fuel?

The illustrative cost comparison of various fueled vehicles is shown in Fig. 2 and 3. Considering the current market prices of the fuels, ammonia is the lowest cost fuel corresponding to about 3.1 US$ in a 100 km driving range. This shows that ammonia is a promising transportation fuel in terms of cost. There is an advantage of by-product refrigeration which reduces the costs and maintenance during vehicle operation. Some additional advantages of ammonia are commercial availability and viability, global distribution network and easy handling experience. Ammonia is a cost effective fuel per unit energy stored onboard compared to methanol, CNG, hydrogen, gasoline and LPG as shown in Fig. 2.

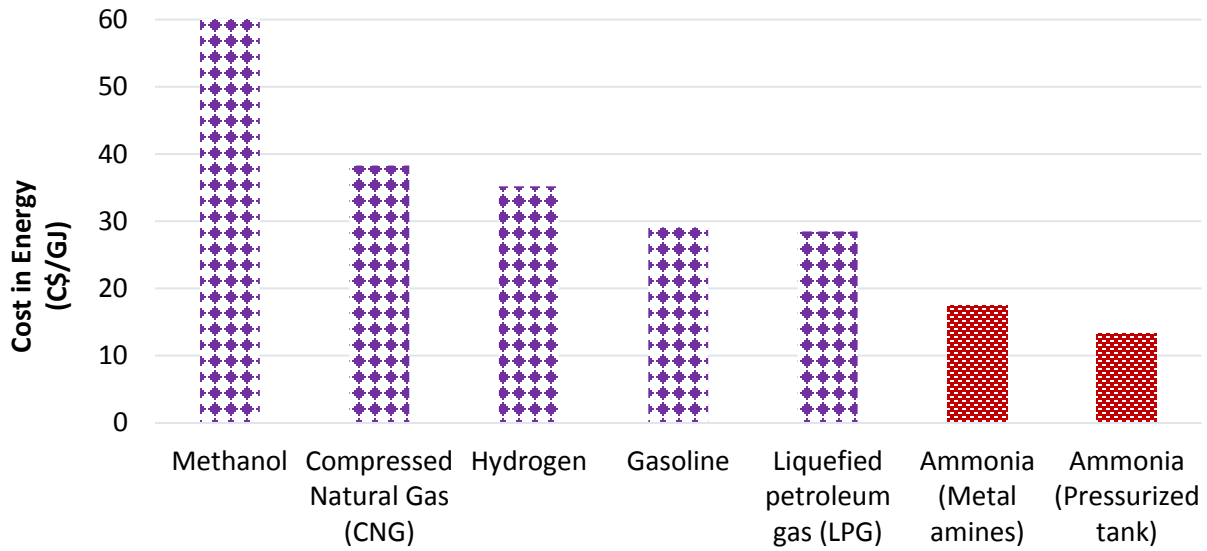

Figure 2 Comparison of various vehicle fuels in terms of energy cost per gigajoule

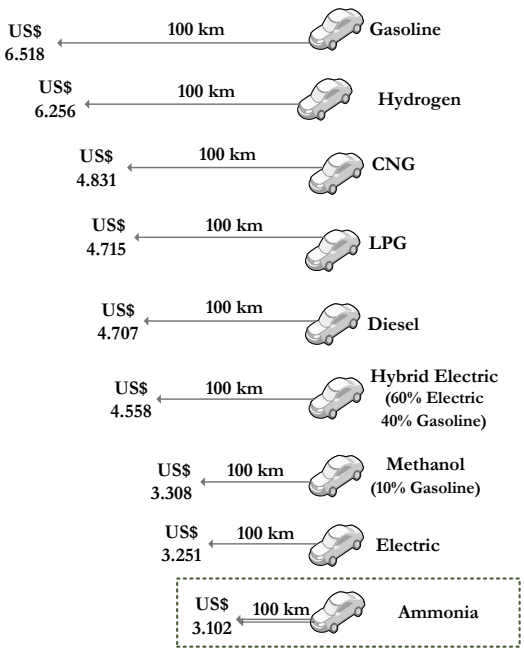

Figure 3 Comparison of driving cost for various fueled vehicles

Table 1 Comparison of ammonia with other fuels

Fuel/storage	**Pressure (bar)**	**Density (kg/ m^3)**	**HHV (MJ/ kg)**	**HHV per Volume (GJ/ m)**	**Energy per Volume (GJ/ m)**	**Cost per Mass (US$ / kg)**	**Cost Per Volume (US$/ m)**	**Cost per Energy (US$ /GJ)**
Gasoline, C_8H_{18}/liquid	1	736	46.7	34.4	34.4	1.03	754.86	21.97
CNG, CH_4/integrated storage	250	188	42.5	10.4	7.8	0.91	170.60	21.29
LPG, C_3H_8/pressurized tank	14	388	48.9	19	11.7	1.06	413.66	21.74
Methanol, CH_3OH/liquid	1	786	14.3	11.2	9.6	0.41	317.80	28.31
Hydrogen, H_2/metal hydrides	14	25	142	3.6	3	3.02	75.49	21.29
Ammonia, NH_3/pressurized tank	10	603	22.5	13.6	11.9	0.23	136.63	10.04
Ammonia, NH_3/metal amines	1	610	17.1	10.4	8.5	0.23	138.14	13.21

In Table 1, the exact fuel energy per mass is given regarding fuel's higher heating value. The volumetric energy of the fuel is found by multiplying the HHV with the density value listed in the third column. Ammonia's HHV is around half of the one of gasoline, and its density is also inferior. Therefore liquid NH_3 stores 2.5 fewer energy per unit capacity than gasoline. If the NH_3 is stored in the form of hexaamminemagnesium chloride to remove the hazard related to its toxicity, the energetic cost to pay for discharging ammonia reduces its HHV. Among alternative fuels, ammonia yields the lowest cost per energy basis. Therefore, it is important to note that low-carbon transportation projects should be eligible for compliance purposes.

8. What is the process of ammonia production?

A most common ammonia synthesis technique is recognized as Haber-Bosch process in the world. In this process, nitrogen is supplied through air separation process. Hydrogen is mainly supplied using steam methane reforming or coal gasification. However the source of hydrogen can be renewable resources. The Haber-Bosch is an exothermic process that combines hydrogen and nitrogen in 3:1 ratio to produce ammonia. The reaction is facilitated by catalyst and the optimal temperature range is 450-600°C.

Alternative production pathways are also available and under investigation including electrochemical and biological routes. These routes can easily be integrated to renewable energy sources for cleaner production. The electrochemical process can be carried out under ambient conditions or at higher temperatures depending on the type of the electrolyte material used. There are various electrochemical pathways such as molten salt, polymer membrane, liquid electrolyte etc. are intensively being researched at the moment [15–20].

The electrochemical process can be carried out under ambient conditions or at higher temperatures depending on the type of the electrolyte material used. For high temperature electrolytic routes of ammonia production, the use of waste heat from thermal or nuclear power plants or heat from renewable energy sources like solar would make the overall process more environmentally friendly.

One of the key advantages of ammonia is to be a storage medium. Renewable energy generation does not often match electrical demand which causes a requirement of storage. Green ammonia can be manufactured from surplus renewable sources, which would reduce the amount of electricity exported to neighboring jurisdictions at a negative cost.

9. What is the source of ammonia and is it cleaner than other fuels?

In terms of conventional resources, naphtha, heavy fuel oil, coal, natural gas coke oven gas and refinery gas can be used as feedstock in ammonia production. Natural gas is the primary feedstock used for producing ammonia in worldwide corresponding to about 72%. However, renewable resources can easily be integrated for ammonia production. In this way, decentralized ammonia production can be realized which further decreases the delivery cost of the fuel. Many studies have been performed to investigate the ammonia production routes and their environmental impacts. Here, some of them are briefly shown.

The production of the different fuels is compared in terms of abiotic depletion of sources as shown in Fig. 4. Ammonia fuel has the lowest abiotic depletion value compared to others although the production process may be fossil fuel based. There are multiple pathways for ammonia production. Ammonia is cleaner when produced from renewable resources. Fig. 5 shows the comparison of ozone layer depletion values for various transportation fuels. Ammonia has

lowest ozone layer depletion even if it is produced from steam methane reforming and partial oxidation of heavy oil.

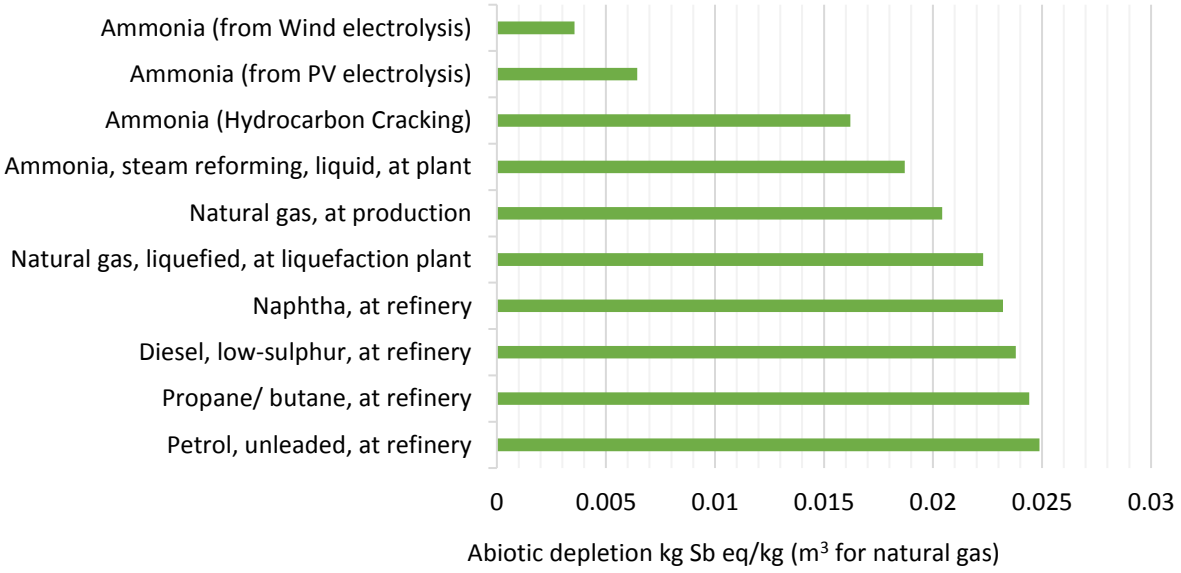

Figure 4 Abiotic depletion values during production of various fuels

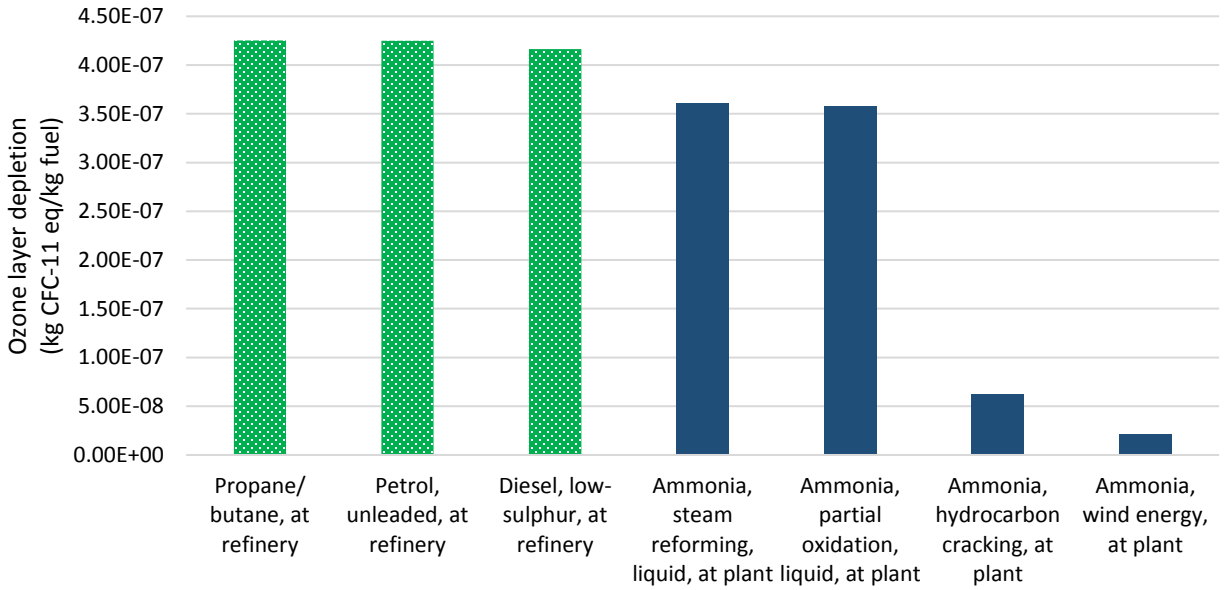

Figure 5 Ozone layer depletion during productions of various fuels

Fig. 6 compares the total greenhouse gas emissions during production of 1 MJ energy from various resources including gasoline, LPG, diesel, natural gas and ammonia. Production of 1 MJ energy from ammonia has lower emissions than gasoline, LPG, diesel, oil and natural gas.

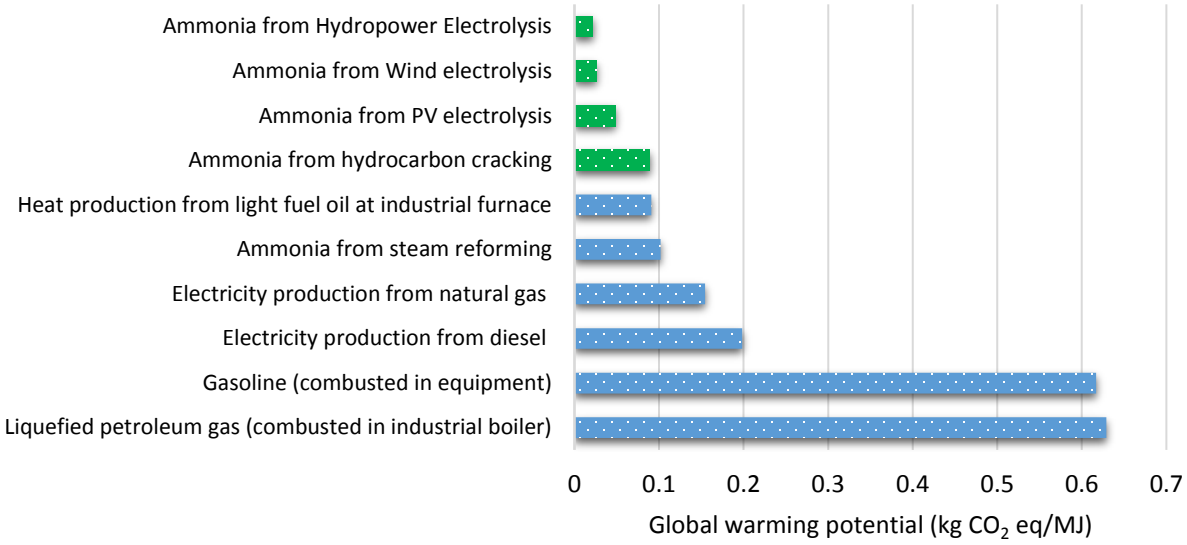

Figure 6 Comparison of global warming potential of 1 MJ energy production from various resources

Giving priority for complete conversion from fossil fuel based fuels to carbon-free fuels will bring short term and long term solutions to combat global warming. Therefore, the activities to lower the carbon intensity of conventional transportation fuels be eligible for compliance purposes

CHAPTER 2:ELECTROCHEMICAL SYNTHESIS OF AMMONIA

Natural gas is the primary feedstock used for producing ammonia in worldwide which increases the fossil fuel dependence and greenhouse gas emissions. Therefore, alternative ammonia synthesis methods are in development stage such as electrochemical ammonia synthesis which is experimentally tested in this chapter.

1. Introduction

The electrochemical process can be carried out under ambient conditions or at higher temperatures depending on the type of the electrolyte material used. For high temperature electrolytic routes of ammonia production, the use of waste heat from thermal or nuclear power plants or heat from renewable energy sources like solar would make the overall process more environmentally friendly. Ammonia production from hydrogen and nitrogen is exothermic in nature and is facilitated by high pressures and low temperatures. Thus a balance between the operating temperature, pressure and the ammonia yield needs to be proven for electrochemical system in determining ammonia production rates. Among solid state electrolyte methods, there are studies in the literature although maximum production rates are lower than liquid electrolyte based methods. A study used a proton-conducting solid electrolyte at 450°C to 700°C with Ru based catalyst. They resulted that the conversion rates are lower compared to nitrogen or steam because of the low conductivity of the working electrode [20]. In another study with a Nafion divider in aqueous 2 M KOH and a Ru on cathode allowed ammonia generation from water and nitrogen at a rate of 2.8×10^{-12} mol NH_3/s cm^2 and coulombic efficiency of 0.9% at 20°C. Also, at 90°C, a maximum rate of 2.1×10^{-11} mol /s cm^2 at 0.2% efficiency was observed [21]. Membrane based applications can be performed at quite lower temperatures than molten salt electrolyte based methods. Having Pt/C on a gas diffusion layer at both electrodes and room temperature, using Nafion as the electrolyte yielded NH_3 at a higher rate of 1.1×10^{-9} mol/s cm^2, which consumed water at the anode and air at the cathode at 0.6% coulombic efficiency [16]. In addition, there is also a molten NaOH-KOH eutectic electrolyte based ammonia fuel cell studied by researchers [22]. Licht et al. [18] obtained about 35% Faradaic efficiency where they supplied water and air to produce ammonia in molten salt electrolyte. In their further research Li and Licht [17] reported that since they used water as hydrogen source, at 200 mA/cm^2, over 90% of applied current generated H_2, rather than NH_3. In this case, hydrogen was cogenerated but required higher potentials because of water splitting voltage.

Numerous electrochemical methods have recently been developed for consideration as alternative syntheses of NH_3 [23–33]. Kugler et al. [32] studied to increase the NH_3 generation rate by applying galvanic deposition of Rh and Ru on Ti felts in which they observed higher formation rates for Rh coatings. Kim et al. [33] performed electrochemical synthesis of ammonia in molten LiCl-KCl-CsCl electrolyte by a mixture of catalysts as nano-Fe_2O_3 and $CoFe_2O_4$. Their maximum formation rate was 3×10^{-10} mol/s cm^2 where they used water and nitrogen for the reaction. Xu et al. [34] investigated generation of ammonia at atmospheric pressure and low temperature electrochemically, using the SFCN materials as the cathode, a Nafion membrane as the electrolyte, nickel-doped SDC (Ni-SDC) as the anode and silver-platinum paste as the current collector. NH_3 was produced from 25°C to 100°C temperature levels when the SFCN materials were utilized as cathode, with $SmFe_{0.7}Cu_{0.1}Ni_{0.2}O_3$ which gives the maximum rates of ammonia formation. Garagounis et al. [35] summarized the test results of studies within the last 15 years using electrolyte cells. More than 30 electrolyte materials with 15 catalysts that were used as working electrodes (cathode) were tested. The polymer Nafion yielded the highest rate of ammonia

formation at a very low temperature. Nafion can also be used as a proton conductor with and a Ru/C cathode which yielded NH_3 from H_2O and N_2 at 90°C. These low operating temperatures are sought after when designing new systems because of the reduced energy input required and lower rate of decomposition of the ammonia formed. As an alternative approach, the use of oxygen ion conductors where steam and nitrogen are introduced together at the cathode should be considered. The rate of NH_3 production was however very small in a demonstration at 500°C but improved by up to two orders of magnitude at higher temperatures as reported by Skodra et al. [36]. Furthermore, NH_3 synthesis using molten salt electrolyte based systems can yield high conversion ratios similar to that of polymer based membranes. Solid-state proton conductors (SSPC) denote a class of ionic solid electrolytes which have the capability to transfer hydrogen ions (H^+) [37]. However, this method has some disadvantages such as high temperature requirement and formation of secondary phases [38–40]. A variety of factors need to be analyzed when selecting the cell material such as system operating temperature, current density, pressure, and conductivity which all affect the ammonia production rate. It is important to note that conductivity of a solid electrolyte increases exponentially with temperature and by reducing cell thickness as reported by Giddey et al. [41]. Kyriakou et al. [42] recently reported extensive literature data about low temperature, medium temperature and high temperature electrochemical NH_3 synthesis routes showing that the synthesis rates can reach up to 3.3×10^{-8} mol/s cm^2. Shipman and Symes [43] presented the recent developments in electrochemical NH_3 production and they categorized the sources of proton as water, hydrogen and sacrificial proton donors. They resulted that the techniques keeping the temperatures in the range of 100°C and 300°C may well demonstrate to be the most efficient.

H_2 can be directly utilized in the electrochemical NH_3 formation as investigated in this study. Most of the literature used water as hydrogen source which also requires water splitting process at the same time with ammonia synthesis. Specifically, for solar energy storage applications, H_2 can act as short-term storage whereas NH_3 can serve as long-term storage medium which reduces the storage losses significantly. Here, electrochemical synthesis of ammonia using H_2 and N_2 at ambient pressure in a molten hydroxide ambient with nano-Fe_3O_4 catalyst is performed. The active surface areas of the Nickel mesh electrodes are increased to allow higher formation rates. The effects of various parameters such as applied potential and current density, reaction temperature on ammonia formation rate are investigated. The nickel mesh electrodes are utilized having large surface area and the reaction temperatures are quite lower than the conventional Haber-Bosch process.

2. Experimental Investigation and Analysis

In this study, H_2 and N_2 are directly used for electrochemical synthesis of ammonia at the electrodes. N_2 receives the electrons from external power supply. Hence nitrogen gas sent via the porous nickel cathode is reduced to nitride according to the following equation:

$$N_2 + 6e^- \rightarrow 2N^{3-} \quad (1)$$

It becomes N^{3-} then after moves to the other electrode where H_2 is being supplied. Hydrogen ions combine with nitrogen ions and form NH_3 at anode electrode and shown the following equation:

$$2N^{3-} + 3H_2 \rightarrow 2NH_3 + 6e^- \quad (2)$$

The anode reaction is also achieved on porous nickel electrode.

The overall reaction is:

$$3H_2 + N_2 \rightarrow 2NH_3 \quad (3)$$

Figure 7 Nickel mesh electrodes in the reactor, molten salt in the reactor

Iron oxide (Fe_3O_4) as nano-powder (20-30 nm, 98+%) is used in the experiments as catalyst. The high surface area of the nano-Fe_3O_4 in the electrochemical synthesis is critical for the reaction to occur and to obtain higher ammonia evolution rates. The reactants, H_2 and N_2, are bubbled through the mesh over the anode and cathode, respectively. The combined gas products (H_2, N_2 and NH_3) exit through two exit tubes in chamber head space. The exiting gases are firstly measured using flowmeters and bubbled through an ammonia water trap then analyzed for ammonia, and subsequently the NH_3 scrubbed-gas is analyzed for H_2 or N_2.

As mentioned earlier, the product gases from the reactor is bubbled through an ammonia trap consisting of a dilute 500 ml 0.001 M H_2SO_4 solution, changed every 15 minutes for ammonia analysis. Ammonia concentration is determined using various techniques to confirm the results. The methods utilized are as follows: ammonia test strips, ammonia gas flowmeters, Arduino ammonia gas sensor and salicylate-based ammonia determination method as the experimental setup is shown in Fig. 7, 8 and 9. For the salicylate-based method, two different solutions are used where one of them contains sodium salicylate and the other one contains sodium hydroxide and sodium hypochlorite. In each case, redundant measurements yield similar ammonia formation values, with the observed reproducibility of methodologies.

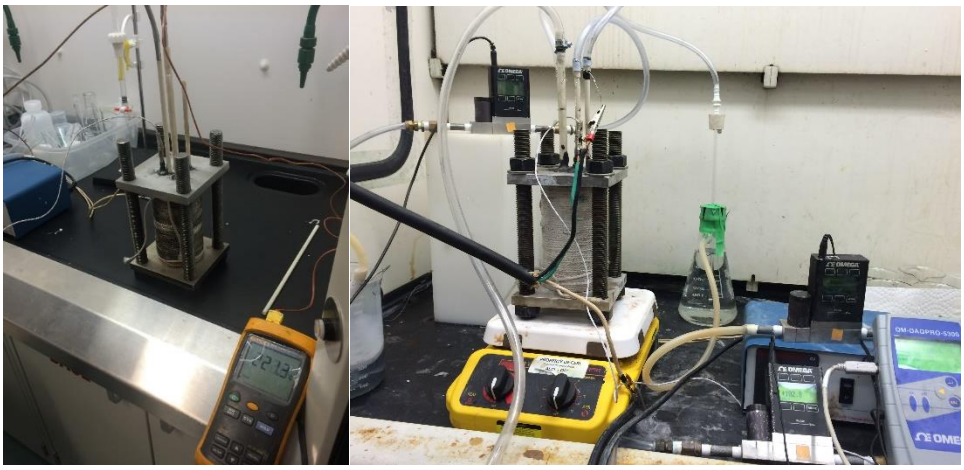

Figure 8 Heating tape used around the alumina crucible and experimental setup with flowmeters, temperature controller and tubing

In addition, the pH level of the dilute H_2SO_4 solutions are recorded before and after NH_3 trapped in the solution in order to observe the dissolved ammonia. Ammonia formation rate is calculated by converting the measured NH_3 to moles per seconds and considering the surface area of Ni electrodes as 100 cm^2. The ammonia formation rate is calculated using the following equation:

$$\dot{m}_{NH_3} = \frac{[NH_4^+] \times V}{t} \quad (4)$$

where $[NH_4^+]$ is the concentration of formed ammonia as mg/L, V is the total volume of H_2SO_4 for trapping ammonia as L and t is the time of collection.

The Faradaic efficiency is calculated based on the moles of electrons consumed compared to the $3e^-/NH_3$ equivalents produced. Thus, the Faradaic efficiency of ammonia generation process is defined as follows:

$$\eta_{Faradaic}\ (\%) = \frac{\dot{n}_{NH_3} \times F \times 3}{i} \quad (5)$$

where F is Faraday constant and i is the current density (A/cm^2).

The energy efficiency of the ammonia production process is also calculated based on lower heating values of reacted hydrogen and ammonia, nitrogen enthalpy and electrical power input as follows:

$$\eta_{Energy}\ (\%) = \frac{\dot{m}_{NH_3} \times LHV_{NH_3}}{(\dot{m}_{H_2} \times LHV_{H_2} + \dot{m}_{N_2} \times h_{N_2} + \dot{W}_{el})} \quad (6)$$

where W_{el} is the total electricity input during the experiment calculated using the total charge, applied voltage and duration.

3. Results and Discussion

The pure alkali hydroxides NaOH and KOH each melt only at temperatures above 300°C. The individual melting temperatures of NaOH and KOH are 318°C and 406°C, respectively. Among various alternatives, these two salts melt at quite lower temperatures which is a highly desired property in order to decrease external heat energy input. Based on common materials, the NaOH-KOH eutectic is of particular attention and melts at 170°C. Ammonia synthesis rates increase when the molten hydroxide (NaOH-KOH) electrolyte is mixed with high–surface area Fe_3O_4 to provide iron as a reactive surface and when nitrogen and hydrogen are present in the reactor. The molten salt medium is supplied electricity between two nickel anode and cathode electrodes. The mixture is prepared in the beginning by simply adding NaOH and KOH pellets in the reactor. After the salts melt, nano-Fe_3O_4 is added to the electrolyte and then stirred. When the mixture is ready, the lid is tightly closed and sealed. In order to yield NH_3 in the reactor, H_2, N_2 and nano-Fe_3O_4 are simultaneously needed. Table 2 shows the experimental conditions for four different runs.

Table 2 Experimental conditions for electrochemical ammonia synthesis

Experiment #	Temperature (°C)	Duration (min)	Current density (mA/cm^2)	Voltage (V)
1	210	15	2	1.4
2	255	30	3	1.5
3	215	45	2	1.3
4	220	25	2.5	1.55

Experiment 2 is performed at constant applied potential of 1.5 V whereas the others are performed at constant current in galvanostatic mode. The temperatures given in the table are average temperatures because, the temperature controller is on/off type and keeping the temperature

constant brings fluctuations. For each run, different ammonia trapping H_2SO_4 solution is used. The unreacted H_2 is also measured using a hydrogen sensor embedded to Arduino board which shows the portion of H_2 which does not react.

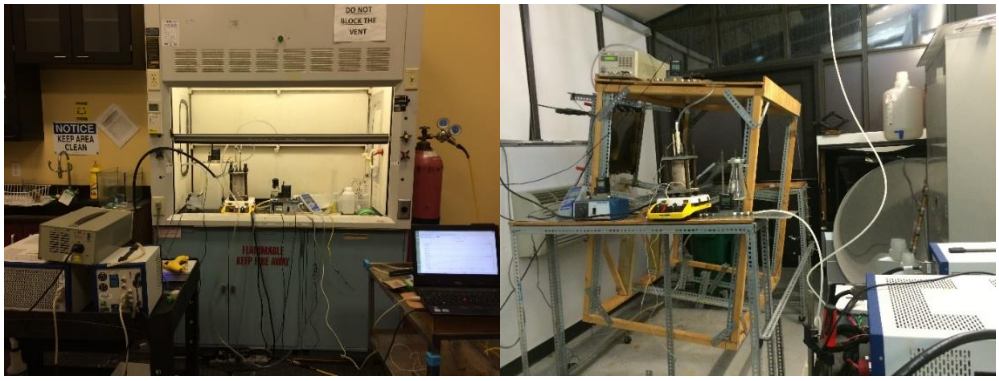

Figure 9 The experimental setup for the electrochemical ammonia synthesis in the fume hood and solar light

The required cell voltage to initiate the reaction of nitrogen and hydrogen in molten hydroxide at 210°C in the existence of nano-Fe_3O_4 is measured to be in average 1.4 V when the applied current is 200 mA between the 100 cm^2 Ni electrodes in the molten NaOH-KOH electrolyte.

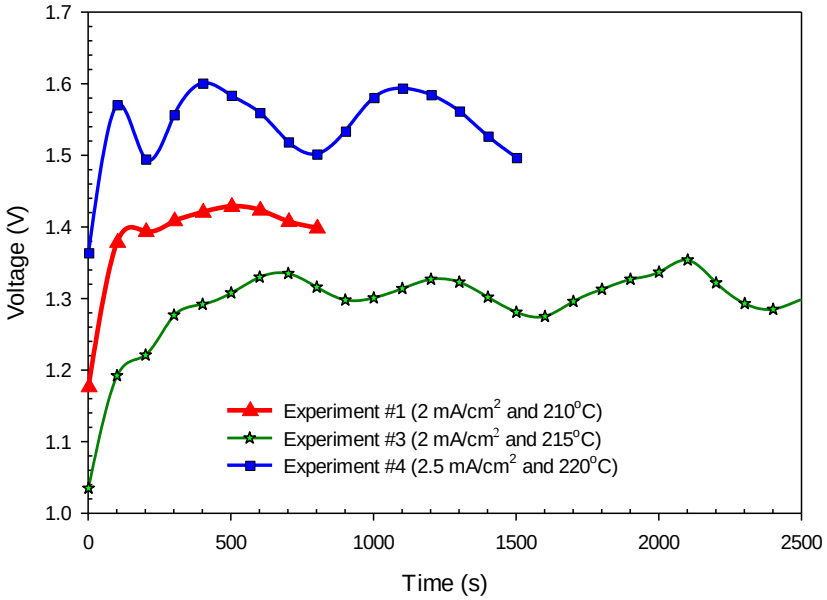

Figure 10 The relationship between voltage and time during several experimental runs at different applied currents and temperatures for electrochemical synthesis of NH_3 using N_2 and H_2 with nano-Fe_3O_4 in a molten salt hydroxide electrolyte

The potential increased to 1.54 V when the current density is increased to 2.5 mA/cm^2 at 220°C as shown in Fig. 10. At 2 mA/cm^2 and 210°C, ammonia is synthesized at a rate of 6.54×10^{-10} mol/s cm^2. At 2.5 mA/cm^2 and 220°C, the ammonia evolution rate decreased to 4.9×10^{-11} mol NH_3/s cm^2. At 215°C in a eutectic $Na_{0.5}K_{0.5}OH$ electrolyte with suspended nano-Fe_3O_4, it is observed

that at 2 mA/cm^2 applied current, NH_3 is generated at a Faradaic efficiency of about 6.3%, which declines to about 0.56% at 2.5 mA cm^2 in the reactor temperature of 220°C. Constant current electrolysis at 2 mA/cm^2 and 2.5 mA/cm^2 are driven at 1.3 V and 1.54 V, respectively at different temperatures as depicted in Fig. 10. It is also observed in the experiments that even though the reactor temperature is below 200°C, ammonia is generated with a similar production rate to above 200°C. The fluctuations in the potentials are caused by the temperature on/off processes to keep the temperature constant during the experiments. When the heater is on, the required potential to drive the reaction decreases as seen in Fig. 10. The potential gradually declines from 1.6 V to 1.5 V during the experiment at constant current density of 2.5 mA/cm^2. It is observed in the experiments that lower current density and lower temperature improve the stability of the rate of NH_3 evolution.

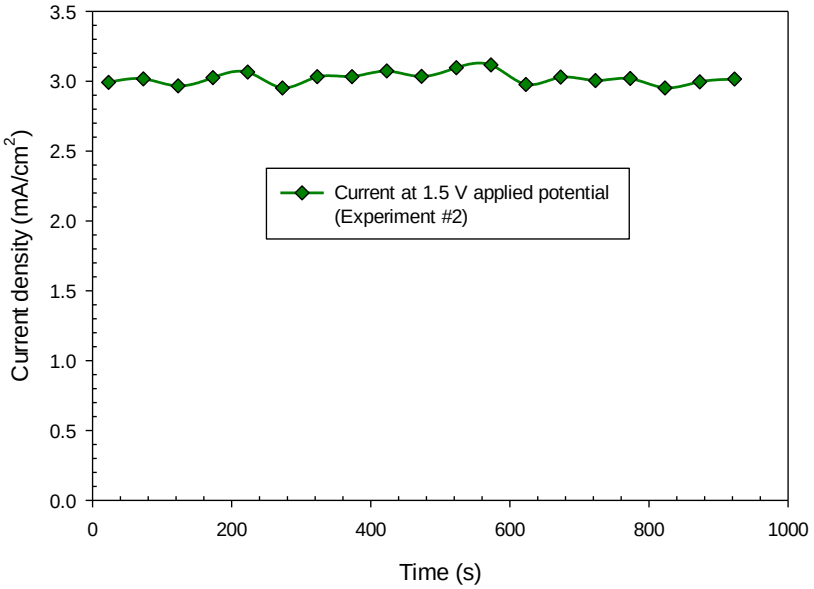

Figure 11 Current density at 1.5 V applied voltage for 100 cm^2 Ni electrodes of electrochemical NH_3 synthesis reactor

Fig. 11 shows the current density across the electrodes of the reactor when constant voltage of 1.5 V is applied. In this case, in average 3 mA/cm^2 current density is measured where the reaction temperature is considerably higher than other experiments which is about 255°C. The greater ammonia generation rate at lower voltages can be because of the lower hydrogen ion stream at the cathode which provides more time for generation of ammonia according to reaction.
Higher NH_3 synthesis rates are obtained within the first hour of the experiments. By the end of the experiment which is close to about two hours, 5.69 mL of NH_3 is formed.

The generated NH_3 is trapped and measured in a room temperature dilute H_2SO_4 trap. A non-dilute H_2SO_4 trap is also tried before the experiments reported here to understand the absorptivity of the solution. However, the ammonia readings were not successful in this case. Hence, dilute H_2SO_4 solutions are utilized for the reported experiments. The conversion efficiency is not only dependent on the hydrogen amount but also amount of catalyst available to stimulate the conversion of N_2 and H_2 into NH_3. In order to make sure that there is enough N_2 to be reacted with supplied H_2, the supplied volume of N_2 is kept quite higher than H_2.

In order to understand the current-voltage characteristics at lower temperature levels such as 200°C, the applied potentials are varied between 1.1 V and 1.5 V as shown in Fig. 12. At 200°C and 1.3 V, the average current density is 2.16 mA/cm^2 whereas it is about 2 mA/cm^2 at 215°C. The given temperatures and current densities are the average values where there are fluctuations because of the temperature controller. The obtained results for different experiments are tabulated in Table 3.

Table 3 Summary of the experimental results showing the NH_3 formation rates and efficiencies

Experiment #	NH_3 formation rate (mol/s cm^2)	NH_3 mass flow rate (g/min)	Faradaic efficiency (%)	Energy efficiency (%)
1	6.54×10^{-10}	6.67×10^{-5}	9.46	6.66
2	6.54×10^{-10}	6.67×10^{-5}	6.30	3.99
3	1.91×10^{-10}	1.94×10^{-5}	2.76	2.07
4	4.90×10^{-11}	5.00×10^{-6}	0.57	0.36

The variations of NH_3 formation rates at different current densities and temperature levels are comparatively shown in Fig. 13. The figure reveals that the temperature and current density are not the sole parameters affecting the performance of the reaction. Although the temperature is high at 2.5 mA/cm^2 current density, the NH_3 formation rate is low.

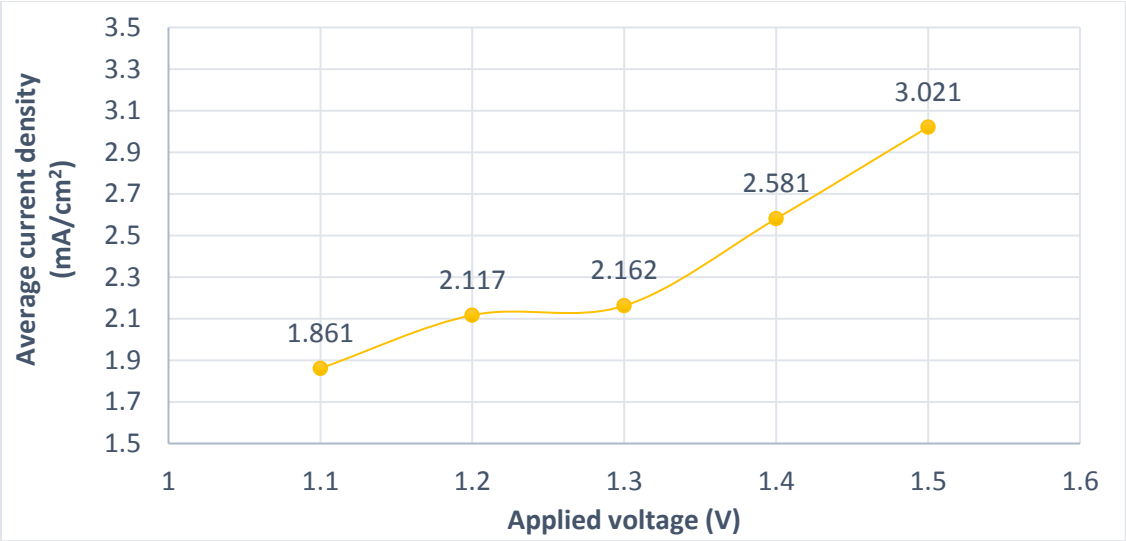

Figure 12 Applied potential-current density relations at 200°C for electrochemical NH_3 formation using N_2 and H_2 with nano-Fe_3O_4 in a molten salt hydroxide electrolyte

In contrast, at higher current densities at 3 mA/cm^2 and higher temperatures at 255°C, the NH_3 formation rate is high corresponding to about 6.6×10^{-10} mol/s cm^2. The differentiations might be caused by the catalyst saturations as well as the changes in supplied H_2 rates. The effects of catalyst quantity and type of electrodes are likely to be investigated in the future work. Furthermore, the electrochemical ammonia synthesis reactor will be integrated to photoelectrochemical hydrogen production cell to develop a clean and environmentally friendly ammonia production technique.

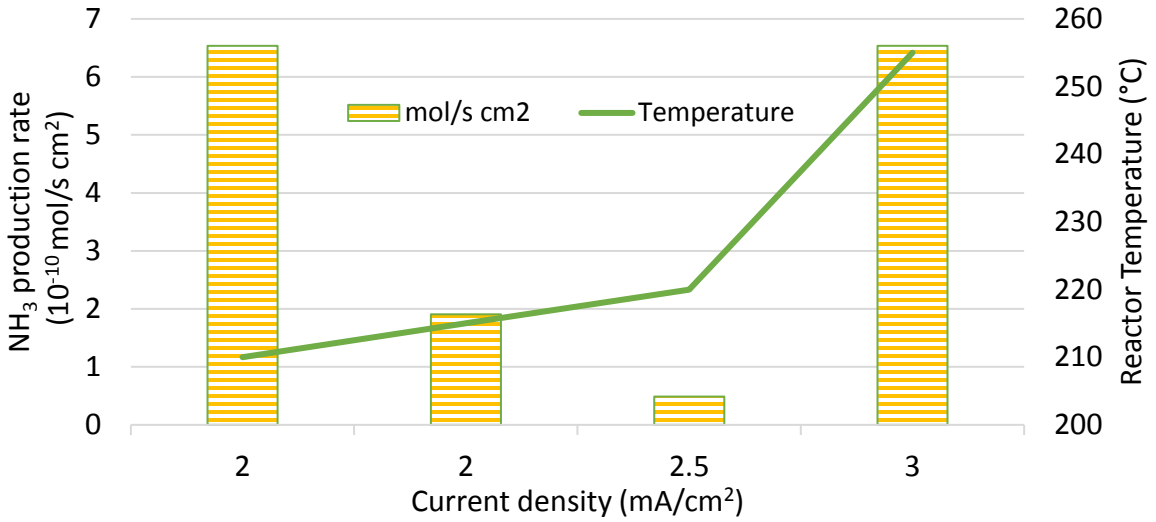

Figure 13 Change of electrochemical NH_3 formation rates depending on the applied current densities and reactor temperature using N_2 and H_2 with nano-Fe_3O_4 in a molten salt hydroxide electrolyte

4. Concluding Remarks

The electrochemical synthesis of NH_3 is a promising alternative to conventional energy intensive NH_3 production plants. Using renewable energy resources to drive the electrochemical NH_3 synthesis, the carbon footprint of current NH_3 production industry can be lowered significantly. Electrochemical NH_3 synthesis routes offer higher integrability to stand alone and distributed NH_3 production which is a carbon free fuel for various sectors. In this study, NH_3 is electrochemically generated at ambient pressure without a necessity of huge compressors using H_2 and N_2 in a molten hydroxide medium with nano-Fe_3O_4 catalyst. The reaction temperature is varied in the range of 200°C to 255°C to investigate the impact of temperature on NH_3 production rates. Having non-corrosive and high surface area nickel mesh electrodes allowed to generate more NH_3. The maximum Faradaic efficiency is calculated as 9.3% with a reaction temperature of 210°C. The NH_3 formation rate is determined to be 6.53×10^{-10} mol/s cm^2 at 2 mA/cm^2 current density.

CHAPTER 3:ELECTROCHEMICAL AMMONIA SYNTHESIS FROM PHOTOELECTROCHEMICAL HYDROGEN

The electrochemical process may be carried out under ambient conditions or at elevated temperatures depending on the nature of the electrolyte material used. For high temperature electrochemical ammonia production modes, the use of waste heat from thermal, nuclear power plants and renewable energy sources such as solar energy would make the process more environmentally friendly. In this section, we report the electrochemical synthesis of ammonia using photoelectrochemical (PEC) H_2 and N_2 at ambient pressure in a molten salt ambient with the catalyst of nano-Fe_3O_4.

1. Introduction

Assisting electrochemical process with solar energy will contribute an environmentally friendly method for ammonia production. Especially for solar energy storage applications, H_2 can act as a short term storage medium, whereas NH_3 can serve as a long term storage medium, which significantly reduces storage and transportation losses. The active surfaces of the nickel mesh electrode are 25 cm^2. The effects of various parameters such as the applied potential and current density, the reaction temperature on the rate of ammonia formation are examined. In this study, the solar light splitting and concentrator has been used for photoelectrochemical hydrogen production and electrochemical ammonia synthesis which has not been tested in the literature. The underlying motivation of this study is the potential for combining photoelectrochemical hydrogen production system with electrolytic ammonia synthesis processes to increase the solar spectrum utilization and ammonia production yield.

2. Life Cycle Assessment of Photoelectrochemical Hydrogen Based Electrochemical Ammonia Synthesis

In this section, the LCA results obtained for PEC based electrochemical ammonia production method using concentrated light are given in detail to reveal the contribution of various sub-processes. There are mainly three processes in the PEC based ammonia synthesis namely; hydrogen production from photoelectrochemical reactor, nitrogen production from air separation and electricity production from PV cells for energizing the process. The boundary of the LCA study for PEC hydrogen production is shown in Fig. 14.

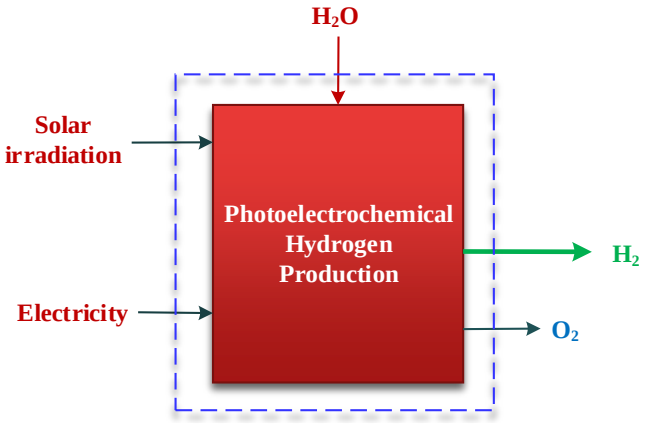

Figure 14 The boundaries of the conducted LCA for PEC hydrogen production

In the second step, electrochemical ammonia synthesis process is simulated as shown in Fig 15.

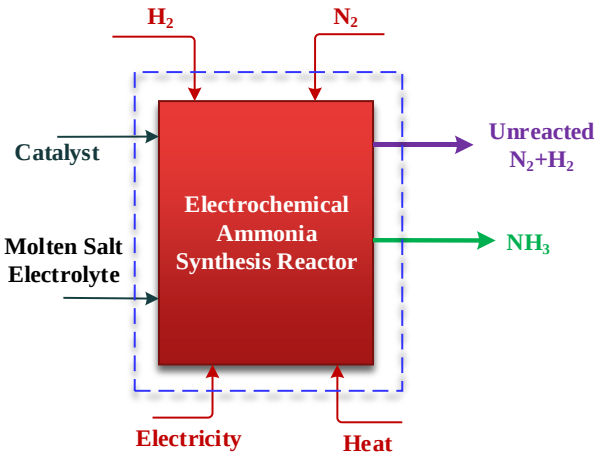

Figure 15 The boundaries of the conducted LCA for electrochemical ammonia synthesis process

The main contributor in all categories is the electricity production from PV cell as shown in Tables 4 to 6. 6.9% of total human toxicity is caused by nitrogen production process whereas 29.9% is due to hydrogen production from PEC system as listed in Table 4. Electricity production from PV is mainly responsible for remaining. There are numerous substances causing toxicity for human health such as arsenic and nickel as shown in Fig. 16.

Table 4 The shares of different sub-processes in human toxicity category for PEC (concentrated light) based electrochemical ammonia synthesis

Inflows	Flow	Unit
Total	100	%
Electricity, production photovoltaic, multi-Si	63.2	%
Hydrogen, PEC cell, PV, Concentrated Light-Integrated System	29.9	%
Nitrogen, gas, at plant	6.9	%
Potassium hydroxide	0.000102	%
Sodium hydroxide	6.96E-05	%
Iron oxide	7.06E-06	%

Arsenic and polycyclic aromatic hydrocarbons are the two fundamental toxic substances (about 64% in total) released to the environment in this method. There are mainly caused by copper and aluminum production processes for PV and support structures as shown in Fig.17. Polycyclic aromatic hydrocarbons are released due to nitrogen production from air separation plant since mix grid electricity is used.

Table 5 shows the shares of main processes contributing to abiotic depletion. Almost half of the total abiotic depletion is because of PV electricity production whereas 25% is due to hydrogen production. The molten salt electrolyte and reaction catalyst have quite small shares in total impact. Furthermore, as shown in Fig. 18, coal and natural gas are two main substances depleting in this method due to high electricity consumption in the PV cell factory and aluminum needed for support mechanism. Crude oil and brown coal have shares of 14% and 7%, respectively as shown in Fig. 19.

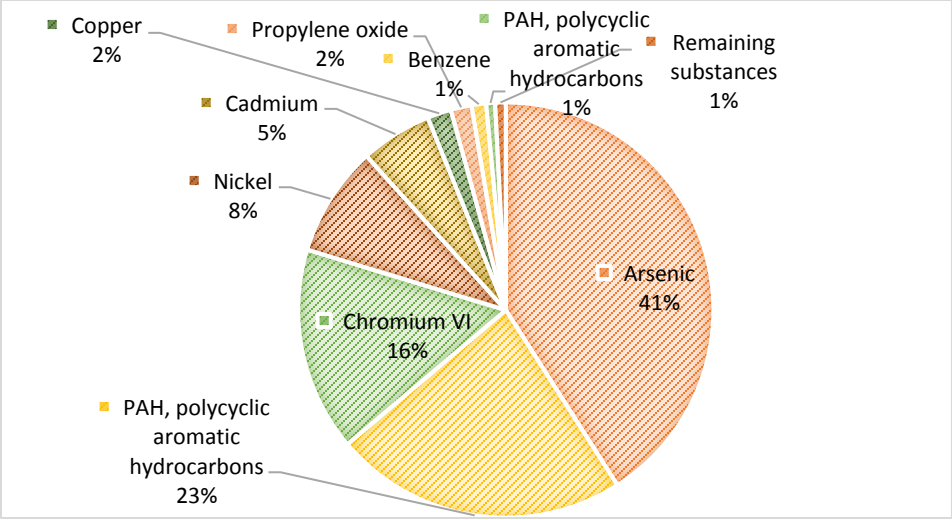

Figure 16 The share of toxic substances for PEC (concentrated light) based electrochemical ammonia synthesis

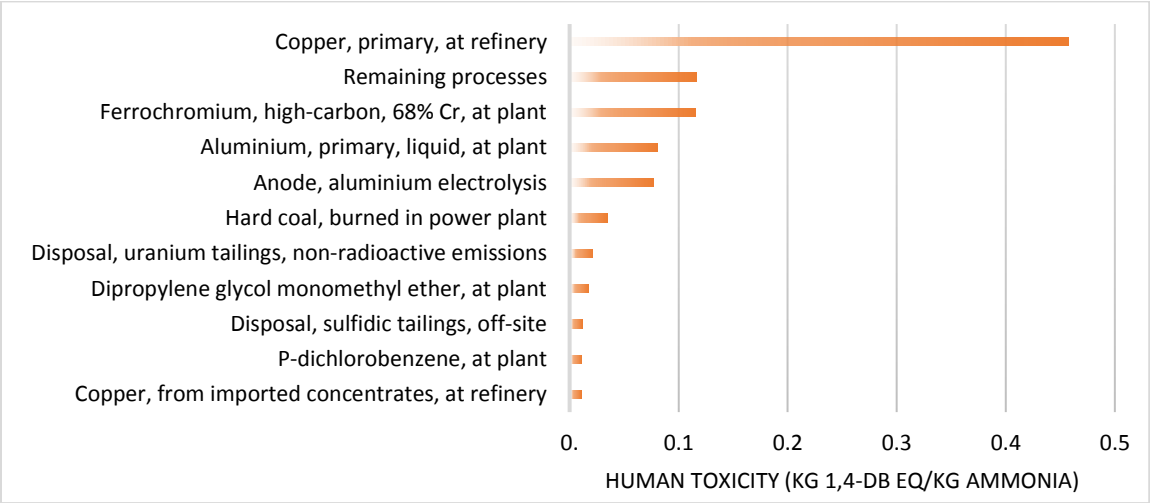

Figure 17 Contribution of various sub-processes to human toxicity potential of PEC (concentrated light) based electrochemical ammonia synthesis

Table 5 The shares of different sub-processes in abiotic depletion category for PEC (concentrated light) based electrochemical ammonia synthesis

Inflows	Flow	Unit
Total	100	%
Electricity, production photovoltaic, multi-Si	51.7	%
Hydrogen, PEC cell, PV, Concentrated Light-Integrated System	24.5	%
Nitrogen, gas, at plant	23.8	%
Potassium hydroxide	0.000256	%
Sodium hydroxide	0.000141	%
Iron oxide	1.83E-05	%

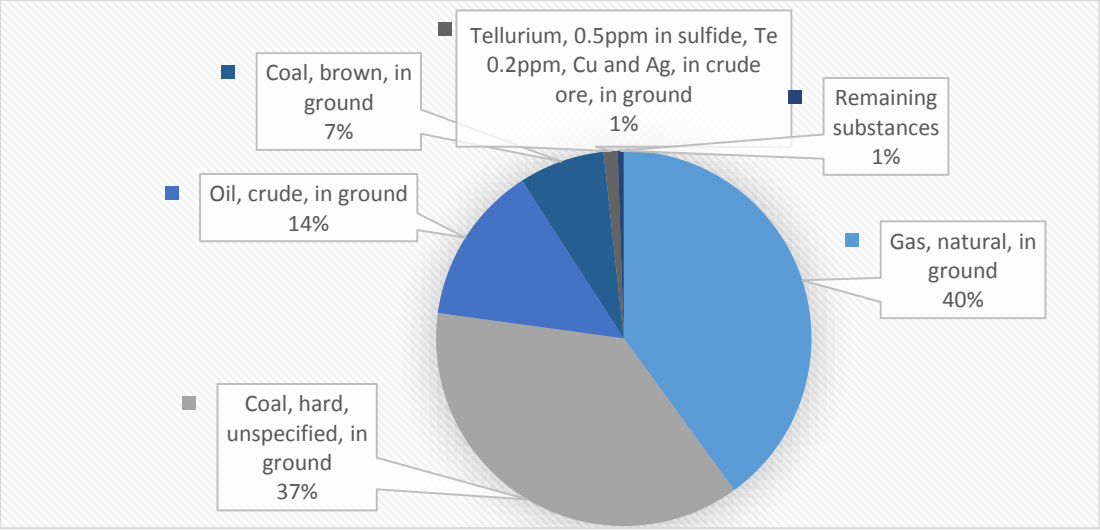

Figure 18 The share of depleting abiotic sources for PEC (concentrated light) based electrochemical ammonia synthesis

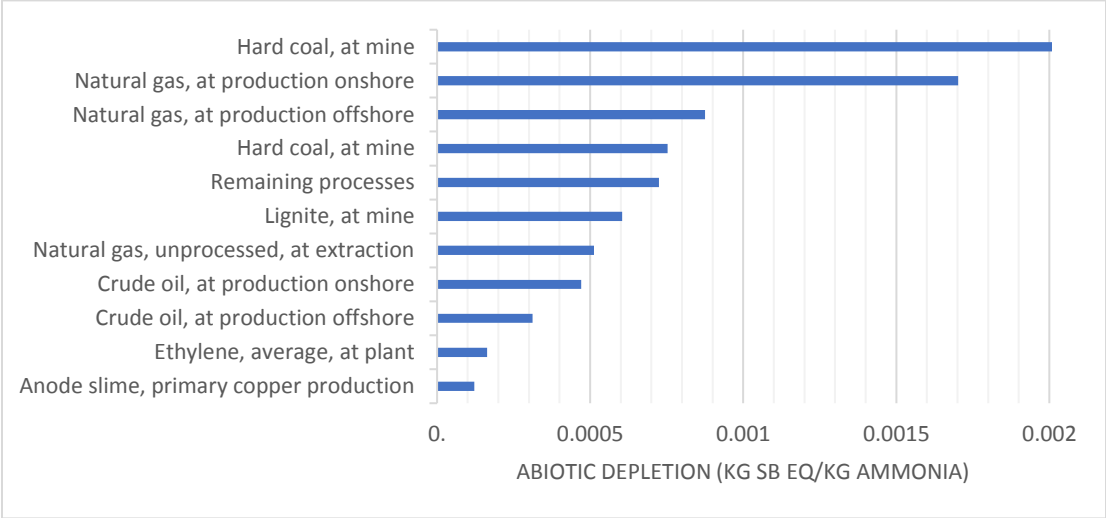

Figure 19 Contribution of various sub-processes to abiotic depletion potential of PEC (concentrated light) based electrochemical ammonia synthesis

The global warming potential of PV electricity production is responsible for almost 50% of total GHG emissions where almost 76% of PV electricity is because of PV cell production process in the factory. The shares of main processes for global warming potential are tabulated in Table 6. Global warming category includes all greenhouse gas emissions however, CO_2 is the main gas emitted to the environment corresponding to about 93% of total in the method as shown in Fig. 20. Sulfur hexafluoride (3%) and methane (2%) are the other gases contributing to total GHG emission. Sulfur hexafluoride emission is mainly due to magnesium production in the plant required for PV cell production. Shown in Fig. 21, electricity production in cogeneration plant and hard coal burned in power plant are mainly because of silicon production required for PV cells.

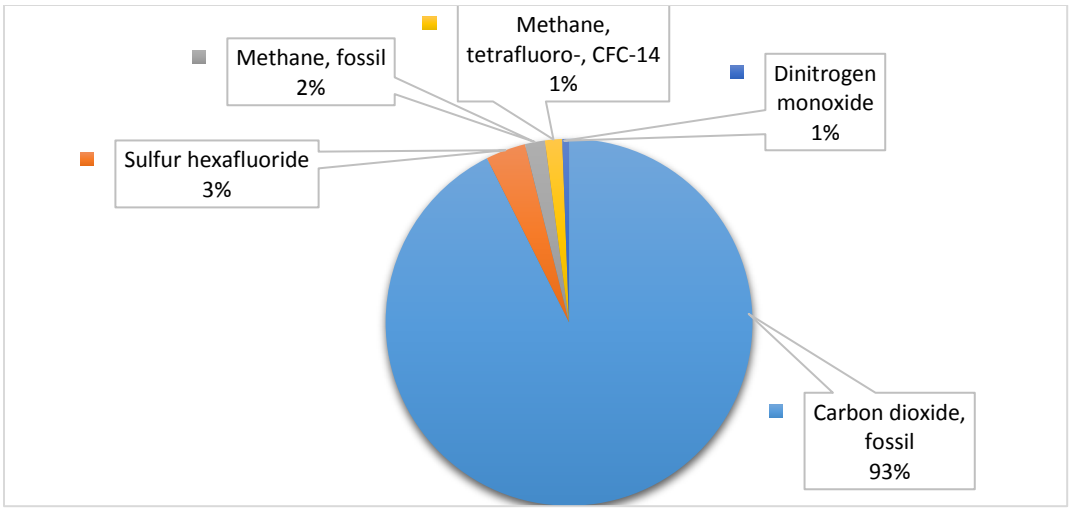

Figure 20 The share of greenhouse gas emissions for PEC (concentrated light) based electrochemical ammonia synthesis

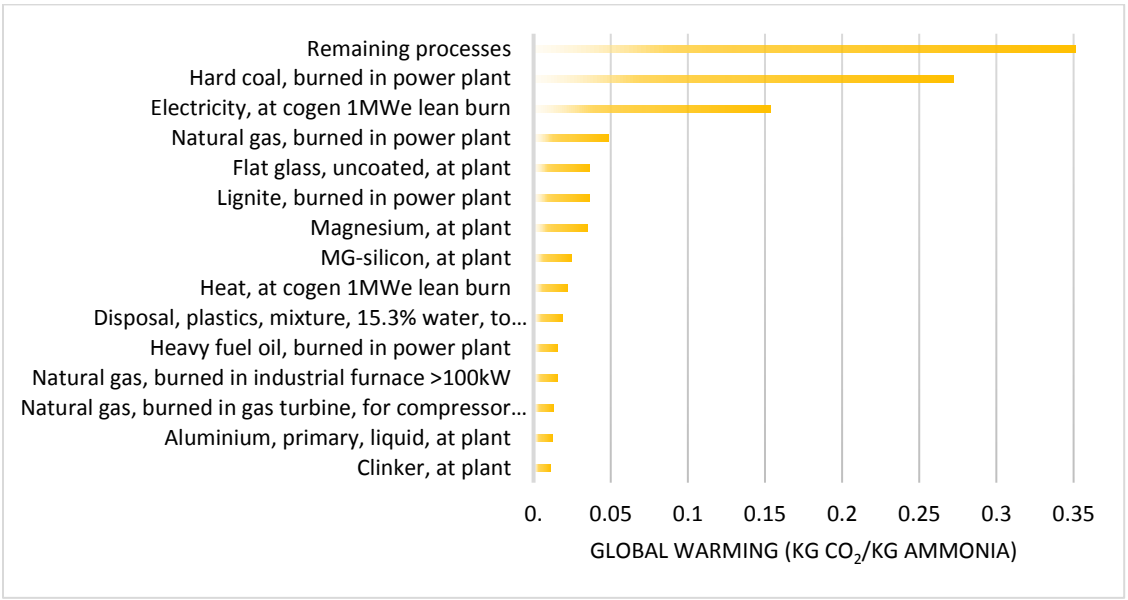

Figure 21 Contribution of various sub-processes to global warming potential of PEC (concentrated light) based electrochemical ammonia synthesis

Table 6 The shares of different sub-processes in global warming category for PEC (concentrated light) based electrochemical ammonia synthesis

Inflows	Flow	Unit
Total	100	%
Electricity, production photovoltaic, multi-Si	51.9	%
Hydrogen, PEC cell, PV, Concentrated Light-Integrated System	24.5	%
Nitrogen, gas, at plant	23.6	%
Potassium hydroxide	0.000248	%
Iron oxide	0.000143	%
Sodium hydroxide	0.000143	%

3. LCA Uncertainty Analyses Results

Defining the uncertainties within the LCA study brings more reliability of the results. The uncertainty analyses are performed in SimaPro software using Monte Carlo technique. The presented results here are only for PEC based (concentrated light) electrochemical ammonia production method using the experimental system defined in the modeling section.

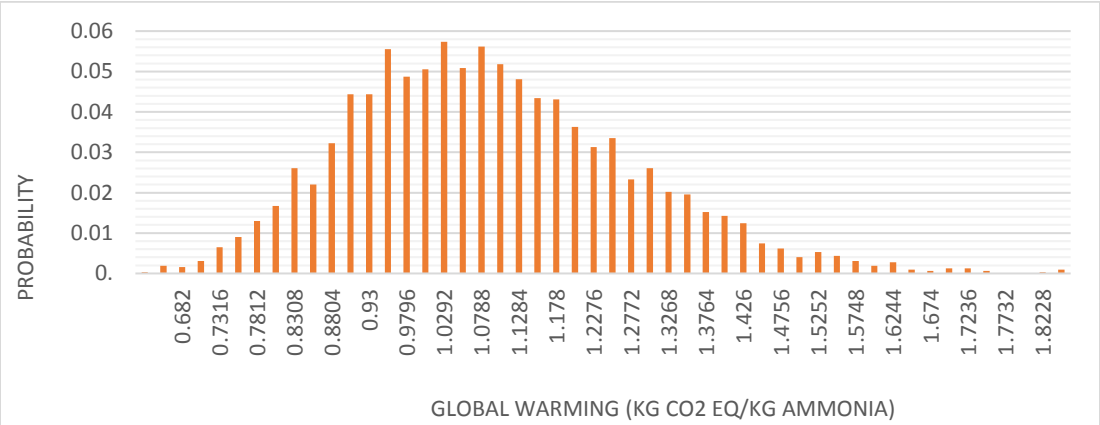

Figure 22 Probability distribution of global warming potential for PEC based (concentrated light) electrochemical ammonia production method

The confidence interval is 95% for the results. The number of runs performed for the results is 3224. The uncertainty analyses results are shown in Table 7 for the selected environmental impact categories. The mean of global warming value is 1.09 kg CO_2 eq. and standard error of mean is 0.00301 kg CO_2 eq. corresponding to 17.1% coefficient of variation which is the lowest among other categories. The highest coefficient of variance is found to be 43.9% for abiotic depletion category

Table 7 Uncertainty analyses results of PEC based (concentrated light) electrochemical ammonia production method

Impact category	Unit	Mean	Median	SD	CV (Coefficient of Variation)	97.50 %	Std.err.of mean
Abiotic depletion	kg Sb eq	0.00822	0.00746	0.00361	43.90%	0.0169	0.00773
Acidification	kg SO_2 eq	0.00637	0.00623	0.00121	19%	0.00903	0.00335
Global warming 500a	kg CO_2 eq	1.09	1.07	0.187	17.10%	1.5	0.00301
Human toxicity 500a	kg 1,4-DB eq	0.949	0.884	0.302	31.80%	1.69	0.0056
Land competition	m^2a	0.0523	0.0495	0.0167	32%	0.089	0.00564
Ozone layer depletion 40a	kg CFC-11 eq	2.75 E-07	2.63E-07	7.65E-08	27.80%	4.57 E-07	0.00489
Terrestrial ecotoxicity 500a	kg 1,4-DB eq	0.00104	0.000999	0.000269	25.70%	0.00168	0.00453

The probability distributions of the selected environmental impact categories are shown in Figs. 22 to 24.

Fig. 25 shows the comparison of uncertainty ranges for the different categories. This method is still in early investigation phase resulting in less reliable data for LCA inventory step. Taking into account the uncertainties of LCA results for PEC based electrochemical ammonia production method, this process can be more environmentally benign than other renewable routes.

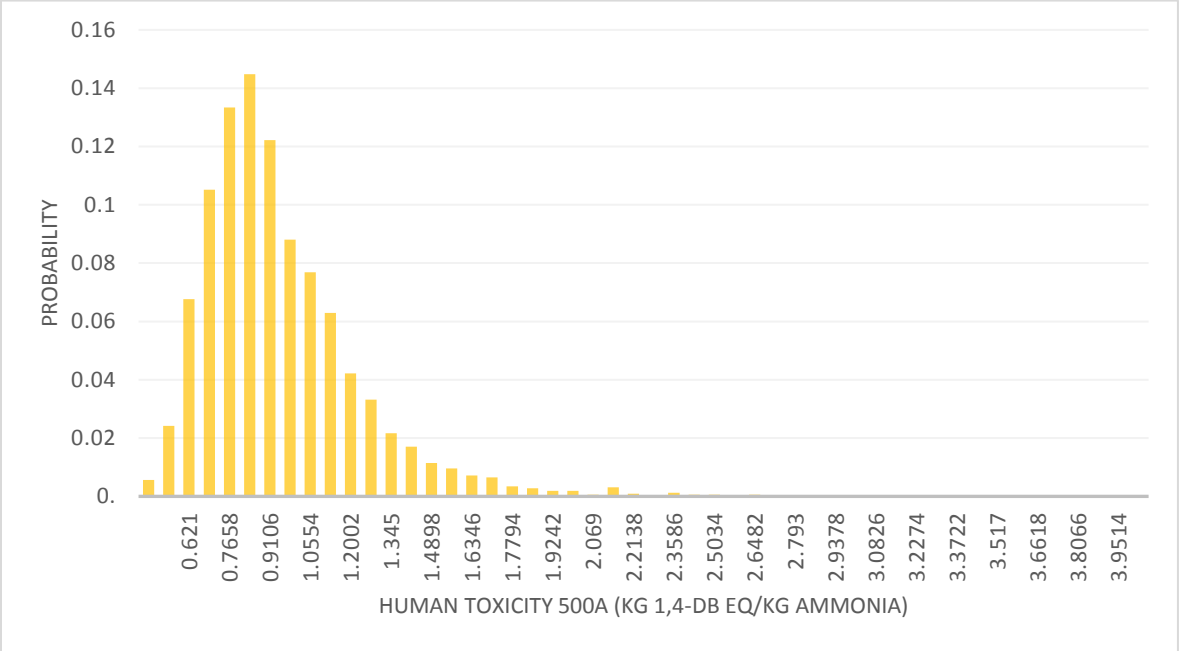

Figure 23 Probability distribution of human toxicity potential for PEC based (concentrated light) electrochemical ammonia production method

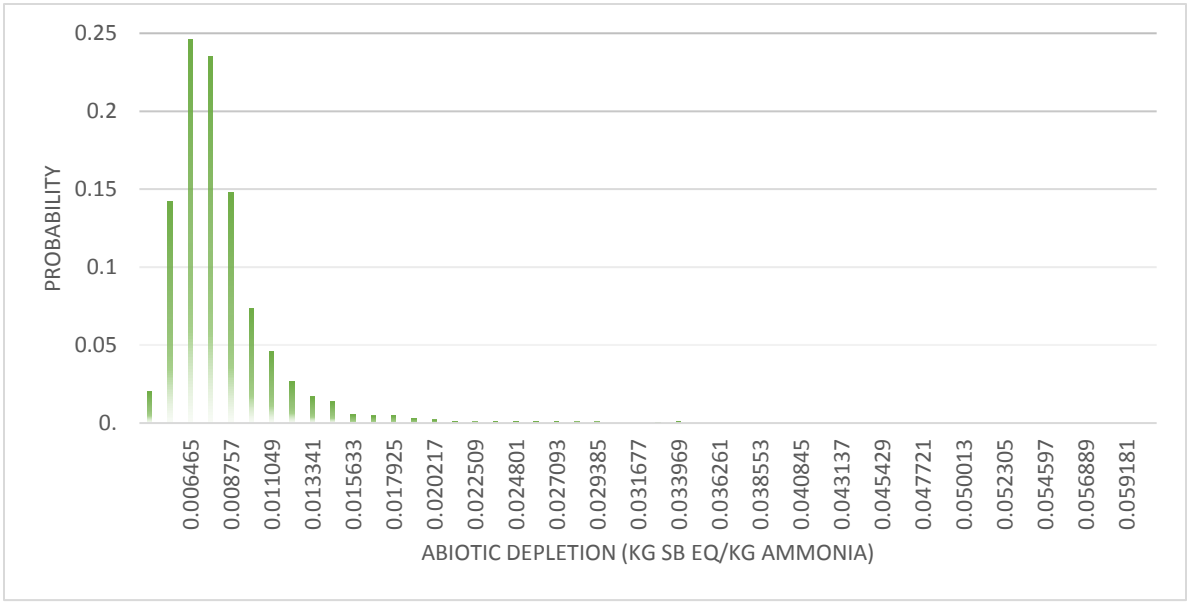

Figure 24 Probability distribution of abiotic depletion potential for PEC based (concentrated light) electrochemical ammonia production method

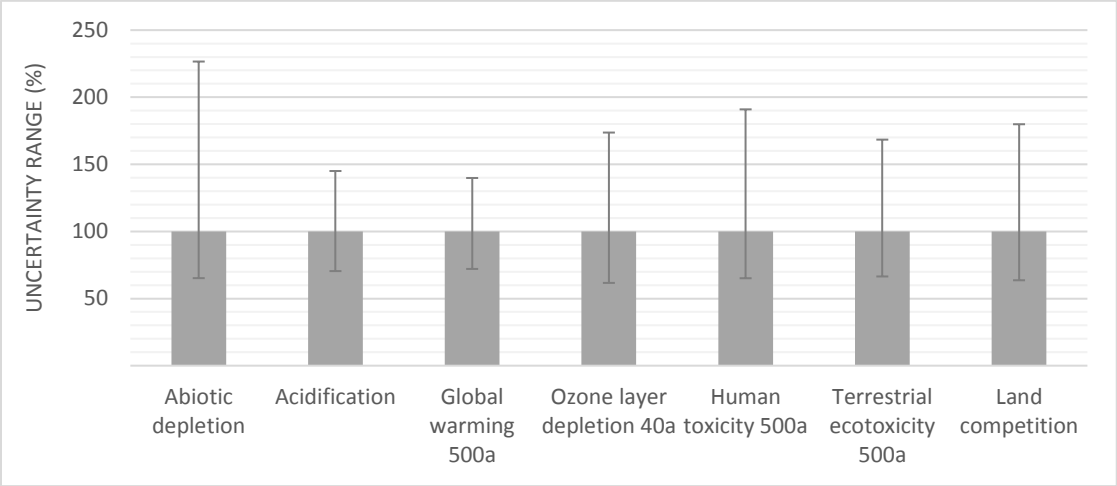

Figure 25 Uncertainty ranges of the selected impact categories for PEC based (concentrated light) electrochemical ammonia production method

4. Experimental Investigation and Analysis

PEC hydrogen generation system in this study comprises of primarily a photoelectrochemical cell with a membrane electrode assembly (Fig. 26), photovoltaic (PV) module, light source (concentrated), electricity supply and optical tools such as Fresnel lens and spectrum splitting mirrors as shown in Fig. 26. The Fresnel lens is utilized for concentrating the light. It is a periodic refractive arrangement of concentric prisms. The cathode plate is electrochemically deposited with copper oxide photosensitive material enhancing the hydrogen evolution as photocathode. In this study, the electrochemical deposition of Cu_2O onto the stainless steel cathode plate is conducted in an electrolyte solution consisting of 0.4 M $CuSO_4 \cdot 5H_2O$ and 3 M lactic acid. The solution temperature is kept constant during deposition by temperature controller where it is set to 55°C. The electrodeposition process continued about 80 minutes in total. The applied voltage for the electrodeposition process is -0.3 V vs. Ag/AgCl.

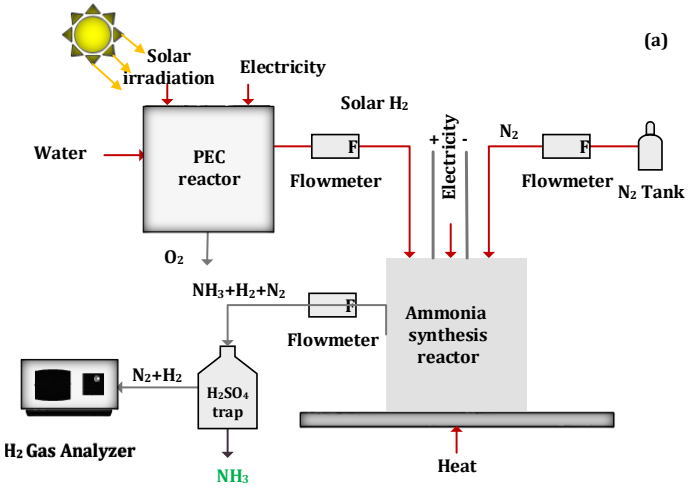

Figure 26 Experimental setup for photoelectrochemical hydrogen production integrated to ammonia synthesis

The ammonia electro-synthesis reactor comprises a nickel mesh cathode and a nickel mesh anode immersed in molten hydroxide electrolyte containing 10 g suspension of the nano-Fe_3O_4 contained in alumina crucible sealed to allow gas inlet at the cathode and gas outlet from the exit tubes as shown in Fig. 27. The reactants, H_2 and N_2, are bubbled through the mesh over the anode and cathode, respectively. The nitrogen gas flow rate is about 80 mL/min in average and hydrogen flow rate is about 10 mL/min in average during the experiments. The combined gas products (H_2, N_2 and NH_3) exit through two exit tubes in chamber head space. The exiting gases are firstly measured using flowmeters and bubbled through an ammonia water trap then analyzed for ammonia, and subsequently the NH_3 scrubbed-gas is analyzed for H_2 or N_2. The electrodes are connected externally by spot welded Ni wires.

Figure 27 The experiments under concentrated sun light for photoelectrochemical hydrogen production integrated to ammonia synthesis

5. Results and Discussion

The photoelectrochemical cell having Cu_2O coated cathode plate is tested for photoelectrochemical characterization at 1.7 V and 3 V. The obtained photocurrent densities are shown in Figs. 28 and 29 for 1.7 V and 3 V, respectively under concentrated and non-concentrated light conditions. The accumulated charges during the hydrogen production experiment at 1.7 V are calculated to be 89.9 C and 108.1 C, respectively for concentrated light and non-concentrated light. Similarly, for 3 V measurements, the accumulated charge is 555 C for concentrated light and 547 C for non-concentrated light. The maximum photocurrent densities for 1.7 V and 3 V are observed to be 0.5 mA/cm^2 and 0.25 mA/cm^2, respectively. During electrochemical ammonia synthesis, to satisfy high hydrogen production rates, the applied potential is selected to be 3 V as shown in Fig. 19. The average current and hydrogen evolution rate at 3 V are measured as 1.85 A and 14.2 mL/min and 1.82 A and 13.8 mL/min for concentrated and non-concentrated light measurements, respectively. The supplied hydrogen to the ammonia reactor is measured to be 10 mL/min in average because of possible losses in tubing. Ammonia synthesis rates increase when the molten hydroxide electrolyte is mixed with high–surface area Fe_3O_4 to provide iron as a reactive surface and when nitrogen and hydrogen are present in the reactor. The molten salt medium is supplied electricity between two nickel anode and cathode electrodes. The mixture is prepared in the beginning by simply adding NaOH and KOH pellets in the reactor. After the salts melt, nano-Fe_3O_4 is added to the electrolyte and then stirred. When the mixture is ready, the lid is tightly closed and sealed. In order to yield NH_3 in the reactor, H_2, N_2 and nano-Fe_3O_4 are simultaneously needed.

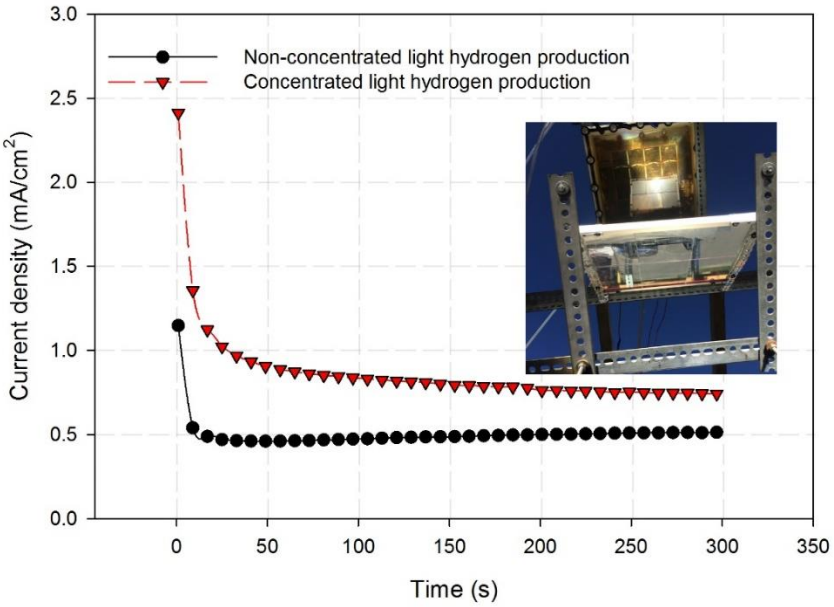

Figure 28 Photoelectrochemical hydrogen production using concentrated light and solar light splitting at 1.7 V applied potential.

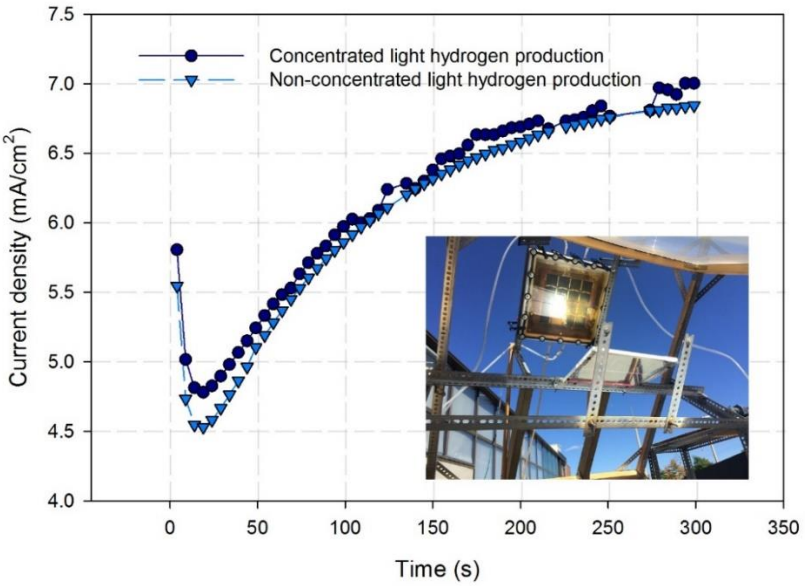

Figure 29 Photoelectrochemical hydrogen production using concentrated light and solar light splitting at 3 V applied potential during electrochemical ammonia synthesis

Table 8 tabulates the experimental conditions and yielded results for two different runs which are performed at constant current modes. Test 1 is performed at current density of 9 mA/cm^2 (0.225 A in total) and Test 2 is performed at 6.2 mA/cm^2 (0.155 A in total) current density. For Test 1, the reactor temperature is 200°C in average and for Test 2, the temperature is about 240°C. For each run, different ammonia trapping H_2SO_4 solution is used. The required cell voltage to initiate the reaction of nitrogen and hydrogen in molten hydroxide for Test 1 at 200°C in the

existence of nano-Fe_3O_4 is measured to be in average 1.75 V when the applied current is 225 mA between the 25 cm^2 Ni electrodes in the molten NaOH-KOH electrolyte.

Table 8 Summary of the experimental results showing the NH_3 formation rates and efficiencies

Parameter	Test #1	Test #2
Experiment time (s)	1000	600
Mass flow rate (g/min)	0.0001125	0.00001875
Volume flow rate (mL/min)	0.1601195	0.02668659
Mol flow rate (mol/s)	1.10×10^{-7}	1.83×10^{-8}
Reactor temperature (°C)	200°C	240°C
NH_3 production rate (mol/s cm^2)	4.41×10^{-9}	7.35×10^{-10}
Current density (mA/cm^2)	9	6.2
Voltage (V)	1.75	1.2
Current (A)	0.225	0.155
Coulombic Efficiency (%)	14.17	3.43
Energy Efficiency (%)	5.50	2.45

The potential decreases to 1.2 V when the current density is to 6.2 mA/cm^2 at 240°C. In Test 1, ammonia is synthesized at a rate of 4.41×10^{-9} mol/s cm^2 whereas in Test 2, the ammonia evolution rate decreased to 7.35×10^{-10} mol NH_3/s cm^2. NH_3 is generated at a coulombic efficiency of about 14.2% at 9 mA/cm2, which declines to about 3.4% at 6.2 mA/cm^2 at 240°C. Constant current electrochemical ammonia synthesis at different applied current densities and temperature are comparatively shown in Fig. 30.

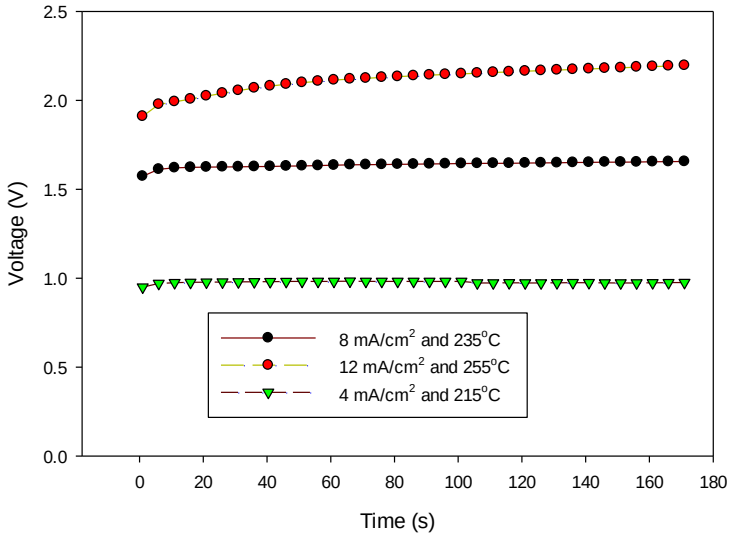

Figure 30 The relationship between voltage and time during several experimental runs at different applied currents and temperatures for electrochemical synthesis of NH_3 using N_2 and H_2 with nano-Fe_3O_4 in a molten salt hydroxide electrolyte

It is also observed in the experiments that even though the reactor temperature is below 200°C, ammonia is generated with a similar production rate to above 200°C. The potential gradually declines from 2.1 V to 1 V for the applied current densities from 12 mA/cm^2 to 4

mA/cm^2. It is observed in the experiments that lower current density and lower temperature improve the stability of the rate of NH_3 evolution.

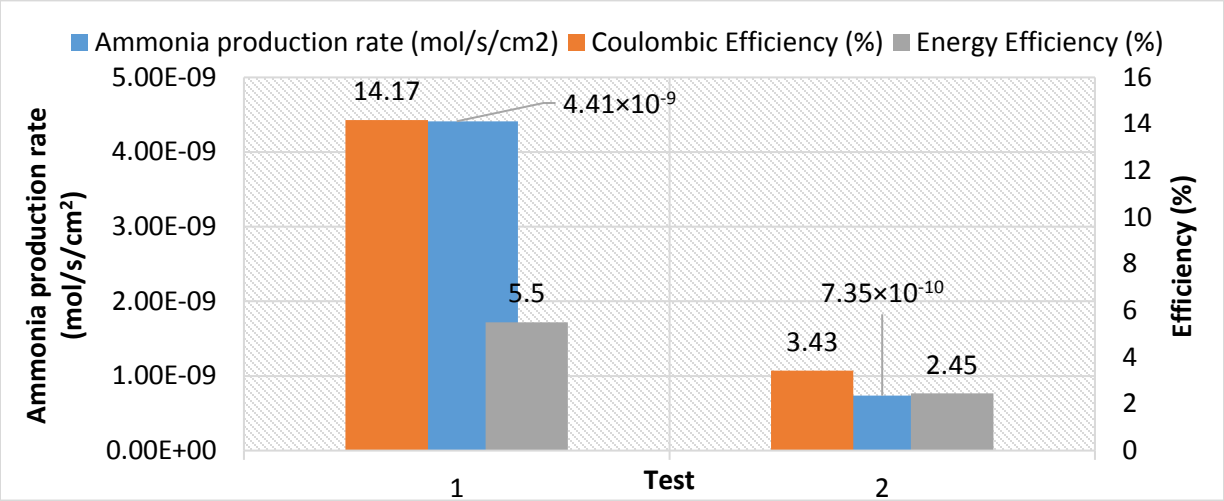

Figure 31 Coulombic and energy efficiencies of two experimental runs for electrochemical NH_3 synthesis using N_2 and H_2 with nano-Fe_3O_4 in a molten salt hydroxide electrolyte.

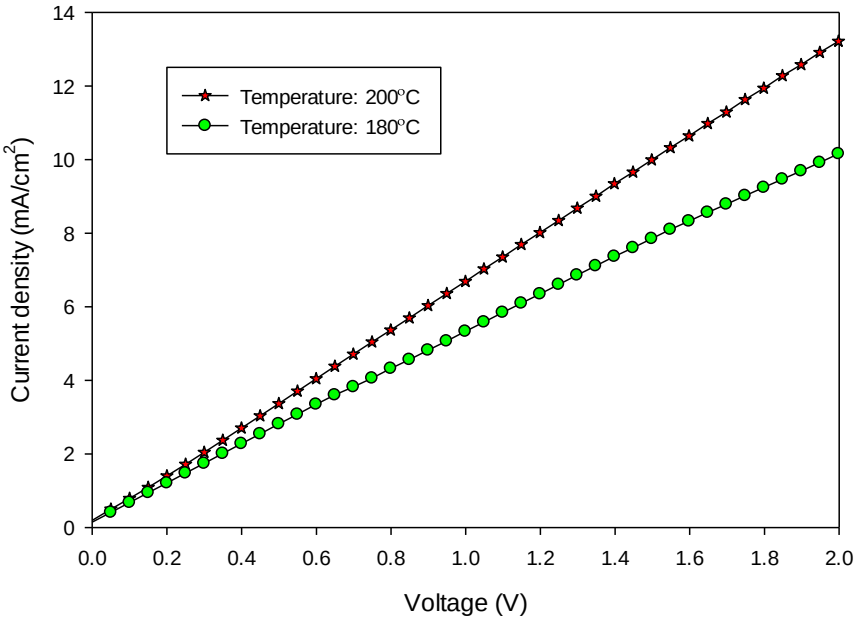

Figure 32 Applied potential-current density relations at 200°C and 180°C for electrochemical NH_3 formation using N_2 and H_2 with nano-Fe_3O_4 in a molten salt hydroxide electrolyte

The measured coulombic and energetic efficiencies of ammonia evolution in time at different temperature levels and conditions in NaOH-KOH molten electrolyte are comparatively illustrated in Fig. 31. The conversion efficiency is not only dependent on the hydrogen amount but also amount of catalyst available to stimulate the conversion of N_2 and H_2 into NH_3. The greater ammonia generation rate at lower voltages can be because of the lower hydrogen ion stream at the

cathode which provides more time for generation of ammonia according to reaction. Higher NH_3 synthesis rates are obtained for Test 1 as illustrated in Fig.31. In addition, the coulombic efficiency is higher for Test 1. At higher current density of 9 mA/cm^2, the NH_3 formation rate yields about 4.41×10^{-9} mol/s cm^2. In order to understand the current-voltage characteristics at lower temperature levels such as 180°C and 200°C , linear sweep voltagram of between 0 V and 2 V as shown in Fig. 32. At 200°C and 1.2 V, the obtained current density is 8 mA/cm^2 whereas it is about 6.1 mA/cm^2 at 180°C. Hence, higher temperatures lowers the required voltage at constant supplied current.

6. Concluding Remarks

Hydrogen and ammonia are two of the most significant clean fuels in the near future. Production of these chemicals are desired to be environmentally friendly. Here, electrochemical synthesis of NH_3 is achieved using photoelectrochemical hydrogen. This method appears to be a potential alternative to conventional energy intensive NH_3 production plants especially for on-site ammonia production. The use of renewable energy resources to promote the electrochemical synthesis of NH_3, the carbon footprint of the current NH_3 production industry can be significantly reduced. The electrochemical synthesis pathways offer a high potential for NH_3 production to separate and distribute a carbon-free fuel for the various sectors. Copper oxide is electrodeposited to have photocathode. NH_3 is electrochemically generated at ambient pressure using photoelectrochemical H_2 in a molten hydroxide medium with nano-Fe_3O_4 catalyst. The reaction temperature is varied in the range of 180°C to 260°C to investigate the impact of temperature on NH_3 production rates. The maximum coulombic efficiency is calculated as 14.17 % corresponding to NH_3 formation rate of 4.41×10^{-9} mol/s cm^2. It is expected that possible problems in the electrochemical synthesis of NH_3 based on liquid electrolytes are further improved by the addition of suitable additives, optimization of the reactor configuration and more resistive materials.

CHAPTER 4:FROM HYDROCARBONS TO AMMONIA

The decarbonisation of fossil fuels, particularly, natural gas, is a promising alternative and compromises definite benefits over the use of carbon capture storage (CCS) technologies. Methane decarbonisation by pyrolysis also called as methane cracking includes the dissociation of methane (CH_4) into its molecular particles: solid carbon (C) and hydrogen (H_2). Its key benefit lies in the lack of CO/CO_2 emissions. Conversely to CCS, it substitutes the managing of CO_2 with a much lower quantity of easier-to-handle solid carbon. Hydrogen signifies a significant clean energy carrier, with an already substantial demand and capable projections for the future energy system. Moreover, carbon is hypothetically marketable as a product for both current and envisaged usages such as carbon fibres, materials and nanotechnology.

1. Natural Gas to Ammonia

Compared to natural gas, there are more environmentally friendly fuels such as ammonia. Ammonia does not emit direct greenhouse gas emissions when utilized in the vehicles. Furthermore, production process of ammonia yields lower environmental impacts compared to natural gas production. Ammonia, which is a sustainable and clean fuel, can also be produced from natural gas and hydrocarbons. Henceforth, in the ideal case, if stranded natural gas reserves can be converted into ammonia and then transported via pipelines/trucks/ocean tankers to the ports, it would have lower total environmental impact both in the production process and utilization process. Furthermore, ammonia is liquid at higher temperatures (-33°C) than natural gas (-162°C) which implies lower energy requirement in liquefaction process of natural gas.

The other option for a more environmentally friendly process can be conversion of LNG to ammonia after being produced and transported via pipelines. Natural gas can be cracked into carbon black and hydrogen using hydrocarbon disassociation technique. In this case, carbon black is also utilized as a useful output for tire, plastic etc. industry. Instead of emitting CO_2 to the environment, produced carbon black is used for various sectors, and greenhouse gas emissions are lowered. Produced hydrogen can be used for ammonia synthesis and stored in the vessels for the overseas transportation. In this manner, a cleaner alternative fuel is consumed and total greenhouse gas emissions are significantly decreased. Ammonia can be produced from any hydrogen including hydrocarbons using cracking of hydrocarbons into hydrogen and carbon. Methane is a favored option for hydrogen production from a hydrocarbon because of its high H to C ratio, availability and low cost. Furthermore, microwave disassociation of methane is a promising option for cleaner ammonia production. Methane is separated into carbon black and hydrogen. The carbon produced can be sold as a co-product into the carbon black market which could be utilized in inks, paints, tires, batteries, etc. or sequestered, stored, and used as a clean fuel for electricity production. The sequestering or storing of solid carbon requires much less development than sequestering gaseous CO_2. Ammonia can also be produced from steam reforming of methane which is a little more energy intensive method. Steam methane reforming is the conversion of methane and water vapor into hydrogen and carbon monoxide which is an endothermic reaction. The heat can be supplied from the combustion of the methane feed gas. The process temperature and pressure values are generally 700°C to 850°C and pressures of 3 to 25 bar, respectively.

There are several technological options for methane dissociation to hydrogen and carbon, which are summarized in Fig. 33. Natural gas power plant electricity can be utilized in ammonia production process from natural gas as it is illustrated in Fig. 34. Produced ammonia can be used in power plants, vehicles and also household furnaces.

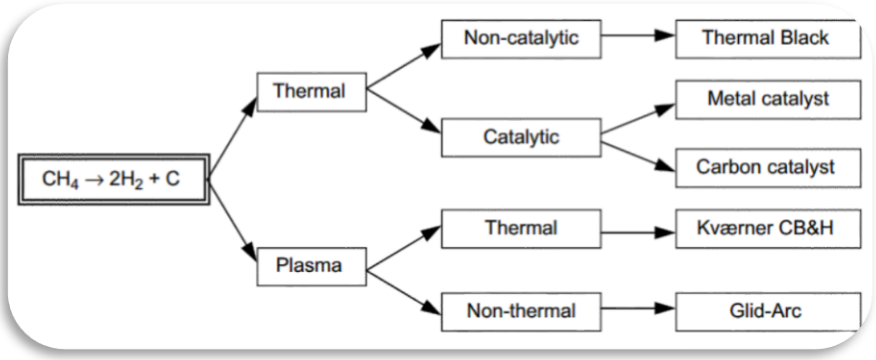

Figure 33 Main routes for decomposition of methane to hydrogen and carbon (modified from [44])

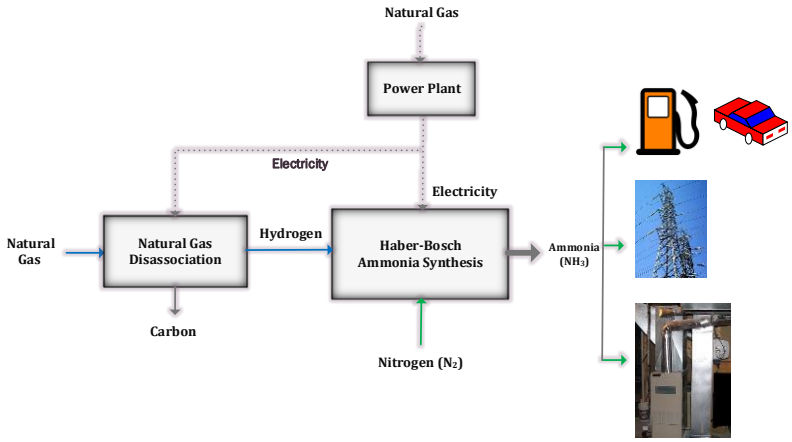

Figure 34 Schematic diagram of ammonia production from natural gas and alternative utilization options

The following Fig. 35 shows an integrated plant for ammonia and urea production which utilizes the captured CO_2 for urea production.

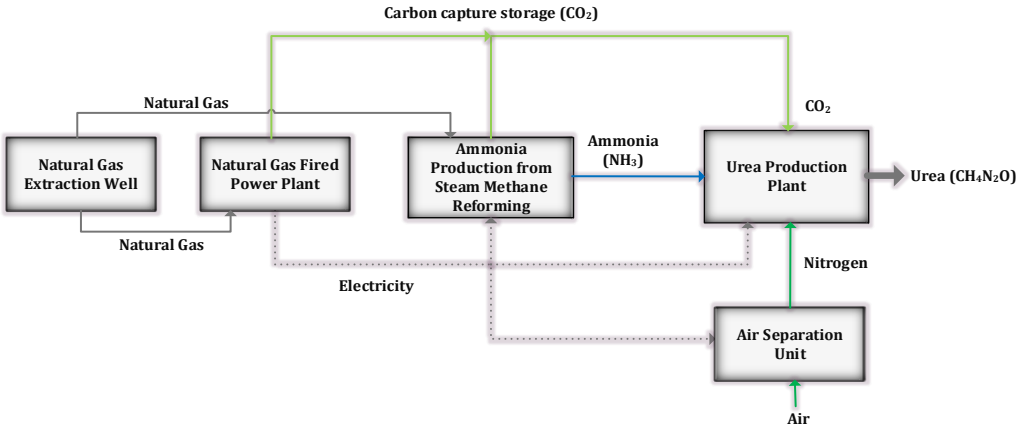

Figure 35 Illustration of ammonia and urea production from natural gas

The efficiency and CO_2 emissions from steam methane reforming, coal gasification and methane pyrolysis are comparatively shown in Table 9. Using CCS technology with steam methane reforming decreases the efficiency down to 54% which is quite similar to methane pyrolysis method. For the microwave dissociation of hydrocarbons for ammonia production, it is seen that the microwave energy may be of sufficient power and duration to cause microwave depolymerization of the high molecular weight materials such as bitumen. Microwave energy is environmentally friendly since it has no harmful effect during hydrocarbon cracking process.

Table 9 Comparison of hydrogen production technologies from fossil-fuels

Process	**Methane steam reforming**	**Coal gasification**	**Methane pyrolysis**
Reaction Heat of reaction (kJ/mol-H_2)	$CH_4+2H_2O \rightarrow CO_2+ 4H_2$ 63.25	$Coal+2H_2O \rightarrow CO_2+ 2H_2$ 89.08	$CH_4 \rightarrow C + 2H_2$ 37.43
Energy efficiency in transformation (%)	74	60	55
Energy efficiency with CCS (%)	54	43	55
CO_2 emission (mol-CO_2/mol-H_2)	0.34	0.83	0.05
Carbon production (mol-C/mol-H_2)	0	0	0.5

It is also remarkable to explain the life cycle emissions comparatively. Production of natural gas from various locations yield higher ozone layer depletion values as seen in Fig. 36. Production of fuel ammonia yields lower acidification values compared to petrol and natural gas production as shown in Fig. 37.

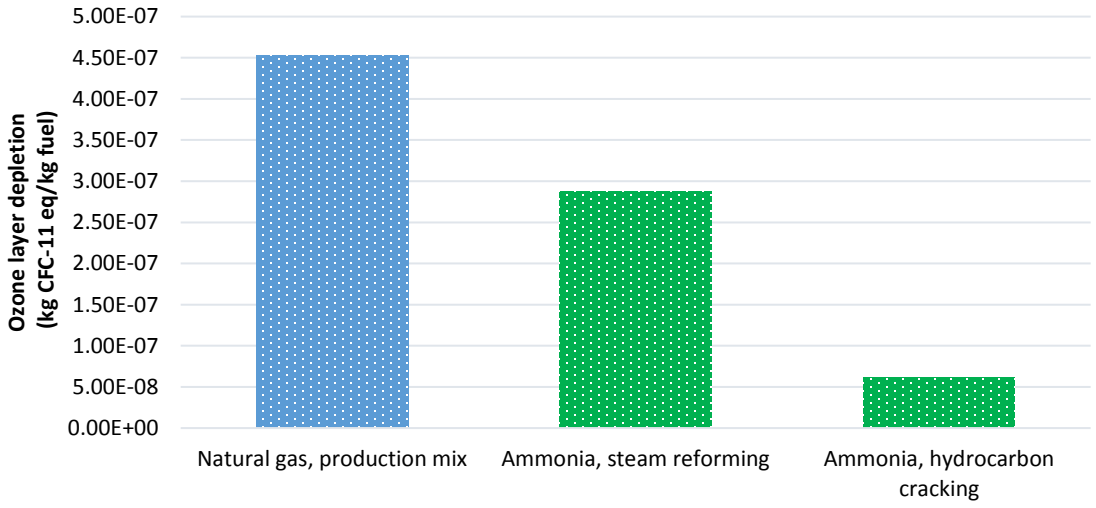

Figure 36 Ozone depletion values during production of one kg of ammonia and natural gas

Fig. 38 shows the comparative cost of ammonia production from renewable and conventional resources. Currently, steam methane reforming is the dominant method of production. However, as seen in the figure, hydrocarbon dissociation yields lower costs than low cost hydropower option and steam methane reforming method. Furthermore, hydrocarbon dissociation also produces carbon black which is a commercial commodity in the market. For example, per each kg of ammonia produced, about 0.5 kg of carbon black can be obtained from methane dissociation. If the price of carbon black is assumed to be 1 US$/kg in the market, the cost of ammonia for the hydrocarbon dissociation scenario decreases down to 0.17 US$/kg.

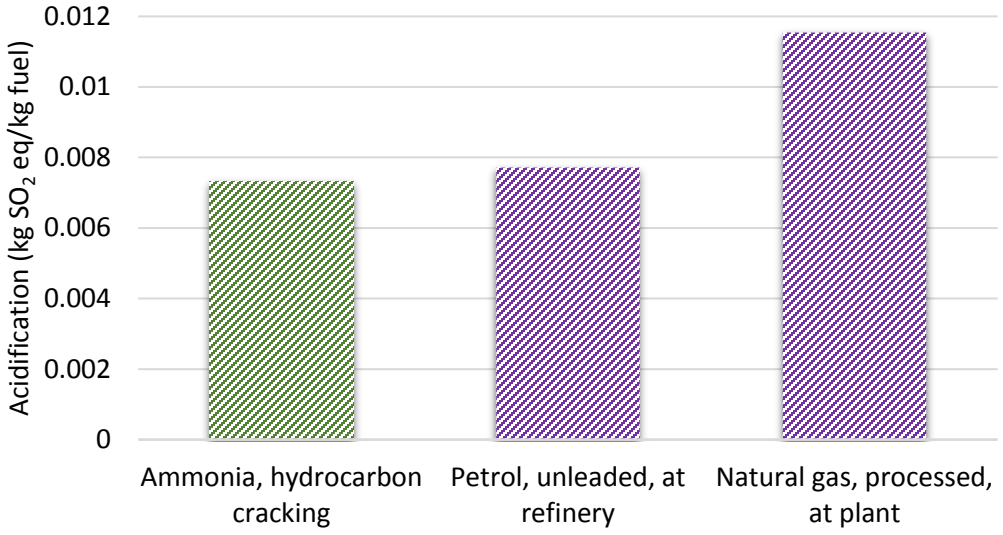

Figure 37 Acidification values of ammonia, natural gas and petrol during one kg fuel production process

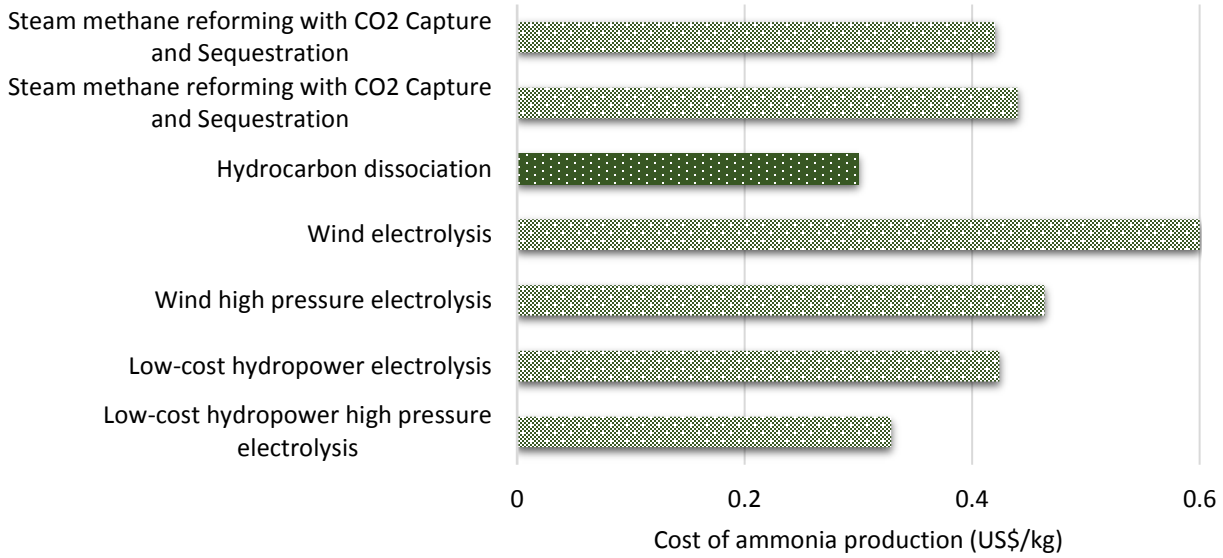

Figure 38 Comparison of cost of production for ammonia using various routes

Fig. 39 compares the total greenhouse gas emissions during production of 1 MJ energy from various resources including gasoline, LPG, diesel, natural gas and ammonia. Production of 1 MJ energy from ammonia has lower emissions than gasoline, LPG, diesel and natural gas.

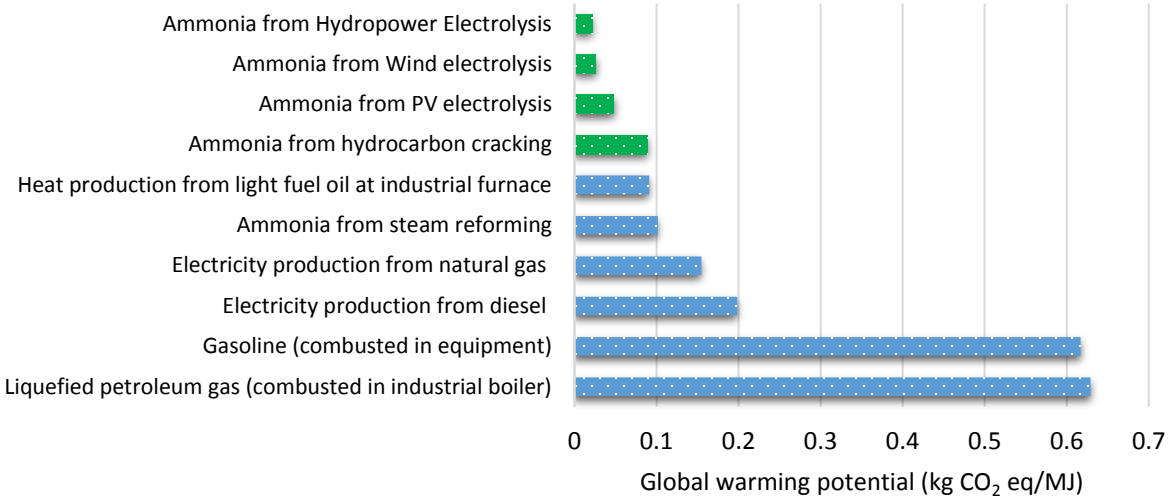

Figure 39 Comparison of global warming potential of 1 MJ energy production from various resources

2. Transport of Natural Gas or Ammonia

Much of this natural gas is considered "stranded" as it is located in regions distant from consuming markets. Liquefying natural gas and shipping it overseas provides an opportunity for these regions to economically develop their natural gas reserves. As unconventional gas production increases, the U.S. is becoming increasingly self-sufficient with respect to natural gas. Pipeline exports from Canada to the U.S. are decreasing. With plenty unconventional resources, industry is shifting its focus from importing LNG into North America to exporting LNG from North America. The export of LNG could facilitate Canadian natural gas production growth and result in significant investment, jobs and economic growth.

LNG is primarily composed of Methane (85.6% – 96.6%), Ethane (3.2% – 8.5%), and Propane (0.0% – 3.0%). The transportation of liquefied natural gas (LNG) refers to any movement or shipping of natural gas while in its liquid form. The two major methods of transporting LNG are by pipeline and vessel. As LNG requires a temperature of -160°C to remain in its liquid form, significant insulation must be incorporated into LNG pipelines in order to maintain this low temperature and ensure no re-gasification occurs. This normally includes a combination of mechanical insulation, for example glass foam and a vacuum layer. This complex insulation system makes LNG pipelines significantly more difficult and expensive to manufacture than standard natural gas pipelines [45].

Figure 40 LNG transport processes

Interconnected elements shown in Fig. 40 include the gas field, liquefaction plant, LNG storage tank, LNG tanker, LNG storage tank, vaporizers, and pipeline systems. In LNG exporting countries, natural gas is extracted from basins and transported by pipeline to liquefaction plants. There, the natural gas is liquefied and stored. The majority of worldwide LNG exports take place at an intercontinental level, meaning that shipping LNG across the ocean is often required. This is done with the use of an LNG vessel, which transports large quantities of LNG between export and import terminals. Several types of LNG vessels exist in the industry today, with the main one being referred to as an LNG tanker. The main components of an LNG tanker are the boiler and pump rooms, a double hull for added strength, bow thrusters, and the LNG storage tanks themselves. Typically, an LNG tanker is built with 4 or 5 individual LNG tanks, as seen in Fig. 41.

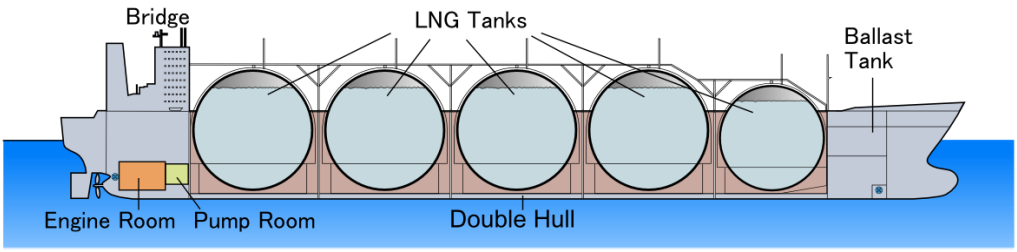

Figure 41 Illustration of an LNG tanker (adapted from [45])

Ammonia tankers are typically refrigerated ships. In addition to ammonia, they can usually transport liquefied propane gas (LPG), propylene, vinyl chloride monomer and other condensable gases. Capacities more than 84,000 m^3 are available. On the other hand, a typical LNG tanker can carry around 160,000 m^3 of natural gas on a single voyage. Ammonia is a more suitable energy carrier to be transported overseas because it is liquid at higher temperatures and require less cooling compared to natural gas.

3. Case Studies for LNG and Ammonia

Natural gas liquefaction costs include:

- liquefaction costs of about US$3.00/MMBTU,
- shipping/fuel costs of about $1.50-$3.50/MMBTU,
- the cost of the gas at about $4.00/MMBTU in a low cost region

Therefore, the total delivered cost corresponds to about $8.50-$10.50/MMBTU relative to a market price of about $12-$15/MMBTU in Europe and Asia based on $100/barrel crude oil as gas in Europe and Asia is typically priced at 11-15% of the price of crude on an energy equivalent basis [46]. The natural gas prices are also derived from another report prepared by International Gas Union [47].

Ammonia distribution costs are considered to be similar to LPG costs. The LPG is kept at approximately -48°C, which is below the boiling point of LPG (propane), which is -42°C. Ammonia distribution would require additional safety equipment, but there are likely to be cost reductions if ammonia were distributed on scales approaching those of current gasoline/LNG distribution. Hence, it seems reasonable to assume that these effects would offset each other, yielding similar costs. A study estimates LPG distribution costs to be around $0.36 to $0.55 per gasoline gallon equivalent (gge), including retail margins. Converting the $0.36/gge cost of distribution equates to approximately $0.62/kg H_2 when distributed as anhydrous ammonia [48]. Here, we employ different cases based on the production cost of ammonia and LNG. For steam

methane reforming based ammonia production, the natural gas cost represents almost 58% of the total ammonia cost as shown in Fig. 42. Therefore, it is highly dependent on natural gas market price. The production cost of natural gas includes the extraction and processing.

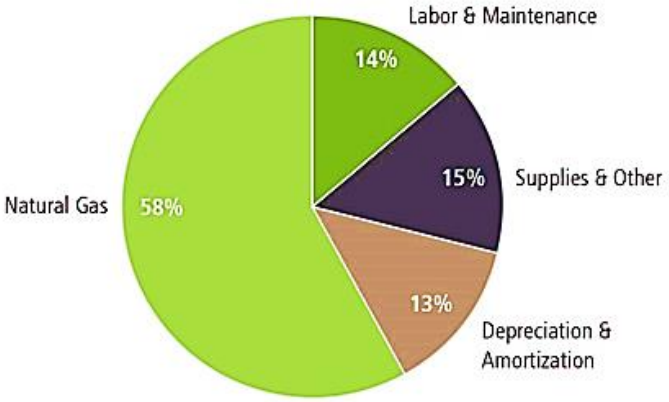

Figure 42 Cost contributions for natural gas based ammonia production plant (adapted from [49])

Case 1: Europe

In this case, ammonia is considered to be produced with a unit cost of 0.44 US$/kg [50,51]. The LNG prices are converted to kg and MJ for comparison purposes as shown in Table 10. For the conversions, 1 MMBTU corresponds to about 1055 MJ. The lower heating value of the LNG is taken as 49.4 MJ/kg [52]. The production cost is cost of gas at the liquefaction plant. After the liquefaction process, the LNG is loaded on the tankers and transported overseas. At the arrival port or plant, the LNG is regasified to be used which is an additional cost. This case represents the average natural gas and ammonia prices in Europe as the illustration of the case is shown in Fig. 43.

Table 10 Unit cost of LNG including the sub-processes for Case 1

LNG	**US$/MMBTU**	**US$/MJ**	**US$/kg**
Production	4.4000	0.0042	0.2060
Liquefaction	3.2000	0.0030	0.1498
Transport	4.1000	0.0039	0.1920
Regasification	0.3500	0.0003	0.0164
TOTAL	12.0500	0.0114	0.5642

The total cost of ammonia and LNG are comparatively evaluated in Table 11 and Fig. 44. The selected ammonia production route is steam methane reforming which receives natural gas as the feedstock. The production plant of ammonia and LNG are assumed to be in the same location and has a distance of 100 km to the port. The land transportation cost of ammonia is calculated based on the average costs per km where a truck's payload capacity is 16 tonne. The truck transportation cost values are taken from the report [53]. Although, there are alternative ways for the transport of ammonia such as pipelines, since there is no ammonia pipeline infrastructure at the moment in Canada, truck transportation is taken into account. It is assumed that 16 tonne liquid fuel can be carried per truck for both fuels. Here, the storage costs of these liquid fuels are not taken into account since they are considered to be transported after the production.

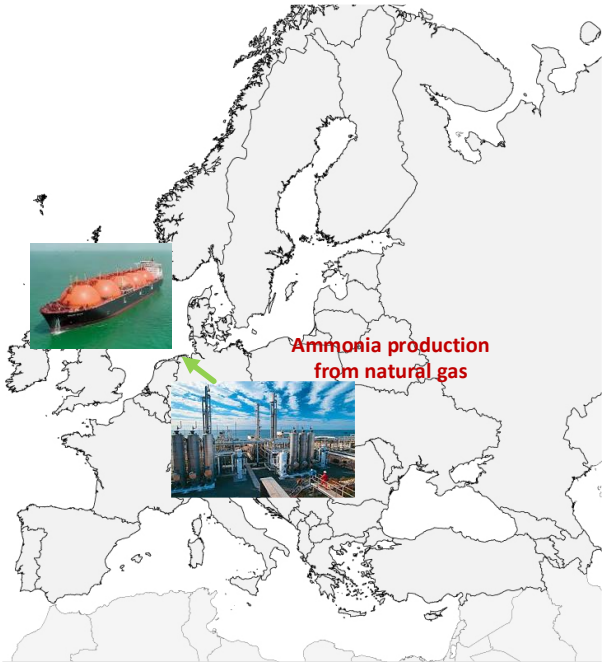

Figure 43 Illustration of the Case 1 for Europe

Table 11 Total unit cost of ammonia and LNG considering production, liquefaction and transport for Case 1

Cost contribution	LNG	AMMONIA
Production cost (US$/kg)	0.206	0.440
Liquefaction cost (US$/kg)	0.149	0
Regasification cost (US$/kg)	0.016	0
Land transportation cost (US$/kg)	0.012	0.012
Tanker overseas transportations cost (US$/kg)	0.191	0.109
Total cost (US$/kg)	0.576	0.562
Total cost (US$/MJ)	0.011	0.030

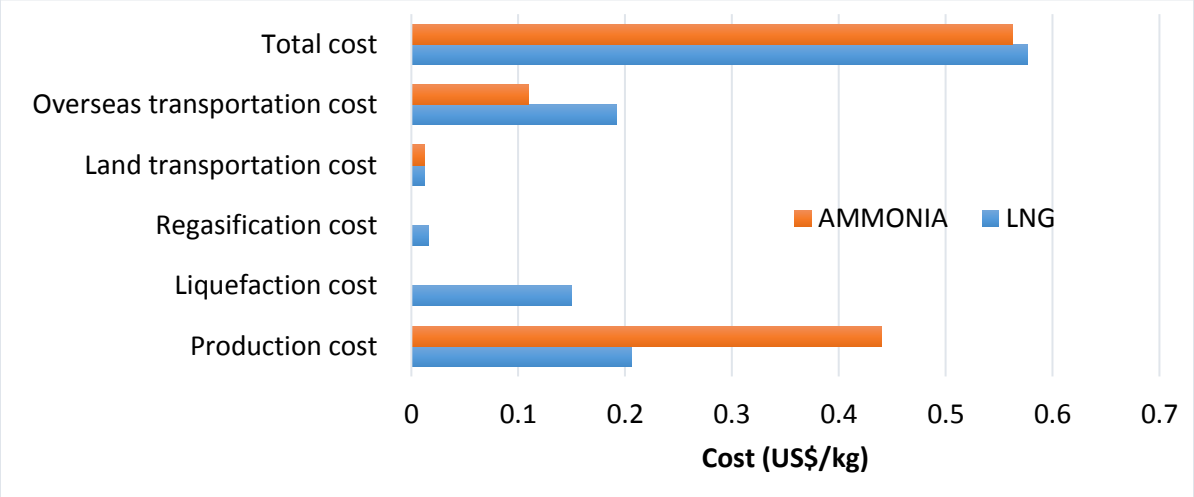

Figure 44 Contribution of sub-processes to total cost of LNG and ammonia for Case 1 in Europe

As shown in Fig. 44, the cost of ammonia at the destination port is slightly lower than LNG although the production cost of ammonia is higher than LNG. Since ammonia is liquid at the production plant, there is no need for additional liquefaction. In addition, regasification cost is neglected for ammonia.

Case 2: U.S

In this case, the production cost of ammonia is taken lower corresponding to 0.22 $/kg [50,51]. The LNG prices are converted to kg and MJ for comparison purposes as shown in Table 12.

Table 12 Unit cost of LNG including the sub-processes for Case 2

LNG	US$/MMBTU	US$/MJ	US$/kg
Production	3.8	0.0036	0.1779
Liquefaction	2	0.0019	0.0936
Transport	3	0.0028	0.1405
Regasification	0.3	0.0003	0.0140
TOTAL	9.1	0.0086	0.4261

The total cost of ammonia and LNG are comparatively evaluated in Table 13 and Fig. 45. The selected ammonia production route is steam methane reforming which receives natural gas as the feedstock. The production plant of ammonia and LNG are assumed to be in the same location and has a distance of 200 km to the port. This case represents the average natural gas and ammonia prices in the U.S. as the illustration of the case is shown in Fig. 46.

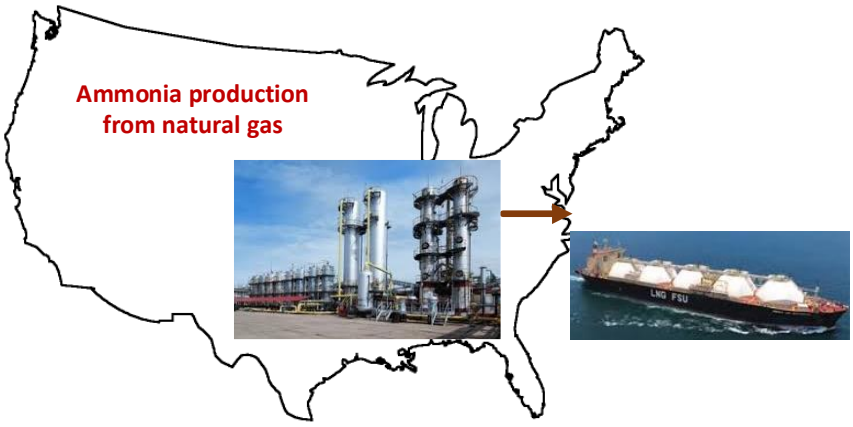

Figure 45 Illustration of the Case 2 for the U.S

As shown in Fig. 46, the cost of ammonia at the destination port is considerably lower than LNG although the production cost of ammonia is slightly higher than LNG. The difference is mainly caused by the liquefaction and regasification processes required for LNG. Because the boiling temperature of LNG is very low compared to ammonia.

Table 13 Total unit cost of ammonia and LNG considering production, liquefaction and transport for Case 2

Cost contribution	LNG	AMMONIA
Production cost (US$/kg)	0.178	0.220
Liquefaction cost (US$/kg)	0.094	0
Regasification cost (US$/kg)	0.014	0
Land transportation cost (US$/kg)	0.025	0.025
Tanker overseas transportations cost (US$/kg)	0.140	0.110
Total cost (US$/kg)	0.451	0.355
Total cost (US$/MJ)	0.009	0.019

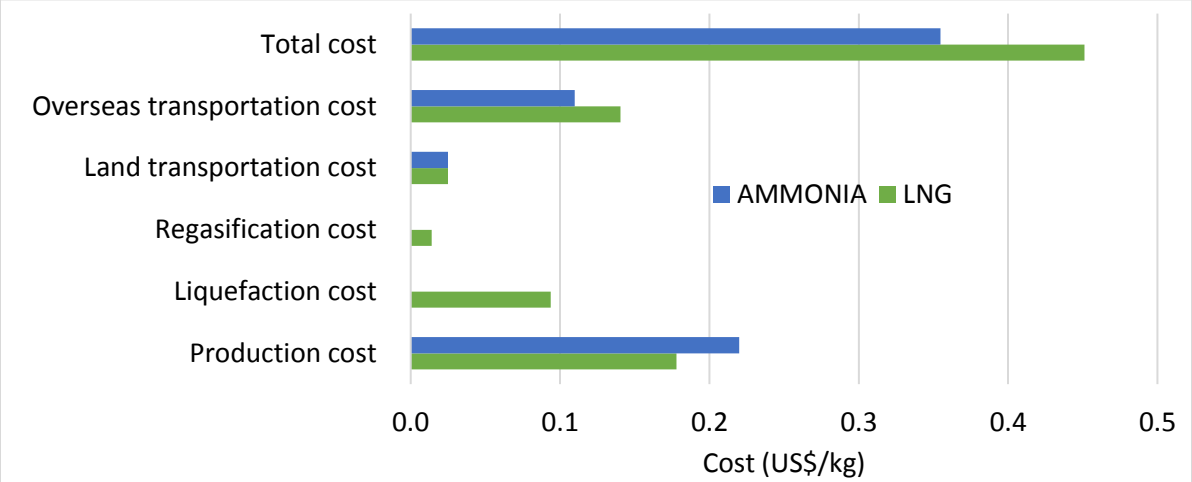

Figure 46 Contribution of sub-processes to total cost of LNG and ammonia for Case 2 in the U.S

Case 3: Middle East

In this case, the production cost of ammonia is taken lower corresponding to 0.1 $/kg [50,51]. The LNG prices are converted to kg and MJ for comparison purposes as shown in Table 14. The cost of natural gas and ammonia in Middle East is lower than other continents. This case represents the average natural gas and ammonia prices in the Middle East as the illustration of the case is shown in Fig. 47.

Table 14 Unit cost of LNG including the sub-processes for Case 3

LNG	**US$/MMBTU**	**US$/MJ**	**US$/kg**
Production	2	0.0019	0.0936
Liquefaction	1.5	0.0014	0.0702
Transport	1.5	0.0014	0.0702
Regasification	0.3	0.0003	0.0140
TOTAL	5.3	0.0050	0.2482

The total cost of ammonia and LNG are comparatively evaluated in Table 15 and Fig. 48. The selected ammonia production route is steam methane reforming which receives natural gas as the

feedstock. The production plant of ammonia and LNG are assumed to be in the same location and has a distance of 300 km to the port.

Figure 47 Illustration of the Case 3 for Middle East

Table 15 Total unit cost of ammonia and LNG considering production, liquefaction and transport for Case 3

Cost contribution	LNG	AMMONIA
Production cost (US$/kg)	0.094	0.100
Liquefaction cost (US$/kg)	0.070	0.000
Regasification cost (US$/kg)	0.014	0.000
Land transportation cost (US$/kg)	0.038	0.038
Tanker overseas transportations cost (US$/kg)	0.070	0.110
Total cost (US$/kg)	0.286	0.247
Total cost (US$/MJ)	0.006	0.013

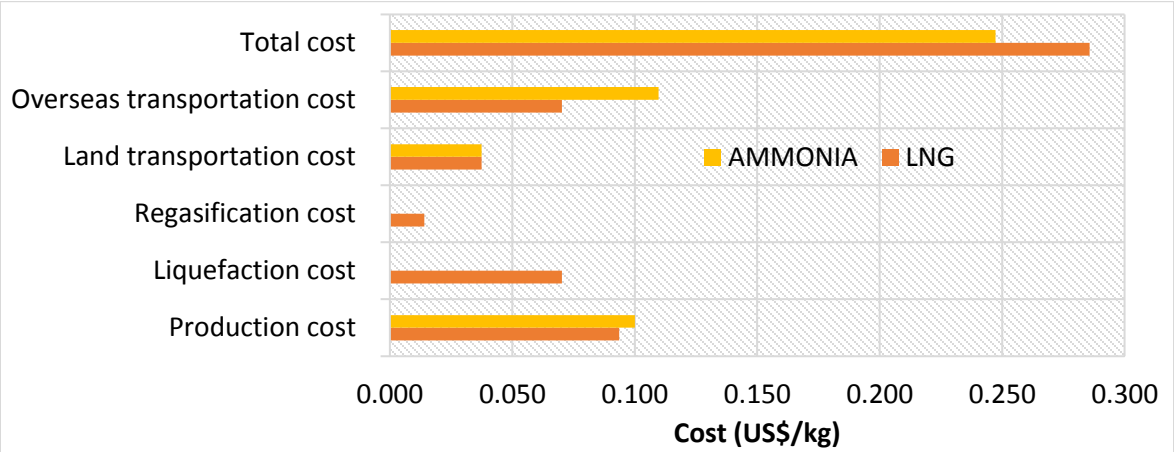

Figure 48 Contribution of sub-processes to total cost of LNG and ammonia for Case 3 in Middle East

As illustrated in Fig. 48, the cost of ammonia at the destination port is 0.04 $/kg lower than LNG. The low cost of natural gas is mainly due the massive resources available in the Middle East. This yields lower costs of liquid ammonia and LNG.

Case 4: Ontario, Canada

In this case, the production cost of ammonia is taken as 0.25 $/kg [50,51]. The LNG prices are converted to kg and MJ for comparison purposes as shown in Table 16. The cost of natural gas is quite low compared to Europe however higher than Middle East. The illustration of the case is shown in Fig. 49.

Table 16 Unit cost of LNG including the sub-processes for Case 4

LNG	US$/MMBTU	US$/MJ	US$/kg
Production	2.1	0.0020	0.0983
Liquefaction	3.0	0.0028	0.1405
Transport	2.5	0.0024	0.1171
Regasification	0.3	0.0003	0.0140
TOTAL	7.9	0.0075	0.3699

The total cost of ammonia and LNG are comparatively evaluated in Table 17 and Fig. 50. The selected ammonia production route is steam methane reforming which receives natural gas as the feedstock. The production plant of ammonia and LNG are assumed to be in the same location (nearby Toronto) and has a distance of about 800 km to the port in Quebec. This case represents the average natural gas and ammonia prices in the Canada

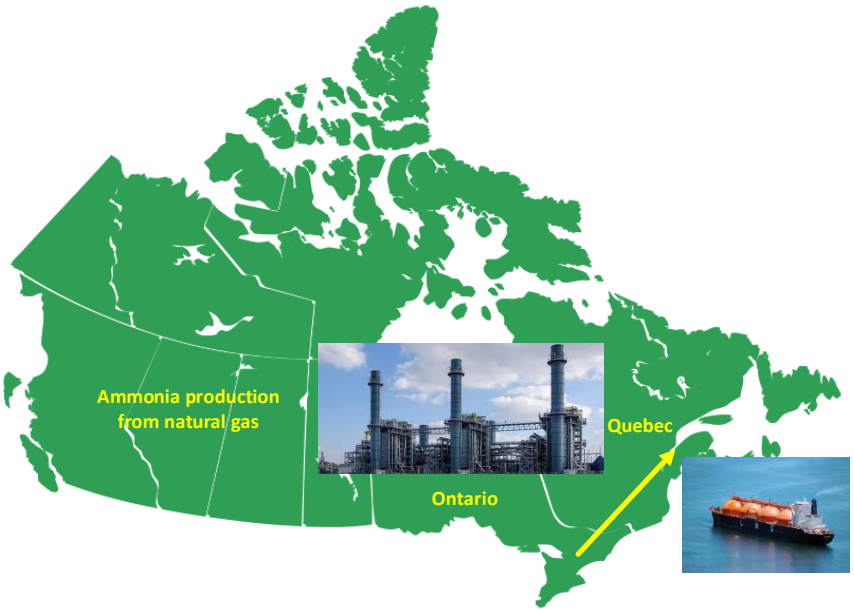

Figure 49 Illustration of the Case 4 for Ontario

Table 17 Total unit cost of ammonia and LNG considering production, liquefaction and transport for Case 4 in Canada

Cost contribution	LNG	AMMONIA
Production cost (US$/kg)	0.098	0.250
Liquefaction cost (US$/kg)	0.140	0.000
Regasification cost (US$/kg)	0.014	0.000
Land transportation cost (US$/kg)	0.100	0.100
Tanker overseas transportations cost (US$/kg)	0.117	0.110
Total cost (US$/kg)	0.470	0.460
Total cost (US$/MJ)	0.010	0.025

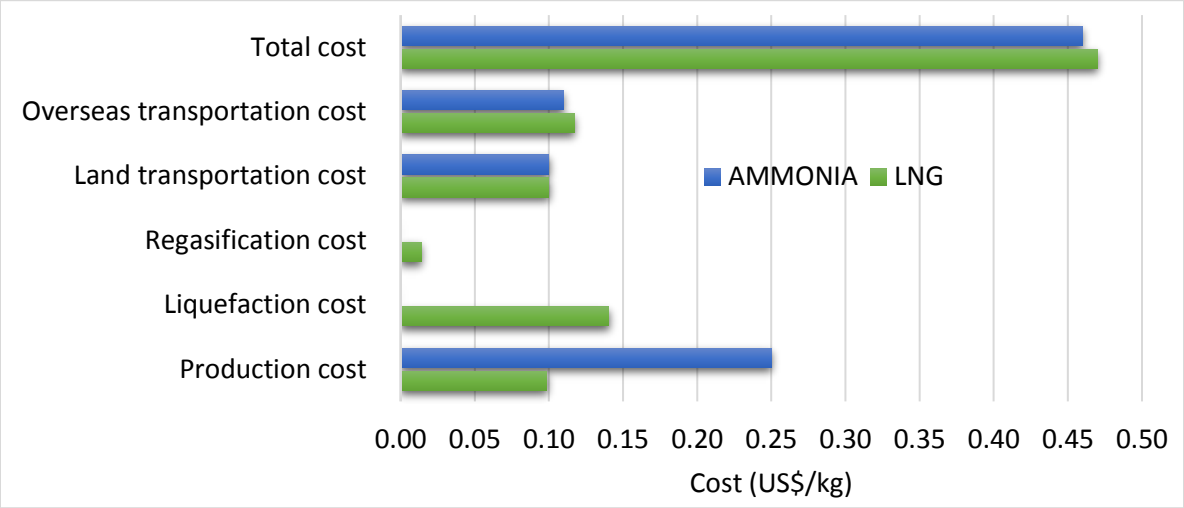

Figure 50 Contribution of sub-processes to total cost of LNG and ammonia for Case 4

As illustrated in Fig. 50, the cost of ammonia at the destination port is 0.01 $/kg lower than LNG in Ontario, Canada.

4. Oil sand to Ammonia

Microwave energy is an alternative type of energy which can be used in oil sand separation. Many of the inorganic particles in processed oil sands carry a charge, and could be influenced by electromagnetic radiation. They are excited at an altered rate than the water and bitumen when irradiated, making a temperature gradient between the different components of the oil sands. The surfactants and other forces cannot cope with this gradient and the solids are able to break free. Since all oil sands are dissimilar, a single frequency or power of microwaves are not available which functions best for all. There have been already some attempts for dissociation of bitumen using microwave energy. Pierre et al. [54] used a 915 MHz microwave to separate a 570 g sample of oil sands. This sample was exposed for 5 min at 500W and extended a last temperature of 315°C. This resulted in numerous layers comprising a bottom layer of sand with an asphaltene-like material on top. A second, noticeably bigger specimen with a volume of about 20 L was exposed for 9 min at 1500W at the same frequency. It got a temperature of 142°C where it exhibited three distinct layers. The bottom layer was typically sand, but also included other solids. The second layer contained a yellowish solution, accounting for all the water and other impurities in the oil

sand. The top layer was black, viscous oil. Bosisio et al. [55] considered microwave-assisted extraction of oil sands. They conducted oil sand extraction experiments under inert atmosphere in a quartz reactor which was located in a rectangular microwave guide (WR 284 wave guide) built-in with a coupling iris and modifiable short circuit. Instance microwave power of 100W at 2450 MHz frequency was realized to the oil sands samples and the different phases of reaction were perceived. The duration of first was 10 to 15s and second-third step were 15s to 15 min. Microwave radiation of oil sands created a crude oil and also small quantities of gaseous yields. Therefore, electromagnetic heating also proved to increase yields of crude oil from 70% to 86%. Lately, Global Research Corporation technologies declared a method using over 8,700 RF microwave frequencies essential to hydrocarbon elements. About 1.2 gal of diesel fuel was extracted from a tire after microwave radiation under vacuum at different frequencies. The company requested to extract oil and gas from diverse feedstocks by microwave radiation such as oil sands, oil shale, used plastics, or rubber with little or no additional processing. Initial testing results formed great amounts of hydrogen and methane gases without CO or CO_2 contaminants [56]. Samples of Lloydminster oil sands (oil–water–solids ratio of 19:40:41) considered principally stubborn to separation were tested with exposure to adjustable frequency microwaves [57]. The tests were able to avoid the FCC regulations because of distinct apparatus to comprise the electromagnetic waves. The aim was to explore what microwave frequency is best for this type of oil sands. All samples separated into a liquid upper layer and a mostly solid lower layer. The degree of separation was calculated by evaluating the oil content of the lower layer. The lower layer of the control specimen, which was not irradiated, had 27% oil content by weight. Tests were achieved by changing frequency and exposure time. Most of the samples presented marginally lower oil content. The best result occurred when the sample was irradiated for a duration of 10 min at 6400±100 MHz, where the lower layer only had 19% oil content. It was described microwave assisted extraction to recover hydrocarbon substances from oil shale, oil sands and lignite in the U.S. Patent 4.419.214 [58][6]. The patent describes how oil sand, oil shale rock and lignite samples were irradiated in a pressure vessel with gaseous or liquefied carbon dioxide and other gaseous or vapor hydrocarbon solvents. For example, oil sand was taken into a microwave feeder pipe and irradiated at 5.8 GHz frequency. Further, BTX (benzene-toluenexylene-ethylbenzene) was pumped through the sand. The extraction solution contained green oil on the top and bitumen was obtained at the bottom. In another example, crushed oil shale rock was irradiated at 915 MHz frequency. After radiation, carbon tetrachloride was injected to extract kerogen and the projected isolated kerogen was 65% of initial organic content of the rock. It is also specified in the review article [59] that oil sands and oil shale samples irradiated to microwaves produced the required heat to dissociate bitumen components to produce a crude oil and distilled kerogen. A laboratory microwave oven was utilized to test oil sand samples from Athabasca and oil shale specimens from Green River and Sunnyside. The authors found that a 128 g sample of oil sand separated into its components when irradiated at 800W for 10 min, followed by 1500W for 15 min.

Microwave energy is environmentally friendly since it has no harmful effect during hydrocarbon cracking process. Optimized ammonia synthesis using the excess heat in Haber-Bosch (which is the most common method for ammonia production) ammonia plant for oil sand bitumen extraction which is used for hydrogen production via microwave dissociation process is possible as shown in Fig. 51.

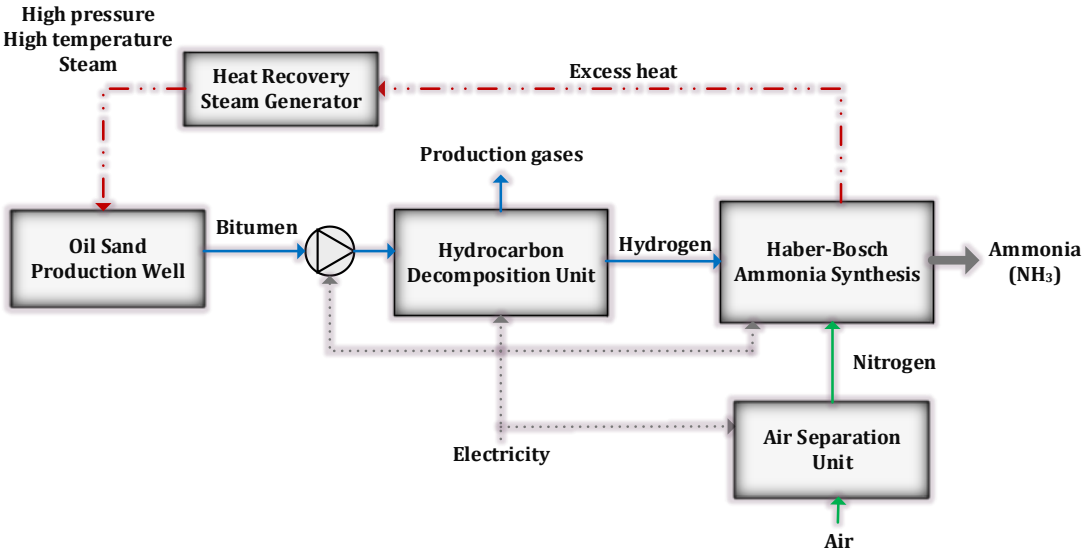

Figure 51 Schematic diagram of oil sand to ammonia plant

Fig. 52 shows the acidification potential (AP) for the selected ammonia production routes. Acidifying substances causes a wide range of impacts on soil, groundwater, surface water, organisms, ecosystems and materials. It is mainly caused by hard coal usage in the electricity grid mixture. The eutrophication category reflects the impacts of to excessive levels of macro-nutrients in the environment caused by emissions of nutrients to air, water and soil. As shown in Fig. 53, the values are close to each other corresponding to 0.0012 kg PO_4 eq/kg ammonia for hydropower route. Fig. 54 shows the ozone layer depletion (ODP) potential of the routes. It may have damaging properties upon human health, animal health, terrestrial and aquatic ecosystems, biochemical cycles and on materials. Hydrocarbon route has the lowest ODP value whereas wind has the highest since it is mainly caused by the transport of natural gas which is used in the power plants where the electricity is supplied to wind turbine production.

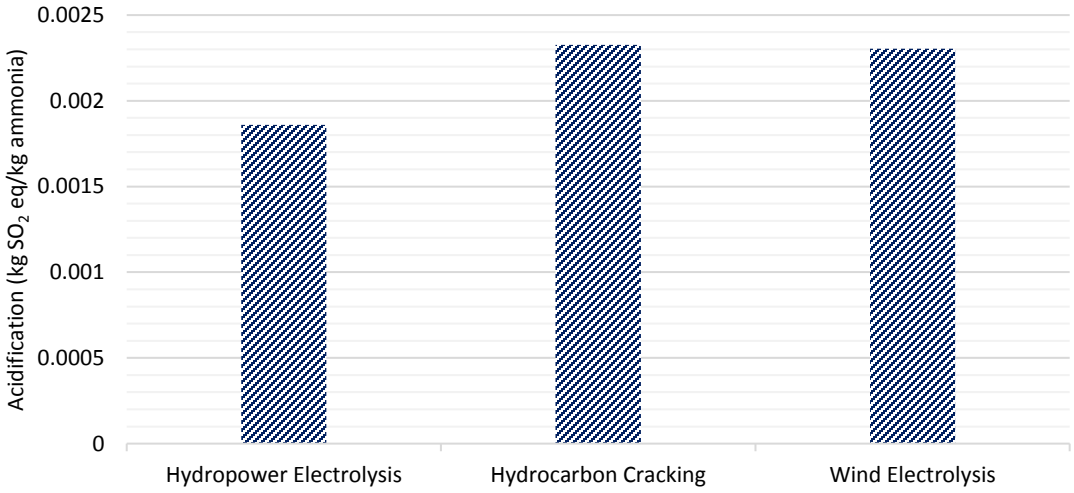

Figure 52 Acidification impact comparison of selected ammonia routes

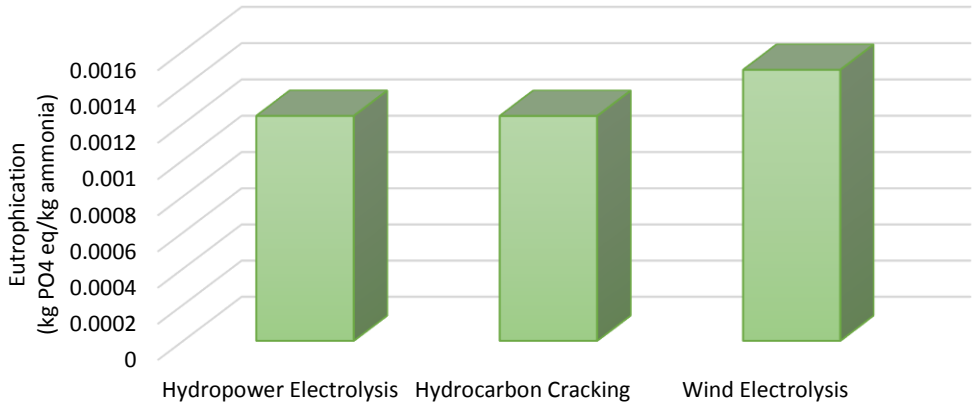

Figure 53 Eutrophication impact comparison of selected ammonia routes

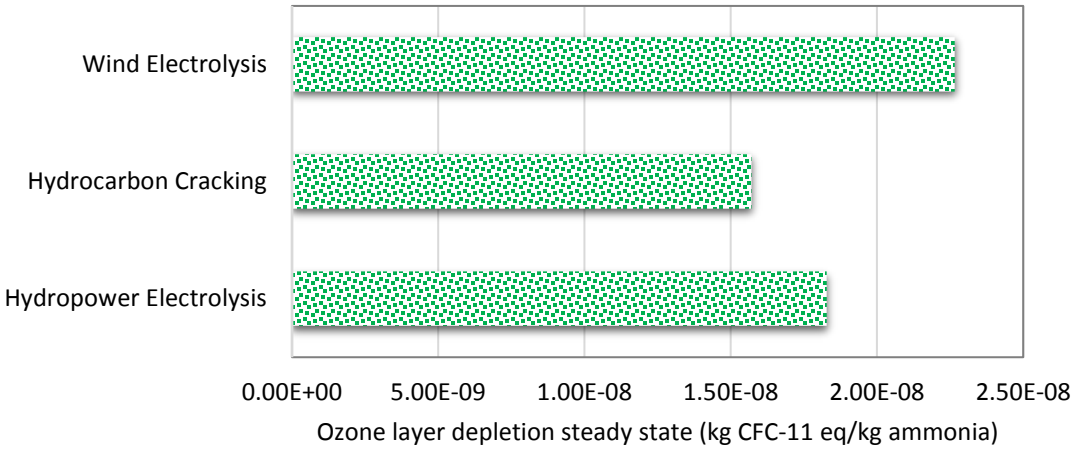

Figure 54 Ozone layer depletion impact comparison of selected ammonia routes

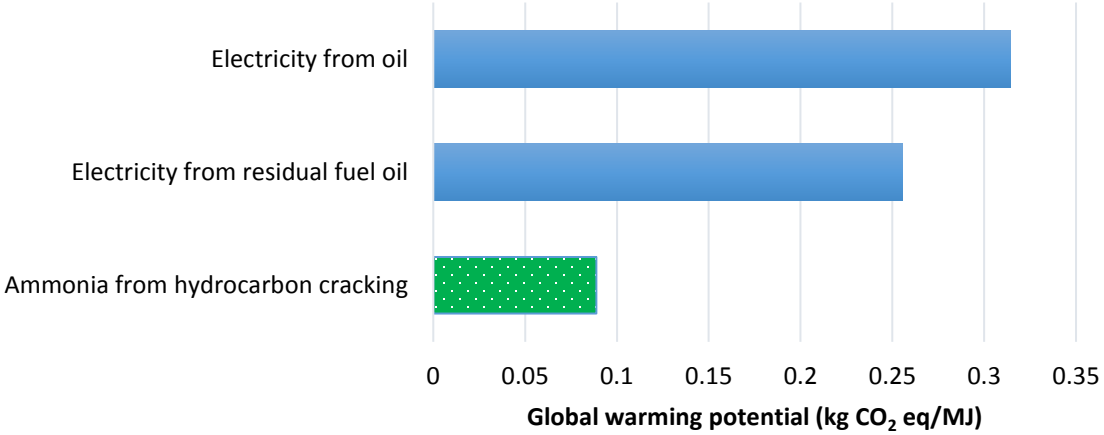

Figure 55 Comparison of 1 MJ electricity production and ammonia production

The production of 1 MJ electricity from residual oil has higher global warming potential than same amount of ammonia production from hydrocarbon cracking method as shown in Fig. 55. This result implies that by replacing ammonia as power generating fuel, total greenhouse gas emissions can be decreased significantly.

5. Concluding Remarks

Utilization of hydrocarbons in an environmentally friendly manner becomes more significant day by day. Dissociation of hydrocarbons such as methane is a promising option especially for British Columbia. Based on the extensive literature review and assessments, the following concluding remarks are noted.

- Hydrocarbons can be used as a source of hydrogen which is required for ammonia synthesis. There are various alternative pathways for hydrogen production from hydrocarbons such as thermal, non-thermal, plasma routes.
- Methane decomposition reaction is moderately endothermic process. The energy requirement per mole of hydrogen produced is considerably less than that for the steam reforming process.
- Hydrogen via thermo-catalytic dissociation of hydrocarbons represents an alternative solution. It is accompanied by the formation of carbon deposits. Methane can be thermally or thermocatalytically decomposed into carbon and hydrogen without CO or CO_2 production.
- It can be estimated that the electric energy supply needed for the cracking operation varies between 4 and 7 kWh per kg of carbon produced or between 1 and 1.9 kWh per normal cubic meter of hydrogen produced.
- Gliding arc discharge reactor is one of the highest efficient route for methane conversion which was experimentally tested by many researchers.
- H_2 production cost that can be expected from industrial methane cracking could be of the order of 1.5 $/kg and NH_3 in the range of 0.3-0.5 $/kg.
- The microwave energy can be of sufficient power and duration to cause microwave depolymerization of the high molecular weight materials such as bitumen.
- For oil sands or extremely high viscosity reservoirs, where the temperature effect on viscosity is significant, electromagnetic heating could be used as a preheating purposes. Because lower frequency waves carry less energy, heating times are considerably longer compared to the higher energy microwaves.
- Optimized ammonia synthesis using the excess heat in Haber-Bosch ammonia plant for oil sand bitumen extraction which is used for hydrogen production via microwave dissociation process is possible.
- The current ammonia retail prices continue to decrease by low natural gas prices. Current retail price is about 550 US$/ton. However, ammonia price is strictly dependent on natural gas price which can be eliminated if oil sand bitumen is utilized.
- Although hydrocarbon dissociation route is a fossil fuel based process, the technology is clean and environmentally friendly close to renewable resources in some environmental impact categories.

CHAPTER 5:AMMONIA IN MARITIME APPLICATIONS

Sea transportation constitutes a large share of global transportation. It is principally used for the transportation of goods, liquid fuels, all type of products and humans. Transoceanic tankers and freight ships need a great amount of energy for operation which is commonly provided by diesel or heavy fuel oils. In order to reduce the total greenhouse gas emissions caused by maritime transportation, ammonia is potential replacement and/or supplements for conventional fuels. Here, zero carbon fuel, ammonia, is proposed to replace heavy fuel oils in the engines of maritime transportation vehicles. Furthermore, it is also proposed to use ammonia as dual fuels to quantify the total reduction of greenhouse gas emissions. An environmental impact assessment of transoceanic tanker and transoceanic freight ship is implemented to explore the impacts of fuel substituting on the environment. In the life cycle analyses, the complete transport life cycle is taken into account from manufacture of transoceanic freight ship and tanker to production, transportation and utilization of ammonia in the maritime vehicles. Several ammonia production routes ranging from municipal waste to wind options are considered to comparatively evaluate environmentally benign methods. Besides global warming potential, environmental impact categories of marine sediment ecotoxicity and marine aquatic ecotoxicity are also selected in order to examine the diverse effects on marine environment. Being carbon-neutral fuels, ammonia, yields significantly minor global warming impacts during operation. The ecotoxicity impacts on maritime environment vary based on the production route of ammonia. The results imply that even if engines are dual-fueled with ammonia, the global warming potential is significantly lower in comparison with heavy fuel oil driven transoceanic tankers.

1. Ammonia production routes

Although steam methane reforming is currently more common technique for hydrogen and ammonia production, by developments in electrolyzer industry, water electrolysis using renewable energy resources become more attractive and practical. Hence, in this study, hydropower and wind energy sources are considered two different pathways for ammonia production. For hydrogen production, electrolysis route is employed where an electrolyzer is used requiring about 53 kWh electricity to generate 1 kg of hydrogen. The source of electricity is taken from wind and hydropower individually for both cases. Haber-Bosch process is utilized for ammonia synthesis in this study. In this process, nitrogen is supplied through air separation process. For the LCA of nitrogen manufacture, electrical work for procedure, cooling water, surplus heat and groundwork for air separation facility are taken into account. The distribution elements were obtained from the heat of vaporization and the specific heat capacity multiplied with the temperature difference from 20°C to the boiling point. SimaPro database has the values of nitrogen manufacture from cryogenic air separation method [60]. Cryogenic air separation process becomes more cost effective compared to non-cryogenic methods at the level of about 200-300 tons per day nitrogen. Since gas phase nitrogen is required in the reaction, the energy requirement is lower because liquefaction is not required. The major input to the air separation plant is electricity required to compress the air. Air is not taken as an input because of inexhaustibility. The separated CO_2 and water vapor are not evaluated as emissions in the process. The transportation is not accounted for the analyses since it is considered that the ammonia synthesis plant is located near air separation plant. The transportation of produced fuels are later considered in the analyses. Producing liquid products from air separation plant requires about two times higher energy than gaseous products. Commercial cryogenic air separation plants require electricity in the range of 0.6 to 1 kWh per kg of liquid nitrogen product. However, as mentioned earlier, gaseous product necessitates lower

power input. Hence, in this study, 0.42 kWh electricity is assumed for nitrogen gas production as taken from GREET 2016 model [61]. The utilized electricity for nitrogen production is US mix grid. For hydrogen generation, hydropower electricity or wind power plant electricity is used. For the transportation of the produced ammonia and hydrogen, an average distance is assumed where 100 km is by lorry with a capacity of higher than 16 tonne and 600 km by rail transport. Dual fuel operation of vessels are also considered in the study as 50% clean fuel and 50% heavy fuel oil.

2. Methodology

The goal of this study is to investigate the environmental impacts of alternative fuels driven marine transportation tankers and ships in comparison with conventional heavy fuel oil from cradle-to-grave: global warming potential, abiotic depletion, acidification, stratospheric ozone layer depletion, marine eco-toxicity and marine sediment ecotoxicity. The motivation behind this study is to decrease the environmental impacts caused by current hydrocarbon dependent marine transportation systems. The results of this study will mainly attract marine transportation sector and academicians working in the area of clean fuel production and utilization technologies. The function of this study is assess environmental impacts per tonne-kilometer cruise travel where the functional unit is 1 tonne-kilometer.

Life cycle analysis includes all stages in a process life namely from the extraction of raw materials through the material processing, manufacture, distribution, use, and disposal or recycling. For this analysis, we account for all the stages in the life cycle of maritime transportation, including feedstock recovery and transportation, fuel production and transportation, and fuel consumption in the ocean tankers and freight ships. The exploration and recovery activities from the well to fuel production and the subsequent transportation to the pump constitute the well-to-pump (WTP) stage. The combustion of fuel during ocean vehicle operation constitutes the pump-to-hull (PTH) stage. These two stages combined comprise the well-to-haul (WTH) cycle.

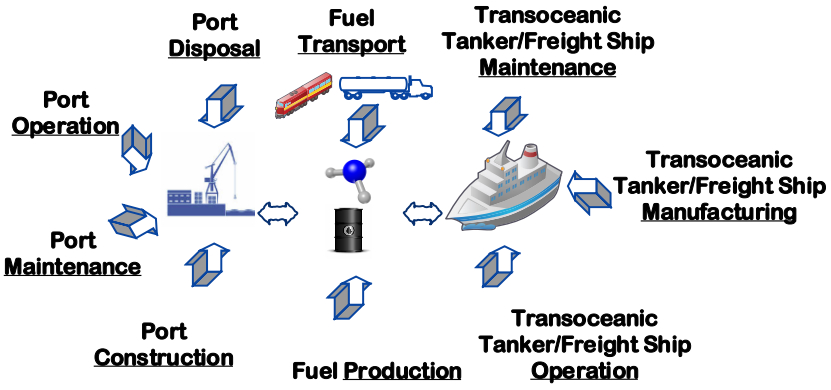

Figure 56 Well-to-haul life cycle phases of maritime transportation

The system boundaries for the LCA analyses are defined as shown in Fig. 56, namely: mining of the raw materials and extraction of the nutrients from these materials, transportation of raw materials and pre-products, generation and supply of required energy, manufacturing of the ammonia and the related field operations. Various environmental impact categories including global warming, marine sediment ecotoxicity, marine aquatic ecotoxicity, acidification, ozone layer depletion and abiotic depletion are selected in order to examine the diverse effects of

switching to clean fuels in ocean transportation. The selected indicators of this method which are utilized in this study are explained as follows [60]:

Depletion of abiotic resources
This impact category is concerned with protection of human welfare, human health and ecosystem health. This impact category indicator is related to extraction of minerals and fossil fuels due to inputs in the system. The Abiotic Depletion Factor (ADF) is determined for each extraction of minerals and fossil fuels (kg antimony equivalents/kg extraction) based on concentration reserves and rate of de-accumulation.

Global warming potential
Climate change can result in adverse effects upon ecosystem health, human health and material welfare. Climate change is related to emissions of greenhouse gases to air. The characterization model as developed by the Intergovernmental Panel on Climate Change (IPCC) is selected for development of characterization factors. Factors are expressed as Global Warming Potential for time horizon 500 years in kg carbon dioxide/kg emission.

Stratospheric ozone depletion
For the reason of stratospheric ozone depletion, a superior portion of UV-B radiation spreads the earth surface because of increasing chlorofluorocarbons (CFCs). This may yield damaging impacts on human and animal health, terrestrial and aquatic ecosystems, biochemical cycles and on substances. Ozone depletion potential of several gasses are specified in kg CFC-11 equivalent per kg emission where the time span is infinity.

Acidification potential
Acidifying substances causes a wide range of impacts on soil, groundwater, surface water, organisms, ecosystems and materials. SO_2 equivalents/kg emission is used to expresses the acidification potential.

Marine aquatic eco-toxicity
Marine eco-toxicity refers to impacts of toxic substances on marine aquatic ecosystems. The characterization factor is the potential of marine aquatic toxicity of each substance emitted to the air, water or/and soil. The unit of this factor is kg of 1,4-dichlorobenzene equivalents (1,4-DB eq) per kg of emission.

Marine sediment ecotoxicity
Marine sediment eco-toxicity refers to impacts of toxic substances on marine sediment ecosystems. The unit of this indicator is kg of 1,4-dichlorobenzene equivalents (1,4-DB eq) per kg of emission.

3. Life cycle phases

Analysis of well-to-haul (WTH) of clean marine fuels is performed in this study where each step is briefly explained in this section. A tonne kilometer by shipping is defined as unit of measure of goods transport which represent the transport of one tonne by a vessel over one kilometer. Marine diesel engines are generally further categorized into two different groups as slow speed (15 knots in average) and medium speed (25-30 knots). Transoceanic tanker and freight ships are slow speed vehicles which include two-stroke cycle with crosshead engines of 4-12 cylinders. In the marine

industry, these engines are used for main propulsion and constitute larger portion of installed power on the ship.

Table 18 Trip scenario for transoceanic freight ship

	Distance	Speed	Time	Load factor
Cruise	2306.041 nmi	18.006 kn	128.073 h	0.6
RSZ1	100.827 nmi	18.006 kn	5.6 h	0.6
RSZ2	25 nmi	18.006 kn	1.388 h	0.6
Hotel1	-	-	22 h	0.19
Hotel2	-	-	22 h	0.19

Each vessel type is characterized by power rating of its two engines - main and auxiliary. For each engine, fuel consumption and emission factors are defined. GREET 2016 software is utilized to find the power ratings and total energy consumptions of the selected ships [61].

In order to determine the average power consumptions, the trip is assumed to be from pacific to international ports. After determining the total trip distances as listed in Table 18 and 19, each trip was divided into segments, including transit through reduced-speed zones (RSZs). Each trip segment may have distinct fuel consumption and emission factors owing to different speeds and load factors and engine/fuel switching. At the origin and destination ports, the vessel will hotel and burn fuel dockside using mainly auxiliary engines. After a vessel leaves port, it travels in an RSZ, during which it uses a lower load factor and consumes less fuel, thereby emitting fewer pollutants, than when traveling at cruising speed. It will pass through an RSZ before hoteling at the port of destination. The GREET marine module aims to model these trip segments, representatively, for different vessel types leaving or arriving at U.S. ports in different regions [61].

Table 19 Trip scenario for transoceanic tanker

	Distance	Speed	Time	Load factor
Cruise	6177.495 nmi	15.049 kn	410.498 h	0.83
RSZ1	40.748 nmi	15.049 kn	2.708 h	0.83
RSZ2	25 nmi	15.049 kn	1.661 h	0.83
Hotel1	-	-	58 h	0.26
Hotel2	-	-	58 h	0.26

Production of transoceanic freight ship

This phase includes the processes of material production, representing the material composition of an average water vehicle used for solid goods transportation. For manufacturing, electricity and heavy oil burned in industrial furnace are included. For the transportation of materials standard distances are applied. Also, waste treatment processes for non-metal components of a water vehicle are accounted for. The exchanges of the ship manufacturing are derived from an assessment of a ship, with a load capacity of 51,500 tonne. The energy consumption in manufacturing is estimated as 50% of the cumulative energy of the used materials. The split of energies is 10% electricity and 90% heavy fuel oil [60].

Production of transoceanic tanker

Similar to transoceanic freight ship, this step includes the processes of material production, representing the material composition of an average water vehicle used for solid goods

transportation. This type of vehicle has higher load capacity corresponding to 100,000 tonne. The energy consumption in manufacturing is estimated as 50% of the cumulative energy of the used materials. The split of energies is 10% electricity and 90% heavy fuel oil [60].

Maintenance freight ship and tanker

This step of the inventory includes the use of paint and emissions of the solvent of the paint as NMVOC. Consumption of lubricates are excluded. It is assumed that the ship is painted 6 times in its entire life span of 25 years. The consumption of lubricates is included in the fuel consumption for vessel operation [60].

Port facilities

Seaport facilities comprise of the construction and disposal of one of the world's biggest port in Rotterdam, Netherlands. The inventory contains the processes of material production, representing the material used in the construction phase of the port. The building activities and electricity consumption are accounted for construction and disposal phases. Emission of NMVOC are included. Also lorry transport of materials to the constructions site are taken into account. The expenditures due to construction and disposal are addressed. The data represent one seaport for both, sea and inland shipping. The material composition of the sealed industrial area is derived from the construction and disposal expenditures of a European highway. The built up is modelled as a steel building. The life time of port is assumed to be 100 years [60].

Operation and maintenance of the port

This inventory includes emissions of to water due to non-removed oil spills. In this step, the land occupation and transformation due to seaport are taken into account. The energy consumption at the port is based on assumptions for the specific electricity consumption at the port in Hamburg, Germany. The land use is further distinguished in built up area (0.6%), road area (45.6%) and water bodies (54.29%). Emission to waters include emission from production sites on the port site, which are not directly connected to the transport activities [60].

Transportation and operation of the transoceanic freight ship

In this step, the full cycle is represented by supply of the fuel, operation of the ship and transport of the goods as 1 tkm. Direct airborne emissions of gaseous substances, particulate matters, dioxins, PAHs, halogens and heavy metals are accounted for. These emissions are caused by heavy oil burning in the engines, hence they are mostly eliminated in ammonia driven ships. Also, the disposal of bilge oil and emissions of tributyltin compounds are included. Individual hydrocarbons are estimated based on the share of diesel engines of road vehicles. Heavy metals are estimated from trace elements in fuel. A distinction between distilled (28%) and residual fuel (72%) is applied. The amount of disposed bilge oil is estimated as 0.6% of the consumed fuel. The average data for steam turbine (5%) and diesel engine (95%) propulsion are considered in the study. The fuel used is for conventional ships is heavy fuel oil and is representative for slow speed engine types about 15 knots. The data represents solid bulk transport of about 40,000 dwt (deadweight tonnage) where the ship is driven by steam turbine and diesel engines [60]. The power ratings of the main engine and auxiliary engines are about 37.5 MW and 8.3 MW, respectively. The average energy consumption for the freight ship is calculated to be 0.214 MJ per mile ton [61].

This step refers to the entire transport life cycle namely; the operation of vessel; production of vessel; construction and land use of port; operation, maintenance and disposal of port;

production and transportation of fuel to the port. Port infrastructure expenditures and environmental interventions are allocated based the yearly throughput (0.37). The vessel manufacturing is allocated based on the total kilometric performance corresponding to about 2,000,000 km and its transport performance. Since transport activity requires loading and unloading, for each transport activity two ports are required [60].

Transportation and operation of the transoceanic tanker

In this step, transoceanic tanker is considered instead of freight ship. Different than the transoceanic freight ship, the average data for steam turbine (62%) and diesel engine (38%) propulsion are considered here. The fuel consumption and emissions are representative for slow speed engine types and a tanker size between 50,000-300,000 dwt. Similarly, the inventory refers to the entire transport life cycle where the functional unit is one tkm. The port infrastructure expenditures and environmental interventions are allocated based the yearly throughput (0.27). The tanker manufacturing is allocated based on the total kilometric performance of 3,920,000 km and its transport performance [60]. The power ratings of the main engine and auxiliary engines are about 15 MW and 2.85 MW, respectively. The average energy consumption for the tanker is calculated to be 0.056 MJ per mile ton [61].

4. Results and Discussion

The methodological analyses are conducted in SimaPro and GREET 2016 software for the evaluation of LCA. The LCA is implemented by employing the impact assessment method of CML 2001.

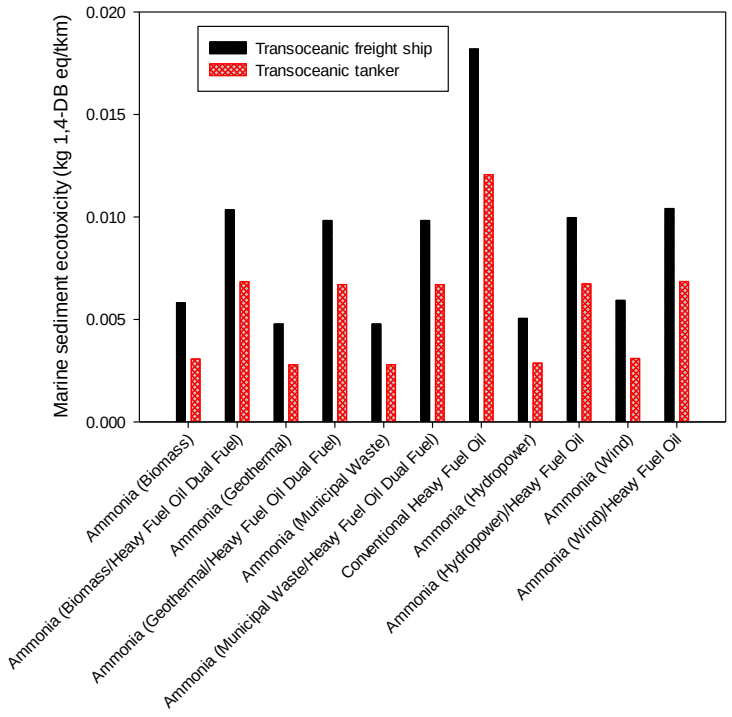

Figure 57 Marine sediment ecotoxicity values of transoceanic tanker and transoceanic freight ship per tonne kilometer for ammonia and conventional heavy fuel oil

The toxic substances on the marine sediment and aquatic environment are the main concerns of marine sediment ecotoxicity and marine aquatic ecotoxicity categories. 1,4-dichlorobenzene equivalents/tkm is used to express each toxic substance. Among the selected fuels, the conventional heavy fuel oil for both tanker and freight ship have the greatest damage on marine sediment and aquatic environment as shown in Figs. 57-61.

In general transoceanic freight ship have higher impact values than tanker because of mainly higher energy consumption rate per tonne-kilometer. Using ammonia (wind energy) in transoceanic tanker as dual fuel with heavy fuel oil lowers the ecotoxicity level about 47%.

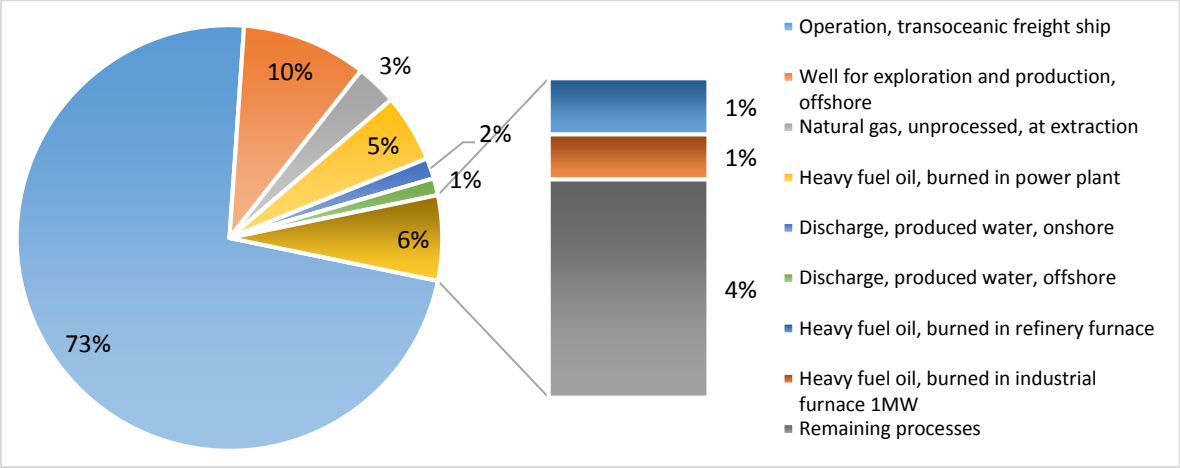

Figure 58 Process contributions to marine sediment ecotoxicity values of transoceanic freight ship driven by dual fuel (50% ammonia from hydropower and 50% heavy fuel oil)

The heavy fuel oil combustion significantly contributes to many of the environmental impacts. Energy production from fossil fuels yield high GHG emission. The contribution of different processes to ecotoxicity of marine sediment and marine aqua is illustrated in Figs. 58 and 59.

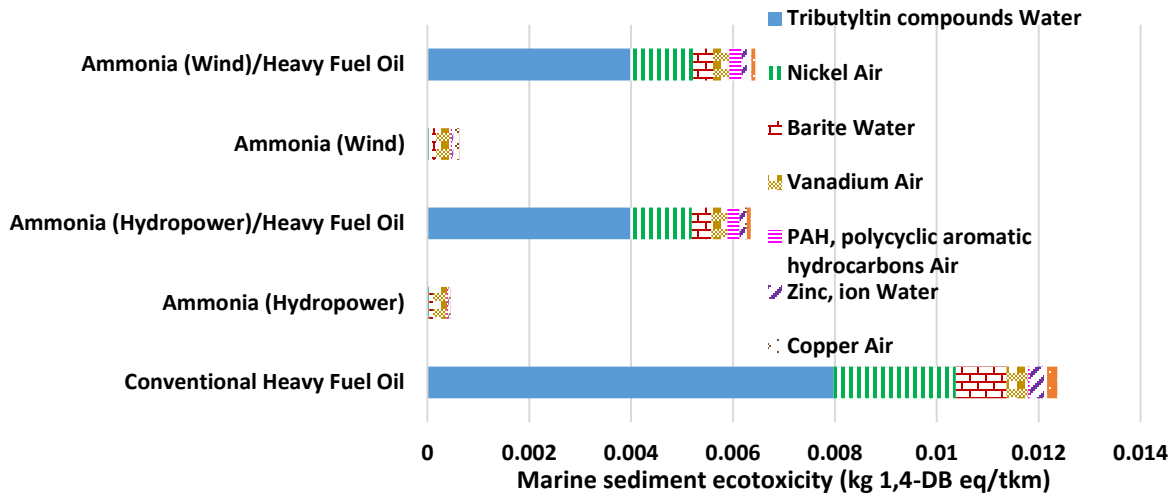

Figure 59 Emissions causing marine sediment ecotoxicity for transoceanic tanker driven by various fuels

Operation of the freight ship is responsible about 73% of marine sediment ecotoxicity for ammonia/heavy fuel oil driven ship whereas exploration and offshore production of heavy oil represents the 10%. This is due to crude oil production which is then used in heavy fuel oil refinery and transported to heavy fuel oil regional storage to be combusted in tanker.
Fig. 60 comparatively shows the materials and emissions causing ecotoxicity. Most of them are related to tributyltin compounds emitted to water because of bottom paintings of the ships. The heavy metals such as nickel and vanadium are due to combustion of heavy fuel oil which can been as the second highest contributor in dual fuel and sole heavy fuel oil options.

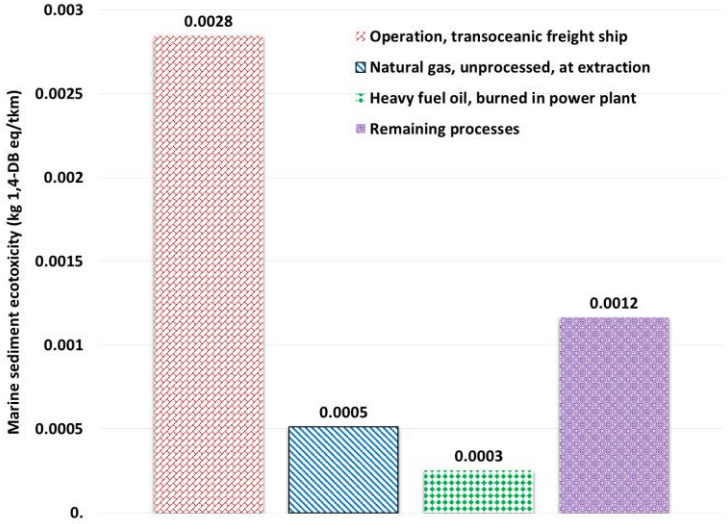

Figure 60 Process contributions to marine sediment ecotoxicity values of transoceanic freight ship fueled by sole ammonia from municipal waste

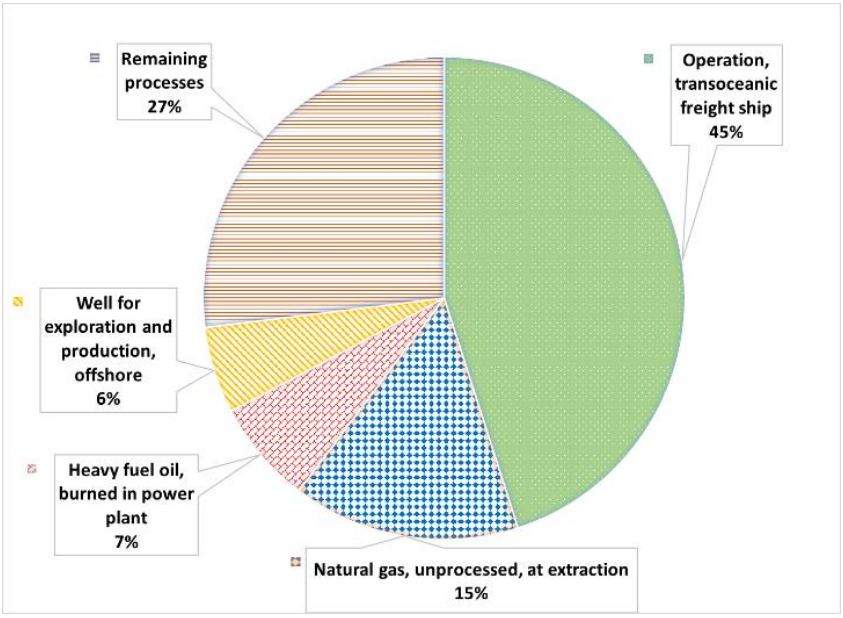

Figure 61 Process contributions to marine aquatic ecotoxicity values of transoceanic freight ship fueled by sole ammonia from geothermal energy

The contributions of different processes to ecotoxicity of marine sediment and marine aqua are shown in Figs. 61, 62 and 63. Operation of the freight ship is responsible about 45% of marine aquatic ecotoxicity as for sole ammonia fueled ship whereas exploration and offshore production of heavy oil represents the 6% and natural gas extraction represents 15% of total. This is due to natural gas and oil fired power plants which is then used for nitrogen production plant. For biomass based ammonia driven freight ship, barium, tributyltin compounds and vanadium are top three substances causing marine aquatic ecotoxicity as shown in Fig. 62 where barium has an impact corresponding to 0.0017 kg 1,4-DB eq per tonne-kilometer. Some of them are related to tributyltin compounds emitted to water because of bottom paintings of the ships

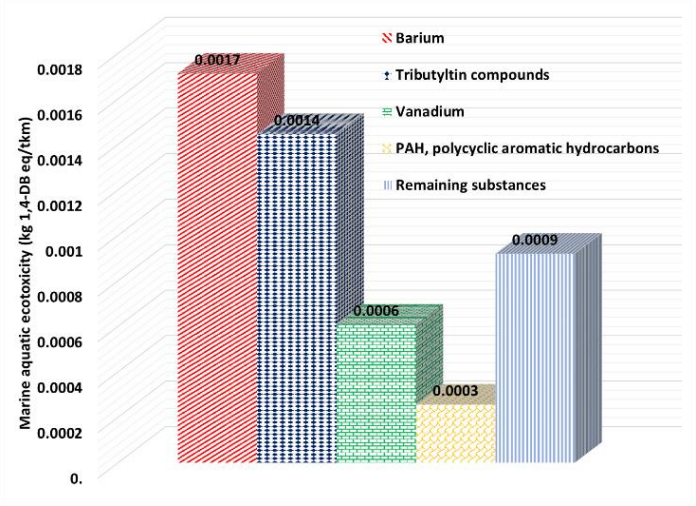

Figure 62 Process contributions to marine aquatic ecotoxicity values of transoceanic freight ship fueled by sole ammonia from biomass energy

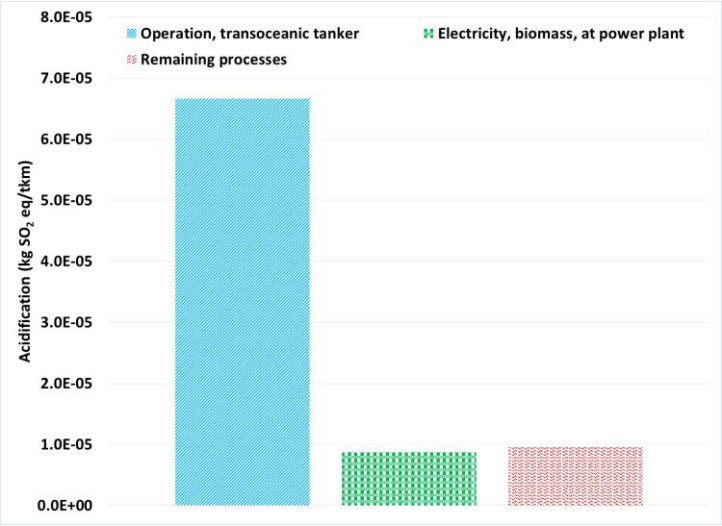

Figure 63 Process contributions to acidification values of transoceanic tanker fueled by ammonia from biomass energy and heavy fuel oil

The source of SO_2 emission is predominantly the operation of tanker and freight ship (96.8%) for conventional heavy fuel oil tankers and ships. It is also high for dual fuel processes as illustrated in Fig. 63.

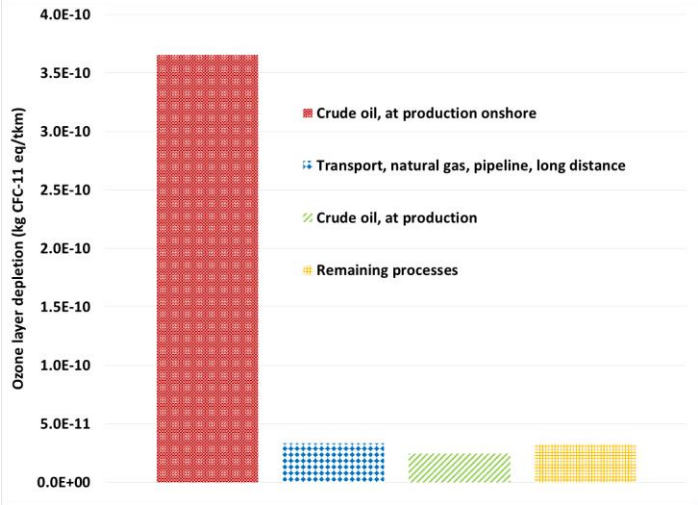

Figure 64 Process contributions to stratospheric ozone layer depletion of transoceanic freight ship by dual fuel (50% ammonia from municipal waste and 50% heavy fuel oil)

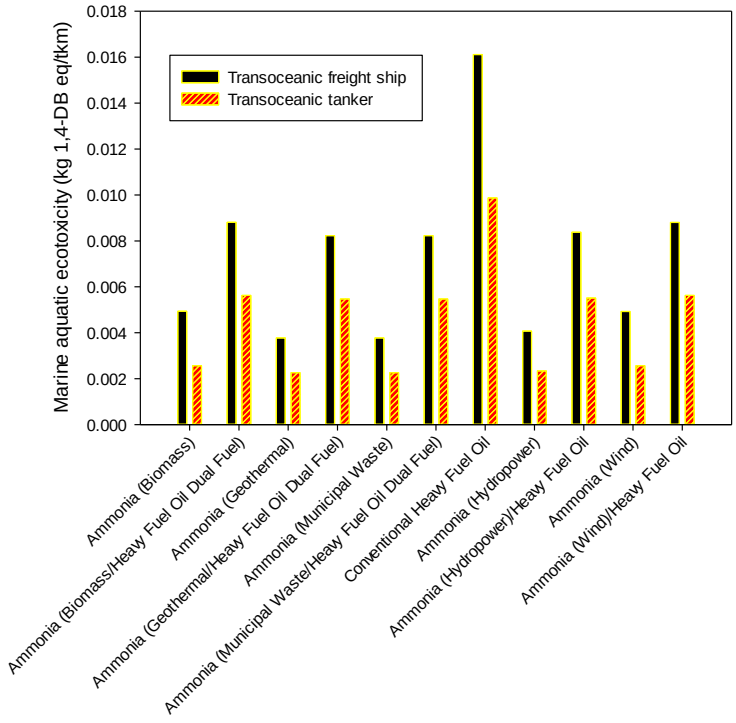

Figure 65 Marine aquatic ecotoxicity values of transoceanic tanker and transoceanic freight ship per tonne kilometer for ammonia and conventional heavy fuel oil

For ammonia and heavy fuel oil driven transoceanic freight ship, crude oil production has the highest share corresponding to about 81.2% as shown in Fig. 64. Operation and maintenance

of the port is responsible for about 16.6% of overall ozone layer depletion whereas the manufacturing of the ship constitutes only 2.2%. Two main substances causing ozone layer depletion are bromotrifluoromethane (Halon 1301) and bromochlorodifluoromethane (Halon 1211) corresponding to about 1.98E-10 and 3.31E-11 kg CFC-11 eq/tkm, respectively. The marine aquatic toxicity results are shown in Fig. 65.

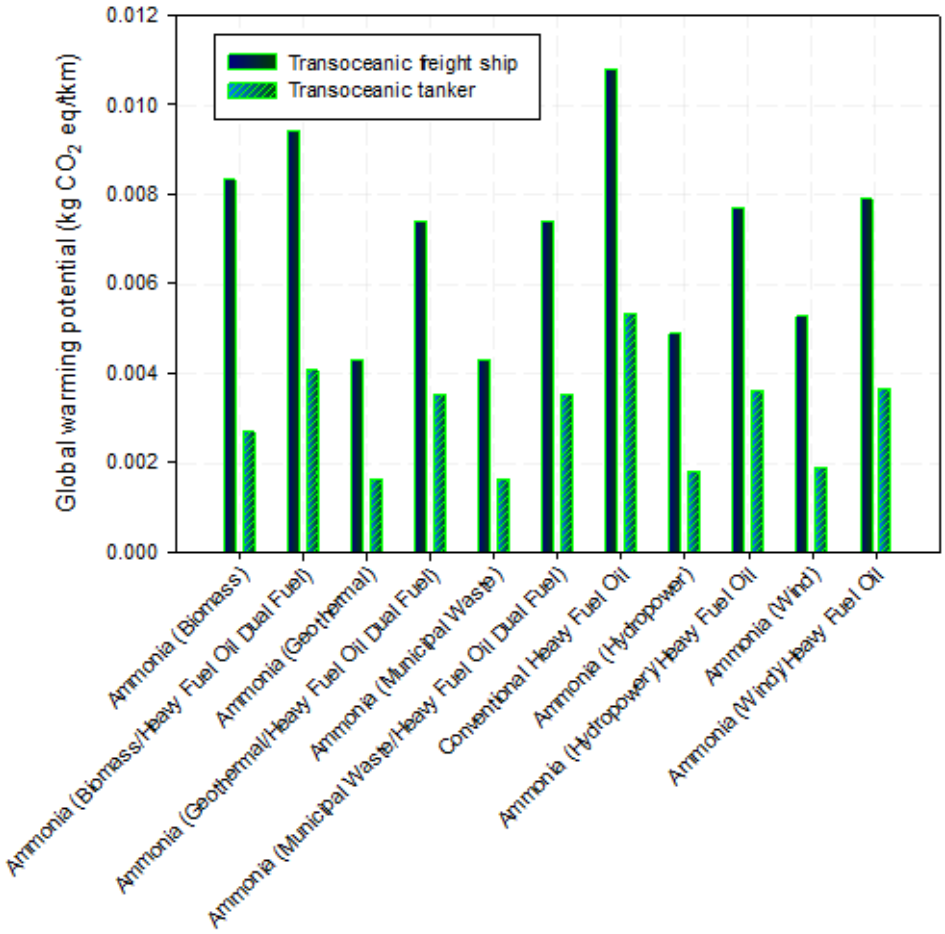

Figure 66 Global warming potential of transoceanic tanker and transoceanic freight ship per tonne kilometer for ammonia and conventional heavy fuel oil

In terms of global warming potential, ammonia (municipal waste) driven transoceanic tanker and freight ship yield the lowest greenhouse gas emissions in the entire life cycle corresponding to 0.0041 and 0.0016 kg CO_2 eq. per tonne-kilometer for freight ship and tanker, respectively as shown in Fig. 66. However, it is very high (about 10 times) for the conventional heavy fuel oil as shown in Fig. 66. The highest values after sole heavy fuel oil are 0.0079 kg CO_2 eq/tkm and 0.0036 kg CO_2 eq/tkm for ammonia (wind)/heavy fuel oil combination, respectively for freight ship and tanker. Using ammonia as dual fuel in the marine engines can decrease total greenhouse gas emissions up to 34.5% per tkm. Similarly, sole ammonia driven transoceanic tanker releases about 0.0018 kg CO_2 eq/tkm greenhouse gas compared to 0.0055 kg CO_2 eq/tkm for sole heavy fuel oil tanker. Process contributions to global warming potentials transoceanic freight ship driven by conventional heavy fuel oil are shown in Fig. 67.

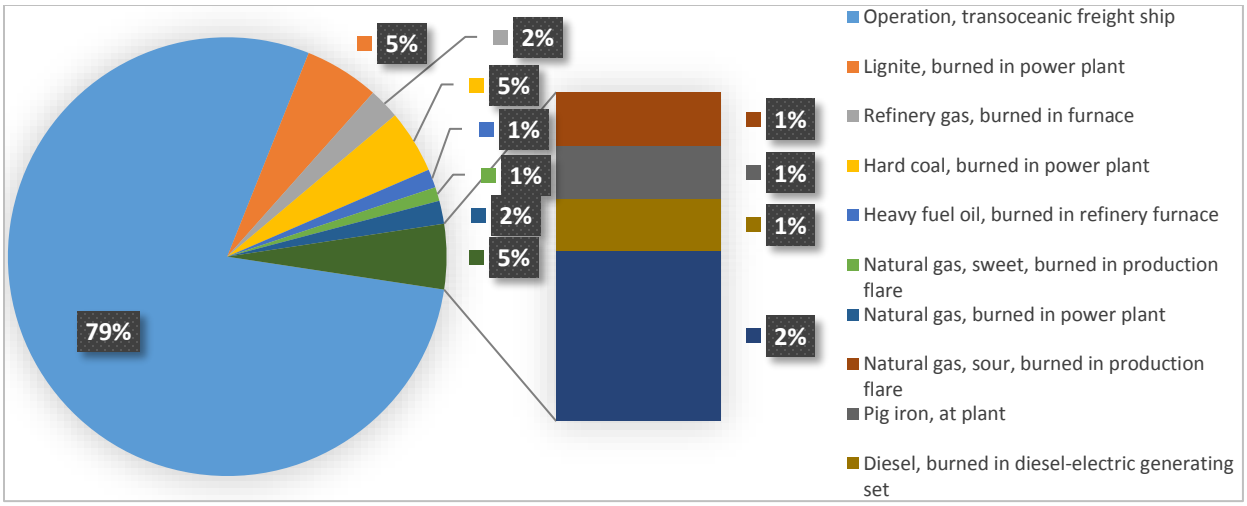

Figure 67 Process contributions to global warming potentials transoceanic freight ship driven by conventional heavy fuel oil

For ammonia (hydropower)/heavy fuel oil driven tanker, total GHG emissions are caused by mainly operation of tanker (64%), maintenance and operation of port (31%) and manufacture of tanker (5%). For the operation of tanker, 49.3% of is caused by heavy fuel oil and only 11.4% is by ammonia utilization.

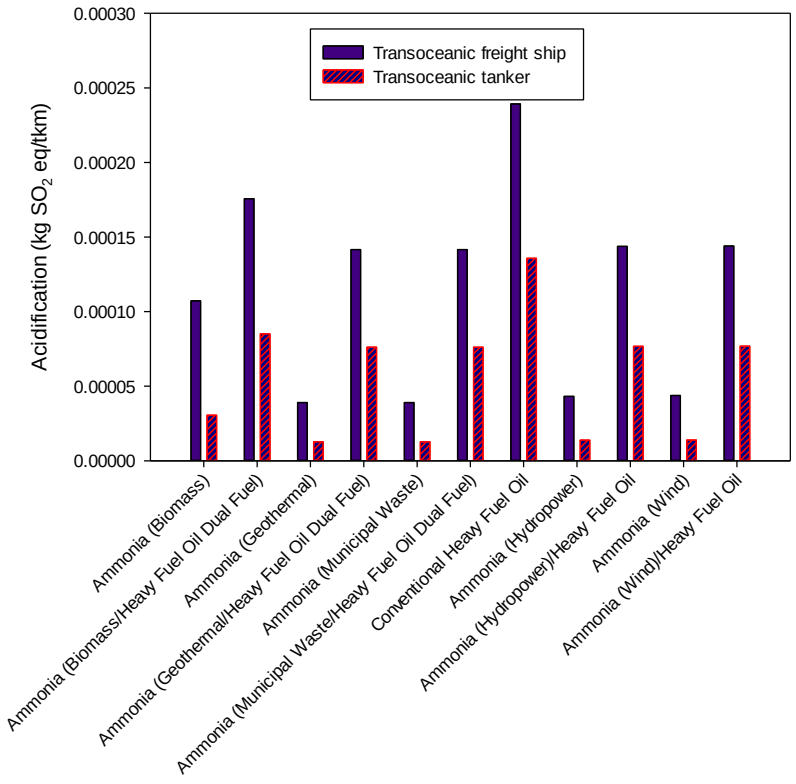

Figure 68 Acidification values of transoceanic tanker and transoceanic freight ship per tonne kilometer for ammonia and conventional heavy fuel oil

The acidification values of heavy fuel oil driven transoceanic tanker and freight ship are mainly caused by SO_2 and NO_x emissions which corresponds to more than 90% of overall acidification value. The source of SO_2 emission is predominantly the operation of tanker and freight ship (96.8%). This is caused by the sulfur content of the heavy fuel oil hence it is mostly eliminated in ammonia as seen in Fig. 68. Acidification values are lowest for hydrogen fueled tankers. The combustion of diesel and heavy fuel oil have the high impact hence, particularly transportation processes with railway and trucks create high emissions leading to higher acidification values. The variation in this impact category for ammonia is because of considerable differences in transportation distances of the hydrogen and ammonia to the port. Because, hydrogen has higher energy content pre mass, the number of transports from production plant to the seaport is lower yielding lower diesel combustion in railway and lorry.

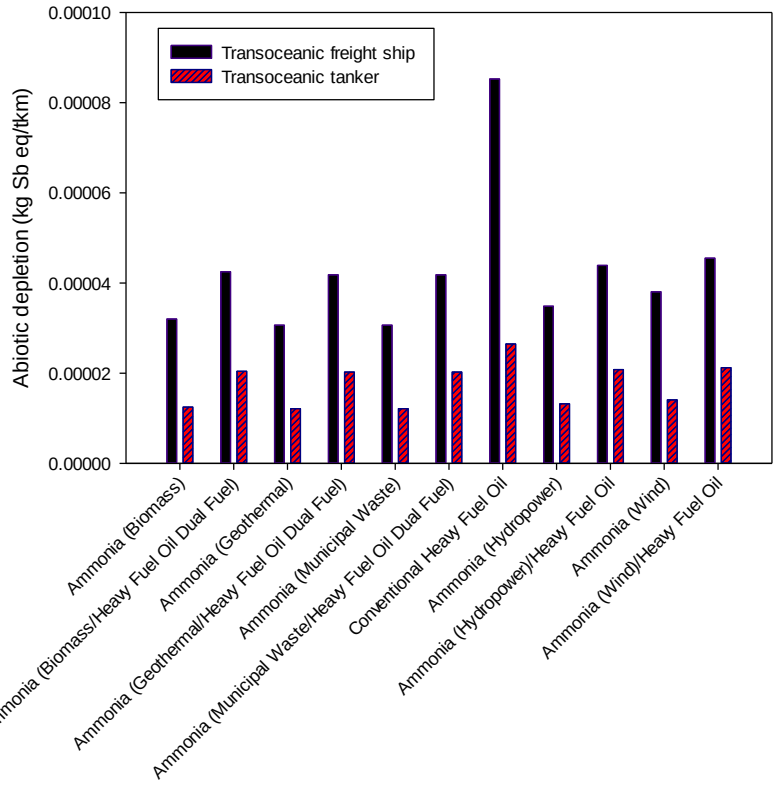

Figure 69 Abiotic depletion values of transoceanic tanker and transoceanic freight ship per tonne kilometer for ammonia and conventional heavy fuel oil

The abiotic depletion impact is calculated to be highest conventional heavy fuel oil followed ammonia (wind)/heavy fuel oil driven freight ships as it is shown in Fig. 69. Abiotic sources are natural sources counting energy sources, such as hard coal and crude oil, which are evaluated as non-living. This is because of fossil fuels are major basis of energy and feed resource, it shows the huge intake of hard coal and lignite (in total 64%) for tonne-kilometer travel of ammonia (wind) driven transoceanic freight ship as illustrated in Fig. 70.

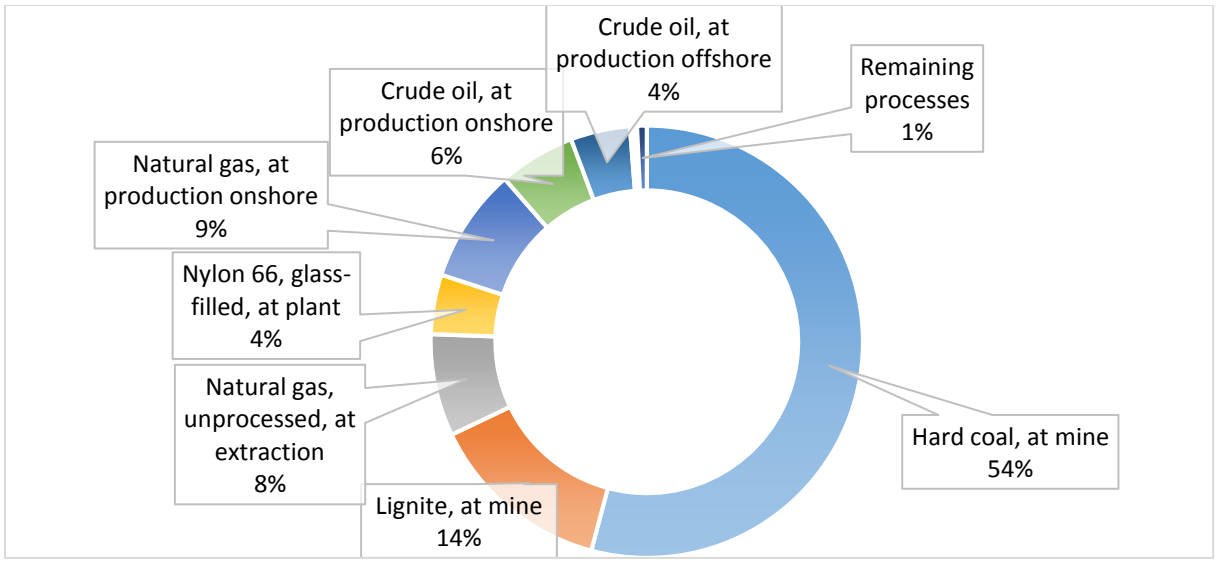

Figure 70 Process contributions to abiotic depletion values of transoceanic freight ship driven by ammonia from wind energy

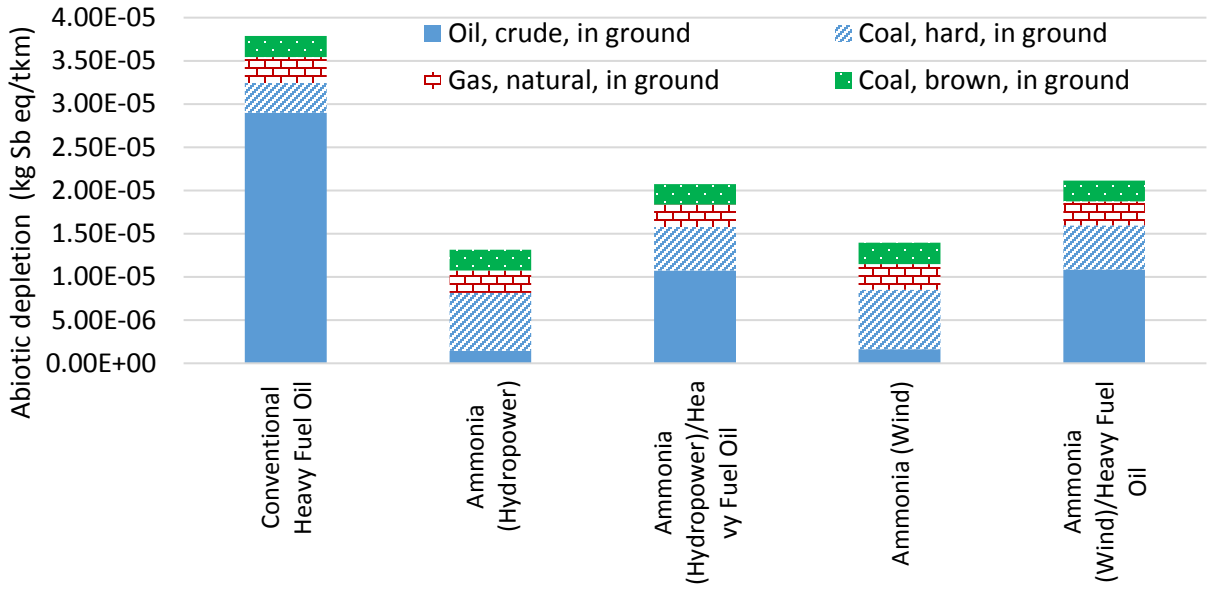

Figure 71 Abiotic substances causing depletion of abiotic resources for transoceanic tanker driven by various fuels

The reason of hard coal and lignite consumption is the electricity US mix usage in air separation plant for nitrogen production of ammonia synthesis process. Nitrogen production constitutes about 40% of overall abiotic depletion whereas hydrogen production from wind electricity is responsible for 16.1% of total abiotic depletion. Note that the operation and maintenance of the port has also a high share corresponding to 29.7% of total where it is similarly originated from electricity mix production. The causes of abiotic depletion values are comparatively shown in Fig. 71. For conventional heavy fuel oil driven transoceanic tanker, crude oil is the main depleted source similar to dual fuel options.

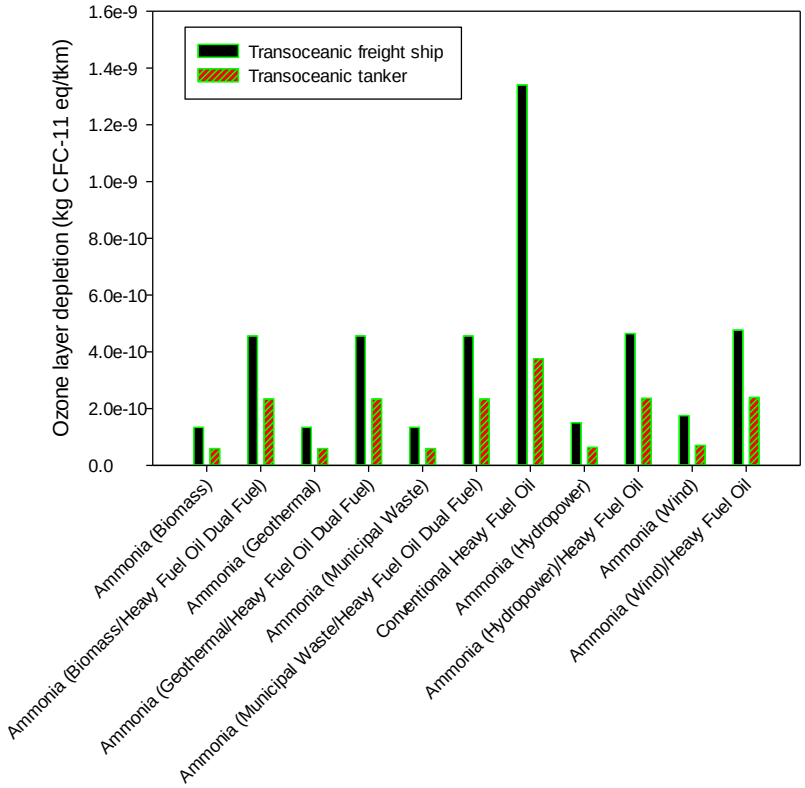

Figure 72 . Stratospheric ozone layer depletion values of transoceanic tanker and transoceanic freight ship per tonne kilometer for ammonia and conventional heavy fuel oil

Fig. 72 presents the life cycle kg CFC-11 eq. emissions of the transoceanic tanker and freight ship with different fuels per tonne-kilometer travelled. It is quite high for heavy fuel oil and dual fuel options while it is considerably less for hydrogen and ammonia fuels. Particularly, hydropower options have the lowest environmental impact in terms of ozone layer depletion.

5. Concluding Remarks

As non-carbon clean fuels for maritime ship engines, ammonia and hydrogen, yield considerably lower global warming impact during operation. The highest GHG values after sole heavy fuel oil are 0.0079 kg CO_2 eq/tkm and 0.0036 kg CO_2 eq/tkm for ammonia (wind)/heavy fuel oil combination, respectively for transoceanic freight ship and tanker whereas it is about 0.011 kg CO_2 eq/tkm for currently used heavy fuel oil freight ship. Using ammonia as dual fuel in the marine engines can decrease total greenhouse gas emissions up to 34.5% per tonne-kilometer. For ammonia (hydropower)/heavy fuel oil driven tanker, total GHG emissions are caused by mainly operation of tanker corresponding to about 64% whereas maintenance and operation of port has a share of 31%. This demonstrates that if clean fuels are even partially replaced with current hydrocarbon derived fuels, total GHG emissions in maritime transportation can be lowered significantly. By development and full utilization of renewable energy based ammonia and hydrogen fuels, GHG emissions during operation of the transoceanic tankers can be even zeroed.

CHAPTER 6:AMMONIA IN AVIATION

Petroleum based fuels have combination of accessibility, ease of handling, energy content, performance, and price because of being a mature product. Therefore, these type of fuels are heavily used by the transportation sector including air, road, and sea. However, limited nature, nonhomogeneous source distribution, changing prices, and end use related emissions of fossil fuels have driven most of the industries such as air transportation to search for other alternatives. The global aviation industry produces around 2% of all human induced carbon dioxide (CO_2) emissions. Specifically, aviation is responsible for 12% of CO_2 emissions from all transports sources whereas it is 74% for road transport [62]. Around 80% of aviation CO_2 emissions are originated from flights of over 1,500 km, for which there is no practical alternative mode of transport. The national and international flights overall the world produced 770 million tons of CO_2 in 2015 [62]. Presently, aviation industry consumes fuels derived from fossil fuels, mostly in specialized forms of petroleum based fuels. Such fuels tend to have higher qualities compared to some conventional applications, such as heating and transportation. Keeping in mind that aircraft fuels have additional requirements compared to land and sea transportation counterparts, such as resistance to extreme temperature changes. Hydrogen and ammonia, have zero or very little emissions when produced using water and renewable energy sources. Possibly, hydrogen, ammonia, methanol and ethanol can eliminate aviation industry's reliance on limited fossil fuel sources with fluctuating prices. Particularly, hydrogen and ammonia can additionally decrease aviation industry's impact on the greenhouse gas emissions considerably.

Table 20 illustrates the specific energy, energy density and density features of various alternative aviation fuels. Liquid hydrogen has the highest specific energy although currently utilized Jet A fuel has the highest energy density. According to the aviation fuel standards, a few of these fuels are not currently suitable for aircraft usage, however, by advancing technologies in engines and combustion, the aformentioned fuels are likely to be alternatives in the aviation industry.

Table 20 Specifications of some alternative aviation fuels

Fuel	Specific Energy (MJ/kg)	Density at 15°C (g/m^3)	Energy Density (MJ/L)
Kerosene (Jet A/Jet A-1)	43.2	0.808	34.9
Liquid Hydrogen	120	0.071	8.4
Liquid Methane	50	0.424	21.2
Methanol	19.9	0.796	15.9
Ethanol	27.2	0.794	21.6
Biodiesel (typical)	38.9	0.87	33.9
Liquid Ammonia	18.6	0.73	13.6

Source: Refs. [63–65]

Fig. 73 plots the mass of fuel essential to provide a definite quantity of energy in comparison with the volume of the equal fuel to give the equal quantity of energy. The quantity of energy, 100 MJ, brings a mutual base for assessment. Inferior values are favoured on both axes.

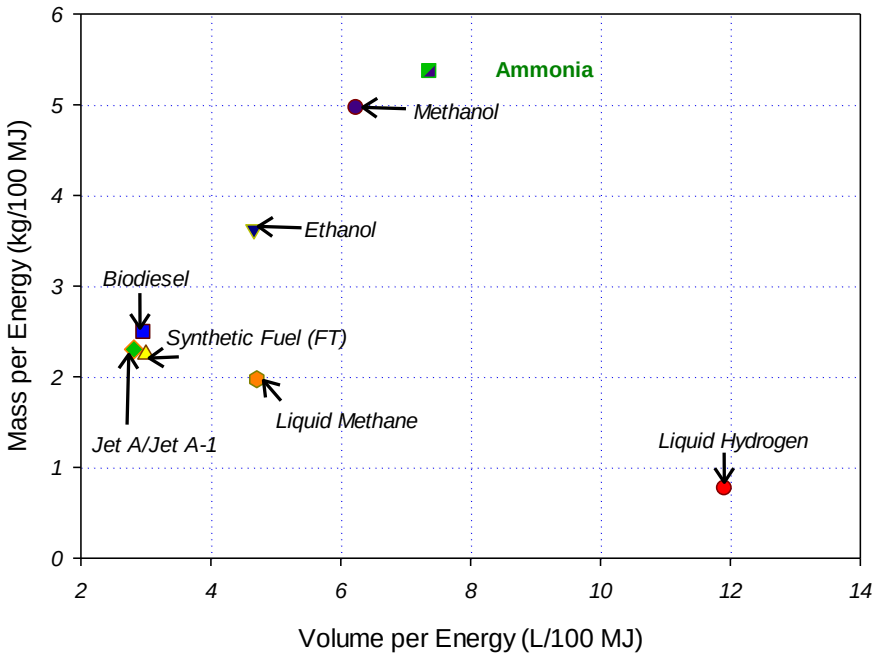

Figure 73 Comparisons of fuel mass and volume per unit energy (data from [66])

Hydrogen has the uppermost gravimetric energy content, however the low density of the liquid yields a very low volumetric energy content. Likewise for liquid methane, the high gravimetric energy content is offset by low density. The gravimetric energy content of the alcohols and biodiesel reveals their oxygen content. Biodiesels are nearer to conventional jet fuel since of the fact that oxygen signifies a smaller fraction of the fuel mass. FT synthetic fuels have a little higher gravimetric energy content than conventional jet fuel, but similarly slightly lower volumetric energy content [66].

In this regard, a life cycle assessment study of an average aircraft transport using various alternative aviation fuels to determine the relative environmental impact of each life cycle phase is presented. Using LCA methodology, the overall life cycle emissions of an aircraft running on various aviation fuels are calculated from well-to-wake. The steps considered in the analyses covers: (i) production, operation and maintenance of the aircraft, (ii) construction, maintenance and disposal of the airport, (iii) production, transportation and utilization of the aviation fuel. The environmental impact categories taken into account in this study are human toxicity, global warming, land use, depletion of abiotic resources and stratospheric ozone depletion.

1. Methodology

The evaluation of the life cycle of alternative fuels include emissions of the fuel cycle. This includes the extraction and transportation of raw materials from the well field or mine to the simple production, processing of these materials in fuel, transport and distribution of fuel in the tank on the plane and finally burn the fuel in the aircraft. The stages of this lifecycle analyzes well to wake as shown schematically in Fig. 74. For this analysis, we account for all the stages in the life cycle of aviation fuels, including feedstock recovery and transportation, fuel production and transportation, and fuel consumption in an aircraft. The exploration and recovery activities from the well to fuel production and the subsequent transportation to the pump constitute the well-to-

pump (WTP) stage. The combustion of fuel during aircraft operation constitutes the pump-to-wake (PTWa) stage. These two stages combined comprise the well-to-wake (WTWa) fuel cycle as illustrated in Fig. 74.

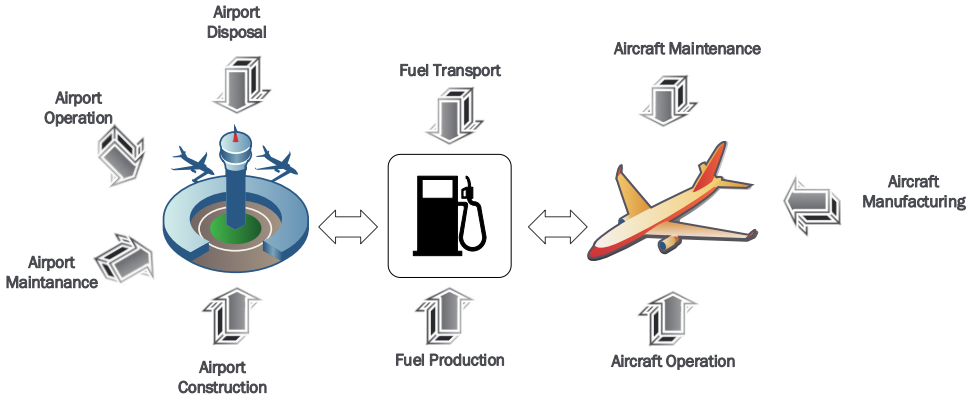

Figure 74 Complete well-to-wake life cycle phases used in the study

A ton kilometer by aviation is defined as the unit of measure of goods transport which represents the transport of one ton by an aircraft over one kilometer. To allocate energy use and emissions of a trip to a passenger, it is assumed that 100 kg of the payload represents an average weight of a passenger and luggage. This is equivalent to a mass allocation of energy and emissions between the passengers and cargo onboard the aircraft. A simple conversion of per-kg results to per-passenger results can be performed using the fixed weight of a passenger plus luggage. This allocation methodology works for all aircraft classes regardless of the split between passengers and cargo payloads onboard the aircraft. It is important that multiplying the passenger-based functional unit by the total passenger-distance flown will not provide the total emissions for a flight because this method will not account for the emissions that were allocated to the cargo in the aircraft. To obtain the total emissions from a flight, it should multiply the payload-based functional unit by the total payload-distance flown.

Environmental impacts are measured by selected environmental impact categories. Estimates of their potential for reducing greenhouse gases instead, compared with results generated for aviation kerosene using data from the results to observe aviation biofuel impacts relative to fossil fuels. It is assumed that sufficient operational fuel properties are modeled with acceptable characteristics of alternative fuels. Hence, the adaptation of the infrastructure of the aircrafts for other fuel combustion purposes are not considered in this study. All of the selected fuels are combusted in the same type of aircraft. Therefore, the aircraft manufacturing and airport operation/maintenance phases are identical for the selected cases. The LCA is performed using SimaPro LCA software in combination with the Ecoinvent database. Ecoinvent contains industrial life cycle inventory data on energy supply, resource extraction, material supply, chemicals, metals, agriculture, waste management services, and transport services. Hence, the inventory data for airport construction/maintenance/operation and aircraft manufacturing/maintenance phases are taken from SimaPro 7.3 software database whereas the other phases are generated based on the previous literature and work. CML 2001 is the selected method to calculate the environmental impact of the inventory data.

2. Description of the Processes

The LCA is divided into three main phases namely; manufacturing of the aircraft, construction and maintenance of the airport and operation of the aircraft.

Aircraft manufacturing

Material consumption values denote the production of one average aircraft in the referring class where the net weight of the aircraft is about 234 tonnes. Interventions for production processes of vehicles are derived from specific exchanges per seat. The aircraft is assumed to have about 367 seats. Inventory data represent 16 European production sites of Airbus company where they are located in Germany, France, Spain and the UK [60]. The inventory data of aircraft include processes of material, energy and water use in vehicle manufacturing. Rail and road transport of materials are considered together with VOC emissions. However, plant infrastructure is not included. Energy consumption for deionized water is included in the electricity value. Material expenditures are not accounted for. Transport of vehicle parts between the different sites is excluded.

Construction and maintenance of airport

In this step, maintenance, construction and disposal of airports are considered. The inventory data for construction and maintenance of the airport include material consumption and energy expenditures related with the construction sealed area such as aircraft parking, runways, etc. at airports. Furthermore, expenditures for buildings are considered. The data include expenditures due to refurbishment and demolition. The airport is chosen as a major one in Zurich, Switzerland and has the following specifications: Foundation layer is 40 cm gravel and a life span of 100 years is considered. Concrete floor is 22 cm with a concrete reinforcement of 1.8 kg steel/m^2 and a lifespan of 30 years is considered. The distance for transport is 25 km. In order to facilitate a first estimate, the following assumptions are made:

- 70% of the built up area is occupied with building halls.
- 30% are multi storey buildings with an average of 5 floors.
- The height between the floors is 2.7 m.

Operation of the aircraft

The fuel consumption and airborne emissions are especially significant for this process. For the airborne emissions, the location of emissions are separated into three main categories; low population density area, stratosphere and unspecified region. The inventory data include consumption of selected fuel, which is jet fuel kerosene in conventional applications, and direct emissions to air as gaseous emissions, particulate emissions, emissions of heavy metals. The results show the average fuel consumption and emission data caused by an average flight. The allocation between intercontinental (94.6%) and intra-European (5.4%) transport performance is made on basis of the yearly transport performance of aircraft departing from Swiss airports. Data refers to average transport conditions of aircraft departure from Swiss airports.

The aviation transportation segment necessitates fuels with great density of energy and hence it is primarily dependent on liquid hydrocarbon fuels. Alternative aircraft fuels need to carry around definite abilities such as good cold flow possessions, thermal steadiness and low freezing point. The fuel needs to be well matched for the current scheme of the aircraft engine. Sustainable aircraft fuels should satisfy low carbon emission in the complete life cycles. The energy crops used

as the production source should not encounter the food manufacture and ecosystem and also do not damage the atmosphere and do not cause deforestation.

As alternative fuels, the following options are taken into account in the operation of the aircraft. The production method of the alternative fuels are also given here

- Hydrogen: 95% hydrocarbon cracking and 5% salt brine electrolysis as conventional methods, hydropower as renewable resource
- Methanol: Steam reforming process of methane
- Ethanol: Direct hydration of ethylene
- Ammonia: Heavy fuel oil and natural gas reforming as conventional methods, hydropower as renewable resource
- Liquefied natural gas: Liquefaction of natural gas in a liquefaction plant
- Jet Fuel (Kerosene): Production from crude oil

Kerosene

In the production of kerosene, all procedures on the refinery site discounting the emissions from combustion services, comprising waste water treatment, process emissions and direct releases to rivers are accounted for. Explanation of all streams of materials and energy because of the throughput of 1 kg crude oil in the refinery. The multioutput process crude oil in refinery delivers the co-products petrol, bitumen, diesel, light fuel oil, heavy fuel oil, kerosene, naphtha, propane/ butane, refinery gas, secondary sulphur and electricity. The influences of handling are allocated to the different products. Main pointers like energy use were projected based on a survey in European refineries. Inventory represents the distribution of petroleum product to the final consumer including all necessary transports. Transportation of product from the refinery to the end user is the full cycle. Operation of storage tanks and petrol stations are also considered. Emissions from evaporation and treatment of effluents are taken into account.

Ethanol

Though technical aspects are available to decrease the dangers throughout usual aircraft operations, important costs would be related with retrofitting present aircraft to admit on ethanol. Furthermore, the usage of ethanol or butanol would yield decreased operative competences and a lower energy efficiency of aircraft processes. The specific energy and energy density of ethanol are each about 40% lesser than the energy density of conventional jet fuel [67]. The production of ethanol in this study is considered from direct hydration of ethylene including materials, energy uses, infrastructure and emissions. The inventory is modelled with data from plants in Europe and India.

LNG

Liquefied natural gas is natural gas that is refrigerated to the liquid phase at around -162.1°C. Natural gas involves typically of methane, with minor quantities of ethane, propane, and butane, along with other hydrocarbons. LNG is utilized as an intermediate for natural gas transportation for over 50 years where the usage continues to grow. Natural gas is one of the greatest plentiful energy sources with considerable new unconventional resources, such as coal bed methane and shale gas, being established around the world. Additionally, methane hydrates can deliver more energy, in the form of methane, than is included in all other fossil fuels. Methane hydrates are methane particles covered in ice and are possibly accessible about the world. Presently, the extraction of methane hydrates is problematic because of the position of deposits. Moreover,

treatment of the ice needs to be completed with attention so that the methane is not emitted into the air. The key benefit of LNG comparative to conventional jet fuel is the possible magnitude of the reserves. The chief drawback is the storing condition in terms of allocating with a fuel that not only has lower energy density than conventional jet fuel, but that is also cryogenic [67]. LNG could not be well-suited with current aircraft and it would also necessitate substantial expansion of the present worldwide distribution network as all of the airports that service LNG-fueled aircraft would need this fuel. Nevertheless, it is also probable that Fischer-Tropsch synthesis of natural gas to a synthetic fuel would be both financially and ecologically superior to LNG [67]. The carbon dioxide emission can be reduced about 25% by the usage of LNG fuel. Engine scheme is a trouble that has to be taken into account for the commercialization of the LNG fuels. The combustion of LNG fuel releases methane, which is one of the main GHG. The dataset in this study defines the liquefaction of natural gas in a liquefaction plant.

Liquid hydrogen

Liquid hydrogen is considered as alternative jet fuel in the last decades. Liquid hydrogen generated more energy per mass in comparison to conventional aviation fuel, however obliges great storage volume. The combustion of liquid hydrogen fuel origins low emission of GHG in comparison to petroleum based jet fuels. There are likewise a few drawbacks of liquid hydrogen. The generation cost, creation of char and tar as by-products are besides to be faced. The other problematic issue related with the usage of liquid hydrogen is that when mixed with air, it can burn in low concentration which will reason safety complications and the storage of hydrogen as liquid is challenging because it needs low temperature. The emission of moderately high volume of water vapor is a problem related with hydrogen aircrafts [67]. For the hydrogen generation in this study, it is assumed that 95% of hydrogen is produced from cracking of fossil fuels, the remaining 5% is from electrolysis of salt brine. The data represent from raw material extraction until delivery at plant for all processes. To compare the production of hydrogen from renewable raw materials, the methods of electrolysis of water from wind, hydropower, geothermal and solar energy are also evaluated. In renewable cases, the hydrogen production is conducted using electrolyzer consuming 53 kWh per kg of hydrogen.

Liquid ammonia

In terms of conventional resources, naphtha, heavy fuel oil, coal, natural gas coke oven gas and refinery gas can be used as feedstock in ammonia production. Natural gas is the primary feedstock used for producing ammonia worldwide. Hence in the current study, it is assumed that 85% of ammonia is produced via steam methane reforming and 15% is produced via partial oxidation of heavy fuel oil. The values represent mostly present state of the art technology used in European ammonia production plants. In order to compare the production of ammonia based on renewable resources, hydraulic, wind, solar and geothermal energy paths are considered in the analysis. For renewables based ammonia production, the hydrogen is initially produced from electrolysis as performed in previous step of hydrogen production and then it is combined with nitrogen in a Haber-Bosch ammonia plant. Manufacturing process starting with heavy fuel oil and natural gas, air and electricity is considered including the auxiliaries, energy, transportation, infrastructure and land use, as well as wastes and emissions into air and water. Transport of the raw materials, auxiliaries and wastes is include. Carbon dioxide is the by-product generated. Transient or unstable operations are not considered, but the production is assumed to be during stable operation

conditions. Emissions to air are considered as emanating in a high population density area. Emissions into water are assumed to be emitted into rivers.

Methanol

The production of methanol also offers an important market for the use of otherwise flared natural gas. Modern natural gas-to-methanol plants are characterized by methanol selectivity above 99% and energy efficiencies higher than 70%. The raw materials, processing energy, estimate on catalyst use, and emissions to air and water from process, plant infrastructure are included. The process describes the production of methanol from natural gas via steam reforming process to obtain syngas for the production of methanol. There is no CO_2 use and hydrogen is assumed as burned in the furnace. Raw materials, average transportation, emissions to air from tank storage, estimation for storage infrastructure are included for the distribution part where 40% of the methanol is assumed to be transported from overseas. The subject matter particulate emissions cover exhaust- and abrasions emissions. Data for distances from production places to Switzerland are estimated with actual plant capacities. Similar overseas distances assumed. Additional 13% is assumed to be from Norway including tanker transport. Other production is within Europe continent.

Maintenance and operation of the airport

Operation of aircraft infrastructure contains the heat and electricity consumption for aircraft maintenance and buildings in the airport. A high amount of the heat is consumed at the airport is produced on-site via natural gas and oil. Additionally, consumption of water, waste of water and disposal of the wastes are considered. The inventory includes energy expenditures and airport energy infrastructure. Transport services on airport site are included. The use and emissions of de-icing materials are taken into account in addition to land transformation and occupation. The data represent a major airport in Europe. The use of de-icing materials is calculated as the geometric mean of 3 years.

Transportation via aircraft

In this step, all the previous processes are included for determining the overall life cycle results per tkm (tonne-kilometer) by considering the operation of aircraft, production of aircraft, construction and land use of airport, operation, maintenance and disposal of airport. Therefore, inventory refers to the entire transport life cycle.

Table 21 Fuel and energy requirements of various fueled aircrafts

Fuel	Energy Consumption (MJ/tkm)	Energy Consumption (MJ/km)	Fuel Consumption (kg/tkm)
Kerosene (Jet Fuel A)	9.35	343.5	0.21
Hydrogen	8.62	316.5	0.07
Ammonia	9.53	350	0.51
Methanol	9.80	360	0.49
Ethanol	9.80	360	0.33
Natural Gas	12.53	460	0.25

Airport infrastructure expenditures and environmental interventions are accounted for using a weighted average of Intra-European and intercontinental freight transport performance at the

airport. Aircraft manufacturing is allocated based on the total life span of an aircraft and its transport performance with a value of 23.5 tonne per aircraft unit. For the manufacturing of aircrafts modern production technologies are taken into account. The fuel and energy requirements of various fueled aircrafts are listed in Table 21 which are taken into account in the analyses.

3. Results and Discussion

The full life cycle of an aircraft running on the conventional jet fuel and various alternative fuels, including hydrogen, are assessed in terms of environmental impact and performance in SimaPro LCA software based on the inventory data. The results presented here are given on per tonne-km basis which represents a wider approach for all aircraft classes regardless of the split between passengers and cargo payloads onboard the aircraft. The analyzed impact categories are: Human toxicity which is related with toxic substances on the human environment and given in terms of 1,4-dichlorobenzene DB equivalents, global warming which represents the greenhouse gases to air associated with the climate change and given in kg CO_2 eq. (equivalents) unit, depletion of abiotic resources which is related to extraction of minerals/fossils and given in terms of kg Sb Antimony equivalents, stratospheric ozone depletion is the ozone depletion potential of various gasses in kg CFC-11 equivalent unit, land use which is the extraction of raw materials, production processes, agricultural land, area of industrial territory, landfill sites, incineration plant area, transport, use processes and given in terms of m^2a. The land use refers to the total arrangements, activities and inputs undertaken in a certain land cover type. The term land use is also used in the sense of the social and economic purposes for which land is managed. In the CML2001 the life cycle impact assessment method, competition is measured as occupied area*time (m^2a) where a represents the annual (year) [60].

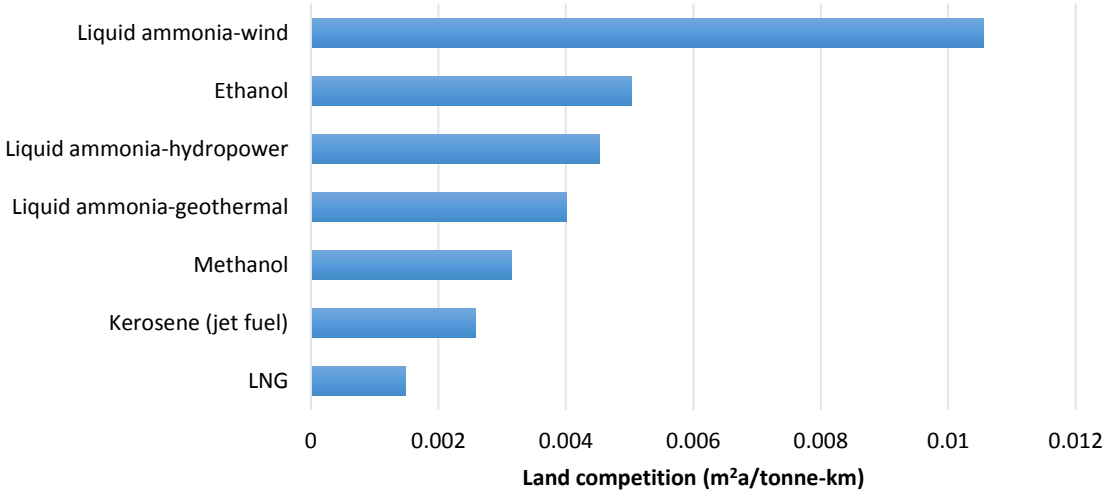

Figure 75 Land use in full life cycle of various fueled aircrafts per travelled tonne-km

The feedstock generation is the process which can cause land employment. Land usage per entity of fuel is lowermost for the LNG case as shown in Fig. 75 due to its higher overall fuel heating value. However land use intensities for jet fuel and methanol pathways are relatively similar and lower than liquid ammonia when compared with the wider collection of alternative fuel pathways. The annual land use intensities liquid ammonia (geothermal based) and LNG in the study are found to be 0.004 m^2/tonne-km and 0.0014 m^2/ tonne-km, respectively. For LNG, the

land occupation and human toxicity potentials are lower than for kerosene. Liquid ammonia from geothermal energy has comparable land use values with methanol and ethanol fueled aircrafts.

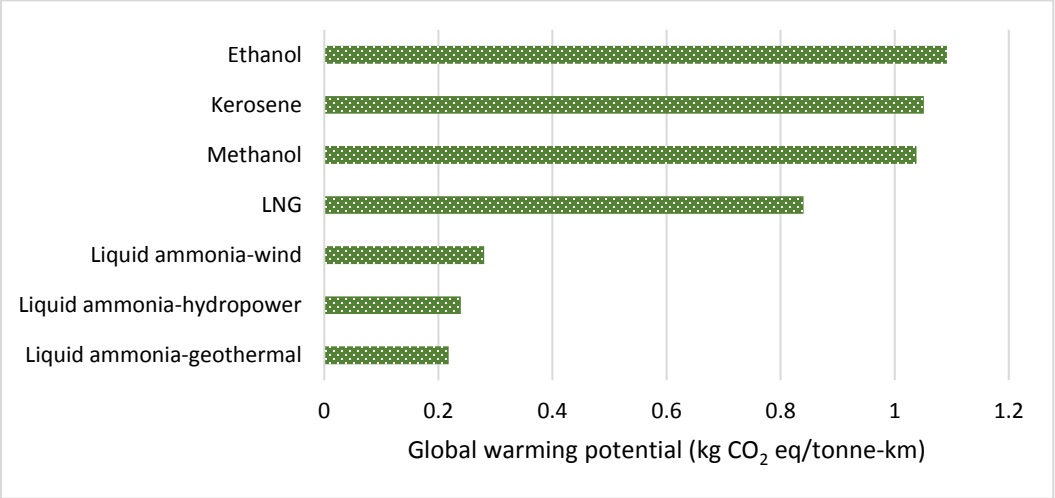

Figure 76 Global warming potential of various fueled aircrafts per travelled tonne-km

Though CO_2 is the furthermost significant GHG and is the major emission from the whole life cycle, quantifying the total amount of greenhouse gases produced is the key to examining the gross warming potential (GWP) of the different systems as shown in Fig. 76. The GWP of the cases is a mixture of CO_2, CH_4 and N_2O emissions. Ethanol fueled aircraft has the highest GWP among others. Liquid ammonia has the lowest values among all other fuels. Using renewable resources such as wind, geothermal and hydropower, the total GHG emissions are considerably lower for liquid ammonia. The overall GWP value of ethanol is the highest corresponding to 1.09 kg CO_2 eq/tonne-km since it comes from ethylene which is a hydrocarbon. Renewable energy usage in the fuel production processes decreases the overall GHG emissions. The hydropower based ammonia fueled aircraft releases about 0.24 kg CO_2 eq per tonne-km. This value goes down to 0.21 for kg CO_2 eq/tonne-km for ammonia fueled aircraft in case the renewable source is geothermal energy.

Ozone depletion potential of several gasses are specified in kg CFC-11 equivalent/kg emission where the time span is infinity. Fig. 77 presents the life cycle kg CFC-11 eq. emissions of the aircrafts with different fuels per kilometer travelled. It is quite high for methanol and kerosene while it is considerably less for liquid ammonia and LNG. Furthermore, utilization of renewable based ammonia is better than kerosene, methanol and ethanol in terms of ozone layer depletion.

In contrast to other categories, LNG has quite higher value in comparison with methanol as illustrated in Fig. 78. This is caused by the exploration and extraction process of natural gas. Similarly, natural gas dependent fuel such as methanol has high abiotic depletion values. Due to higher fuel flow rate for ammonia, it yields about 0.01 kg Sb eq/tonne-km. However, renewable based ammonia driven aircrafts can significantly decrease the depletion of abiotic resources down to 0.0014 kg Sb eq/tonne-km which corresponds to about 10% of conventional steam methane reforming based ammonia fueled aircraft.

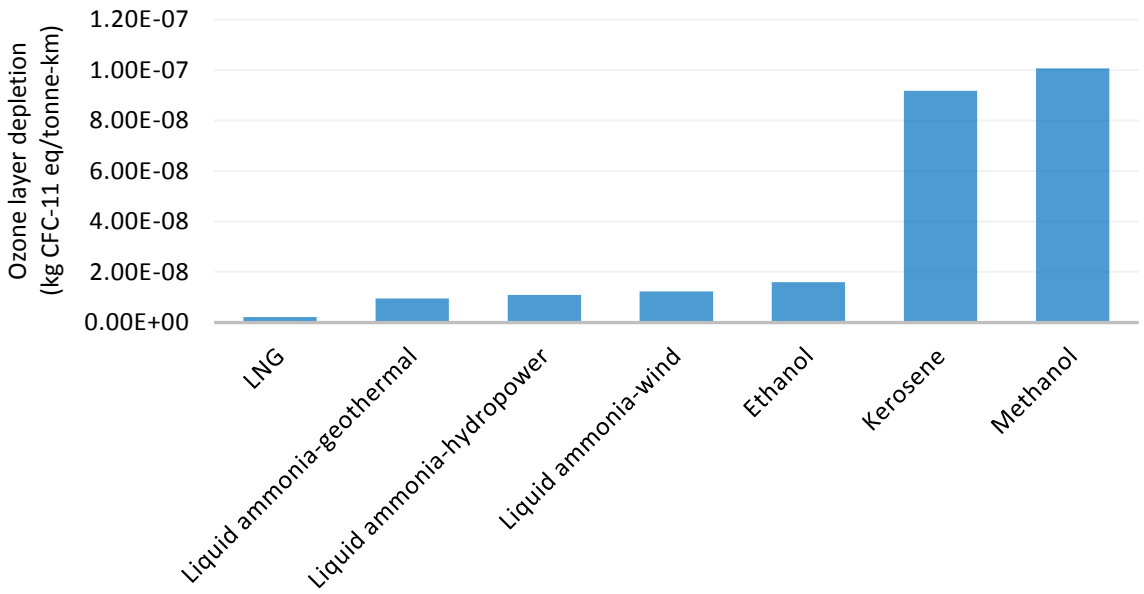

Figure 77 Ozone layer depletion values of various fueled aircrafts per travelled tonne-km

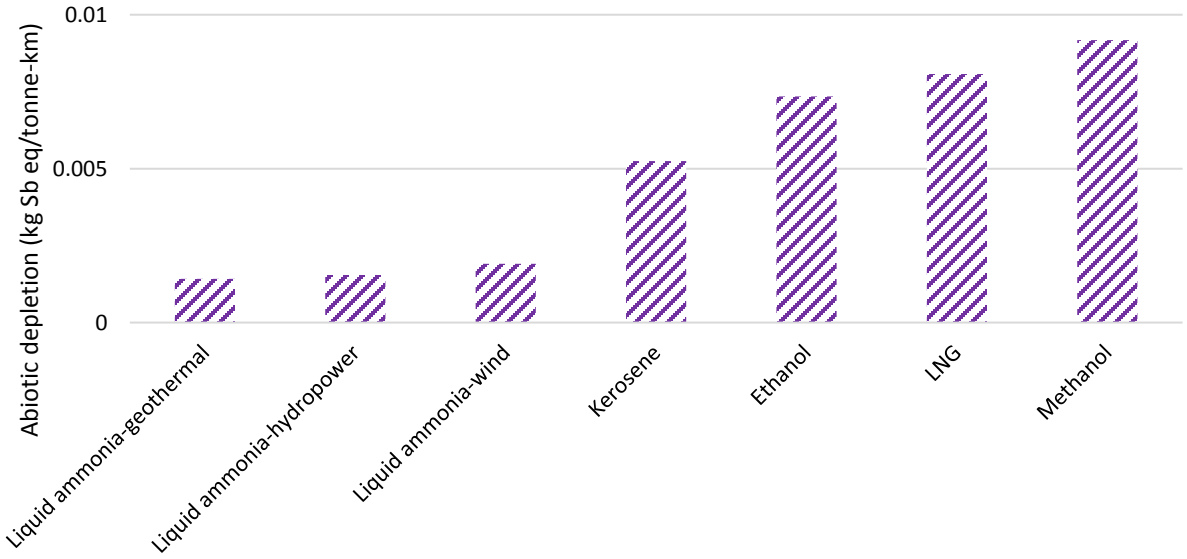

Figure 78 Abiotic depletion values of various fueled aircrafts per travelled tonne-km

Among all alternative aviation fuels, the kerosene jet fuel, methanol and ethanol human toxicity values are greater as shown in Fig. 79. On contrary, LNG and liquid ammonia have significantly lower toxic impacts on humans. Geothermal based ammonia fueled aircraft has the lowest human toxicity value among others whereas methanol has the highest value. It is attributed to operation of aircraft with a share of 93%. Natural gas burned in the furnace has a portion of 3% where it is also utilized in the methanol production process. Copper and ferrochromium are used for steel and building materials during the construction of the airport. Ammonia fuel from geothermal resource

has comparable toxicity value corresponding to 0.04 kg 1,4- DB eq/tonne-km with LNG corresponding to 0.03 kg 1,4- DB eq/tonne-km.

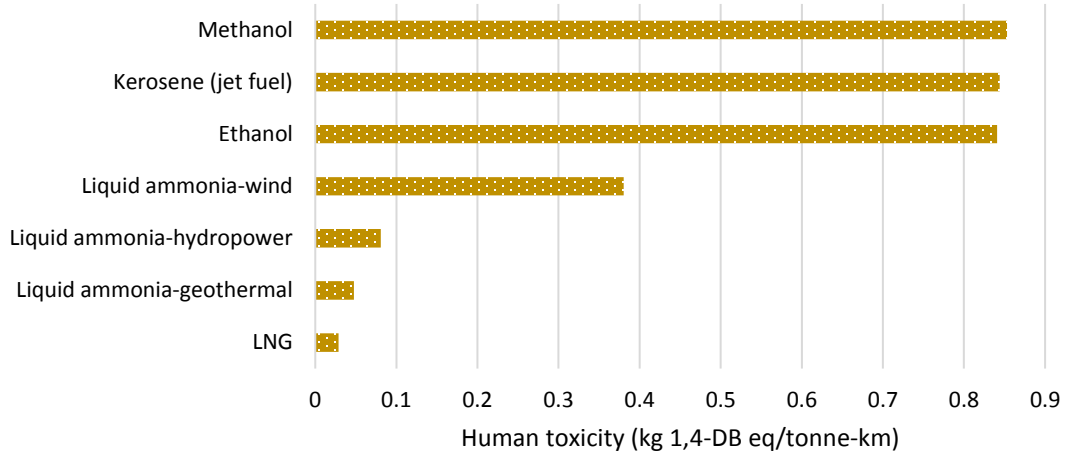

Figure 79 Human toxicity values of various fueled aircrafts per travelled tonne-km

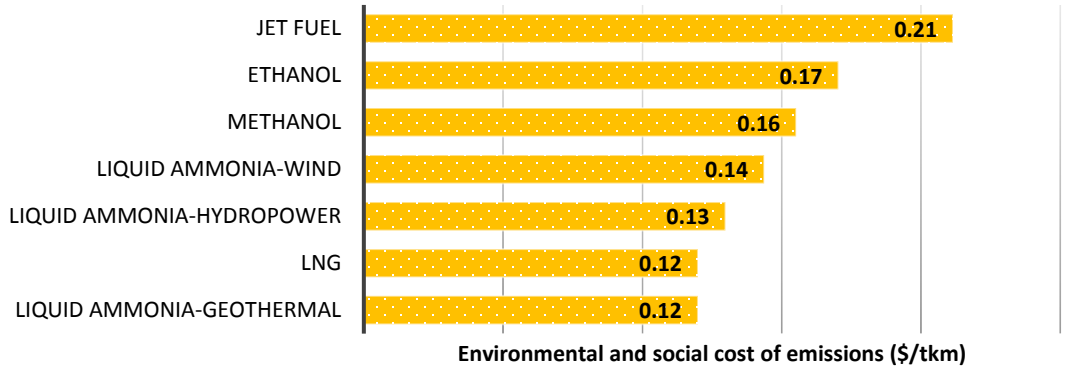

Figure 80 Total environmental and social cost of emissions for various fueled aircrafts from conventional and renewable resources

The marginal external price of a unit of GHG emissions is identified as environmental and social costs of emissions. In the literature, these values are estimated by using an integrated assessment (IAM) framework. IAM framework employs: a reference socio-economic situation, a model of the connection between emissions and temperature variation, and a link between the temperature variation and financial damages. Fig. 80 shows the calculated environmental and social cost of emissions. Since, they are associated with the amount of various type of emissions, kerosene jet fuel and fossil fuel based ammonia represent higher costs.

The environmental and social costs methodology is essential, for the reason that it gives a unique perspective on the economic impact of emissions on environment and human health. Environmental and social costs of HC, CO, NO_x, PM, and CO_2 emissions of various fueled aircrafts are evaluated in terms of USD/tonne-km as shown in Fig. 81 and Table 22.

Table 22 Environmental and social cost of emissions for complete life cycle of various fueled aircrafts from conventional resources

		Environmental and social cost of emissions (USD/tonne-km)						
Substance	Environmental and social impact (USD/kg)	Methanol	kerosene	liquid ammonia-hydropower	liquid ammonia-wind	liquid ammonia-geothermal	methanol	LNG
Particulates, < 2.5 um	229.2	0.0122	0.011	0.018	0.025	0.012	0.0942	0.0629
Carbon monoxide	4.16	0.0281	0.005	0.035	0.036	0.034	0.02794	0.0316
Nitrogen oxides	24.8	0.0240	0.113	0.055	0.056	0.053	0.02386	0.0121
Hydrocarbon	8.27	0.0314	0.008	0.007	0.009	0.007	0.02315	0.0124
Carbon dioxide	0.07	0.074	0.073	0.015	0.018	0.014	0.07086	0.057

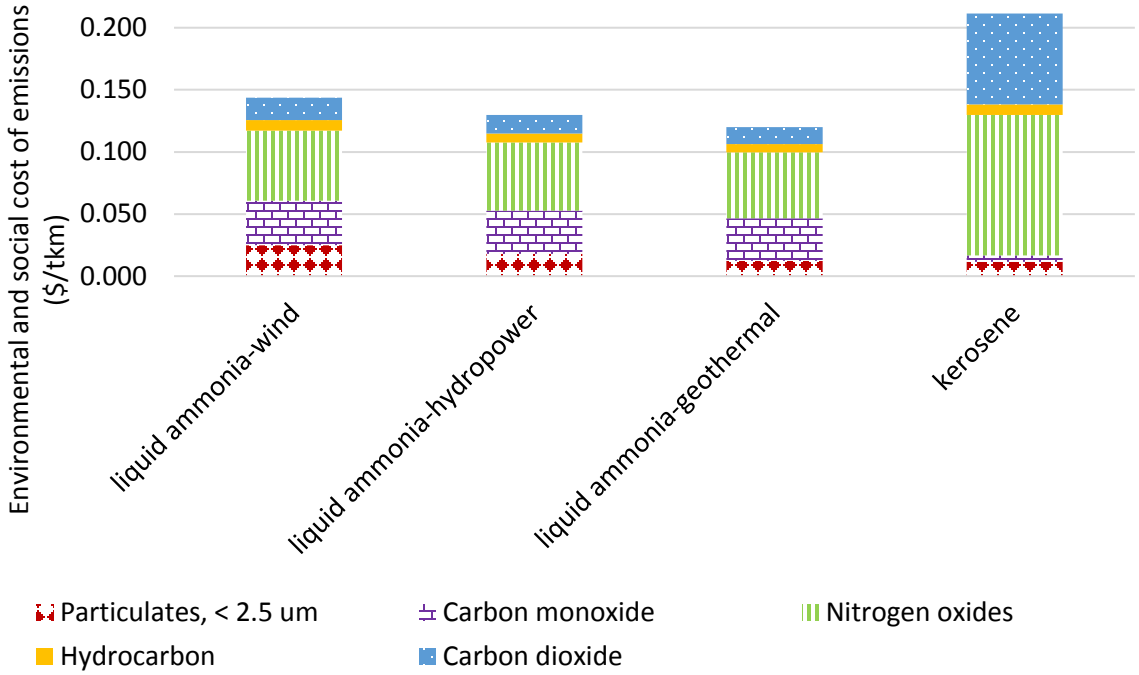

Figure 81 Comparison of total environmental and social cost of emissions for renewable based ammonia driven aircrafts and kerosene driven aircraft

However, as illustrated in Fig. 80, renewable based ammonia yields lower environmental and social cost of emissions in comparison with kerosene. Specifically, Fig. 81 shows renewable only based routes for ammonia in comparison with kerosene. It is noted that the total environmental and social costs for renewable based ammonia fueled aircrafts are considerably lower than conventional kerosene jet fuel.

Fig. 82 and Table 16 illustrate the cost of flight for a 5600 km distance in which alternative fuels are used for the aircrafts. Although LNG represented better environmental performance, the cost of aircraft operation in terms of fuel is the highest for ethanol and LNG.

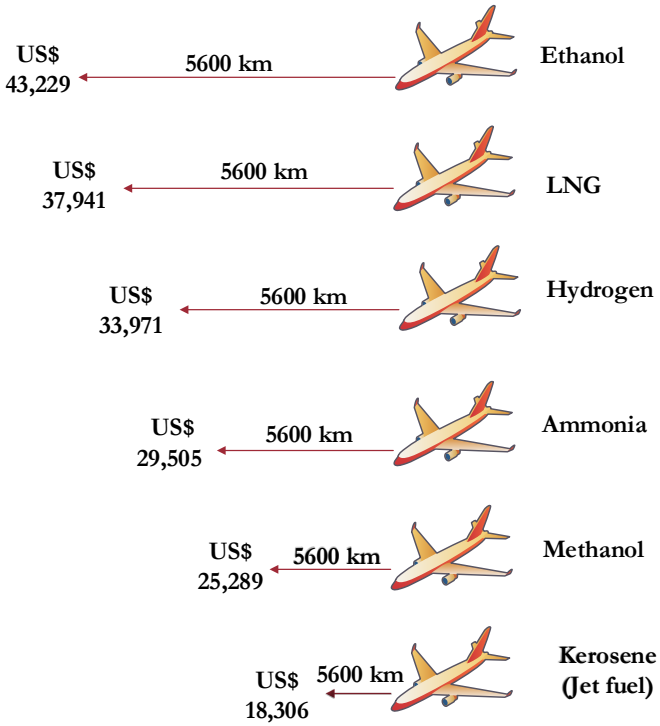

Figure 82 Comparison of fuel costs during the operation of aircrafts for the given range

In the cost calculations, current conventional based routes are taken into account for comparison purposes. Hydrogen fueled aircraft has lower cost compared to these two alternatives. Since the production of kerosene from crude oil is a more mature technology, it represents the lowest cost among all. Liquid ammonia is also low cost alternative compared to hydrogen as seen in Table 23. Hydrogen has the highest cost per unit mass, however, having higher heating value makes hydrogen a cost effective solution. Liquid ammonia here is considered from steam methane reforming, hence developing renewable technologies will enable lower cost of operation for liquid ammonia driven aircrafts.

Table 23 Average fuel consumption rates and fuel costs for selected alternative fuels

Fuel	Fuel Consumption (kg/km)	Fuel Consumption (kg/tonne-km)	Fuel Cost (USD/kg)
Kerosene (Jet fuel)	7.99	0.217	0.409
Methanol	18.06	0.492	0.250
Ammonia	18.82	0.512	0.280
Hydrogen	2.64	0.071	2.300
LNG	9.46	0.257	0.716
Ethanol	12.47	0.339	0.619

Source: Refs. [60,61]

The performances of the aircrafts are also compared in terms of energy and exergy efficiencies in Fig. 83. In the calculations, two different efficiencies are taken into account namely: production efficiency and combustion efficiency. The production efficiency represent the process

from raw material to final product as fuel. The combustion efficiency is the process of utilization in the aircraft. Although, there can be storage and transportation losses, the overall efficiency can be calculated based on these two main efficiencies by neglecting the storage and transportation efficiencies. Here, conventional method (SMR) is taken into account for hydrogen and ammonia rather than renewable based options.

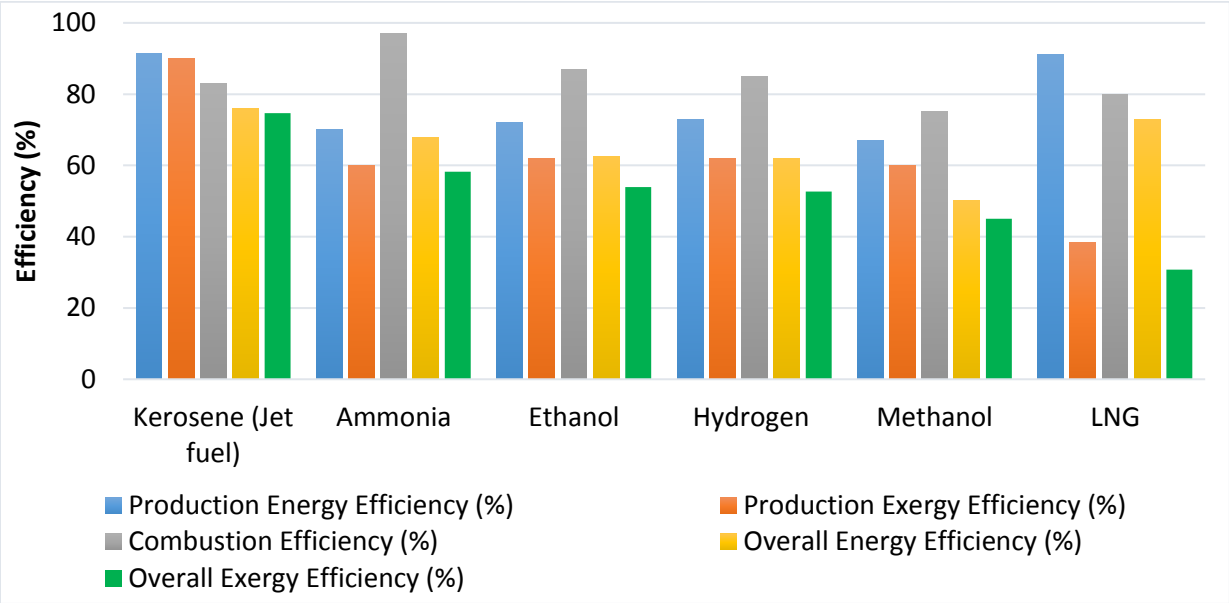

Figure 83 Comparison of energy and exergy efficiencies of various fueled aircrafts

The efficiency values are taken from the open literature [11,68,69] and calculated accordingly. Kerosene has the highest production energy and exergy efficiencies yielding the highest overall efficiency. Liquefaction of natural gas in an energy intensive process causing lower exergetic efficiency, hence lower overall efficiency for utilization in aircrafts. Ammonia has high combustion efficiency which results in the second highest overall exergy efficiency among the other alternative fuels. Overall efficiencies of methanol are lower than other fuels. It is noted that the selected alternative fuels may represent higher efficiencies but also higher environmental impacts depending on the production process and technology.

4. Concluding Remarks

In this study, a well-to-wake approach is used in order to determine the overall life cycle emissions of an aircraft running on various conventional and alternative fuels. Operation of the aircraft, construction, maintenance and operation of airport, manufacturing of the aircraft, production and utilization of fuel are considered as a complete LCA cycle. Although there are modifications required to achieve the aviation fuel qualifications for such alternative fuels, the long term viability and environmental sustainability promote them attractive solutions for the future of aviation industry. The following conclusion remarks can be derived from this study:

- Alternative aviation fuels including ammonia and LNG are more environmentally friendly options than kerosene.
- Renewable sources based ammonia routes represent the most preferable option in terms of environmental impact.

- Global warming potential of LNG (0.84 kg CO_2 per tonne-km) and methanol (1.03 kg CO_2 per tonne-km) driven aircrafts are lower than currently used kerosene based jet fuels.
- Renewable resources based ammonia production considerably lowers the environmental impacts corresponding to 0.23 kg CO_2 per tonne-km for hydropower route.
- Operation of the aircraft has almost equivalent share (40.7%) with operation and maintenance of the airport (44.6%) in total GHG emissions. Hence, the energy supply of airport facilities are also critical when complete life cycle is evaluated.
- The environmental cost analyses reveal that nitrogen oxides are the highest contributor followed by carbon dioxides.
- The cost of flight is currently lower for kerosene jet fuels however by developing technologies the cost of flight for ammonia can compete with conventional jet fuels.

CHAPTER 7:AMMONIA IN ROAD TRANSPORTATION

Current vehicles can be converted to run on ammonia by minor modifications. The general requirements for the conversion of a diesel vehicle engine to dual fuel ammonia engine can be written as follows:

- Installation of separate low pressure ammonia injectors
- Replacement of copper and brass parts with stainless steel parts.
- Specific arrangement to reduce the injected flow rate of diesel
- Replacement of gaskets, nuts and bolts interacting with ammonia with stainless steel.
- Installation of control unit for ammonia injection
- Installation of temperature and pressure measurement units at intake manifold, engine cooling fluid, ammonia flow regulator and exhaust.
- In case of on-board hydrogen production, a decomposition unit which reduces total diesel consumption to increase the ammonia combustion performance.
- Installation of non-corrosive fuel ammonia tank

Ammonia can be used for multiple purposes in the vehicle. It is a fuel, refrigerant and reduction agent. The patent developed by UOIT proposes the utilization of ammonia in these major areas. The requirements for patent US8272353 B2 "Apparatus for using ammonia as a sustainable fuel, refrigerant and NOx reduction agent" [70] can be summarized as follows:

1. *Configuration: ammonia-fueled system for vehicular power and cooling generation*

- Adaptation of fuel storage tank to store ammonia
- A heat exchanger operably connected to the fuel tank
- A decomposition and separation unit operably connected to the heat exchangers and having a hydrogen conduit and a nitrogen conduit,
- The decomposition and separation unit is adapted to separate the heated ammonia into hydrogen and nitrogen and stream them into the hydrogen and nitrogen conduits
- an internal combustion engine operably connected to the hydrogen conduit.

2. *Configuration: ammonia-fueled hybrid system for propulsion, power, heating and air-conditioning*

- a thermally insulated fuel tank adapted to receive ammonia;
- a condenser operably connected to the fuel tank;
- an evaporator operably connected to the fuel tank,
- the condenser and the linear piston;
- a selective catalytic reductor operably connected to the fuel tank and operably connected to the generator,
- the selective catalytic reductor is adapted to combine ammonia with nitrogen to reduce the production of nitrogen oxides.

3. *Configuration: ammonia based fuel-cell system with combined power, heating and refrigeration*

- the fuel tank adapted to receive ammonia;
- a heater operably connected to the fuel tank;
- a fuel-cell operably connected to the heater;

- a turbocharger operably connected to the fuel-cell;
- an electrical drive generator operably connected to the turbocharger.

4. Configuration: ammonia based cooling system

- a thermally insulated tank adapted to receive ammonia;
- a heat exchanger; and a throttling valve operably connected between the tank and the heat exchanger;
- adjusting the throttling valve adjusts the evaporation temperature of the ammonia in the tank.

5. Configuration: a fueling system

- a decomposition and separation unit adapted to receive ammonia, delivering hydrogen and nitrogen as separate streams;
- a nitrogen expanding turbine operably connected to a heat recovery heat exchanger.

6. Configuration: an ammonia fueled internal combustion engine

- a thermally insulated fuel tank adapted to store ammonia;
- a mechanical refrigeration unit having a sub-cooler coil immersed in ammonia in the fuel tank;
- an internal combustion engine operably connected to the fuel tank and the mechanical refrigeration unit.

Conversion process to ammonia vehicle is quite similar with compressed natural gas and propane vehicles. If current fuel tank size of a vehicle is used for ammonia only, the range would be about 50-60% of gasoline only vehicle. The estimated conversion costs of a conventional diesel/gasoline passenger vehicle to various alternative fueled vehicles are given below.

- Propane Conversion Kit: $600-$1300
- Compressed Natural Gas Conversion Kit: $4000-$8000
- Ammonia Conversion Kit: $5000-$10,000

1. Life Cycle Assessment of Vehicles

A characteristic life cycle of a vehicle technology can be categorized into two main steps, namely fuel cycle and vehicle cycle. In the fuel cycle, the processes beginning from the feedstock production to fuel utilization in the vehicle are considered as shown in Fig 84. In the vehicle cycle, utilization of fuel is considered. The results presented here are given on per km basis based on the fuel consumption rates given in Table 24.

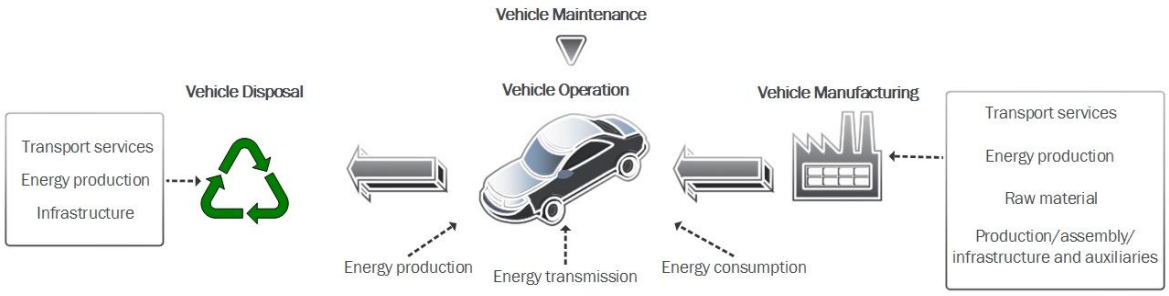

Figure 84 Complete life cycle of vehicles including fuel/vehicle cycle.

Table 24 Energy consumptions per km for the selected vehicles

Fuel		Fuel/Energy Consumption	Unit
Gasoline		0.0649108	kg/km
Diesel		0.0551536	kg/km
M90	Methanol (90%)	0.1180535	kg/km
	Gasoline (10%)	0.0060664	kg/km
Hydrogen		0.0195508	kg/km
Ammonia		0.0926600	kg/km
EV		0.2167432	kWh/km
HEV	Electric (50%)	0.1083716	kWh/km
	Gasoline (50%)	0.0324554	kg/km
CNG		0.0603914	kg/km
LPG		0.0576296	kg/km

Source: [71]

The specific conditions for the selected vehicles are presented herein:

- Gasoline: All processes on the refinery site excluding the emissions from combustion facilities, including waste water treatment, process emissions and direct discharges to rivers are accounted for. The inventory data also includes the distribution of petroleum product to the final consumer including all necessary transports. Transportation of product from the refinery to the end user is considered together with operation of storage tanks and petrol stations. Emissions from evaporation and treatment of effluents are accounted for. Particulate emissions cover exhaust- and abrasions emissions.
- Diesel: Diesel is evaluated as low-Sulphur at regional storage with an estimation for the total conversion of refinery production to low-Sulphur diesel. An additional energy use (6% of energy use for diesel production in the refinery) has been estimated. The other processes are similar to gasoline. Particulate emissions cover exhaust- and abrasions emissions.
- CNG: Natural gas with a production mix at service station is taken into account. The inventory data contains electricity necessities of a natural gas service station together with emissions from losses. The data set represents service stations with high (92%), medium (6%) and low (2%) initial pressure. VOC emissions are obtained from gas losses and contents of natural gas. Particulate emissions cover exhaust- and abrasions emissions.
- Hydrogen: Hydrogen is produced during cracking of hydrocarbons. It includes combined data for all processes from raw material extraction until delivery at plant. The output fractions from an oil refinery are composite combinations of mainly unreactive saturated hydrocarbons. The first processing step in converting such elements into feedstock suitable for the petrochemical industries is cracking. Particulate emissions cover exhaust- and abrasions emissions. In order to have comparable results where hydrogen comes from non-fossil fuels such as solar PV and nuclear, they are also taken into account in the analyses by applying water electrolysis route. The electrolyzer is assumed to consume about 53 kWh electricity for one kg of hydrogen production.
- Ammonia: Ammonia synthesis process is Haber-Bosch which is the most common method in the world. Ammonia production requires nitrogen and hydrogen. In this study, hydrogen is assumed to be from hydrocarbon cracking as explained in the previous paragraph. In the life cycle assessment of nitrogen production, electricity for process, cooling water, waste heat and infrastructure for air separation plant are included. Particulate emissions cover exhaust- and

abrasions emissions. In order to have comparable results where ammonia comes from non-fossil fuels such as solar PV and nuclear, they are also taken into account in the analyses. The generated hydrogen from electrolyzers are used for ammonia synthesis plant.

- EV: Electricity consumption is included. Particulate emissions comprise exhaust and abrasions emissions. Heavy metal emissions to soil and water caused by tire abrasion are accounted for. In the electricity usage process, electricity production mix, the transmission network and direct SF6-emissions to air are included. In order to present a renewable based scenario for electric vehicles, a mixture of renewables for energy requirement during the operation are also evaluated consisting of 25% biomass, 25% solar PV, 25% wind power and 25% hydropower.
- HEV: Hybrid car is assumed to be 50% electric and 50% gasoline with ICE. Electricity and gasoline consumptions are included. Particulate emissions comprise exhaust and abrasions emissions. Heavy metal emissions to soil and water caused by tire abrasion are accounted for. For the hybrid vehicle's electricity, a mixture of renewables for energy requirement during the operation are also evaluated consisting of 25% biomass, 25% solar PV, 25% wind power and 25% hydropower.
- Methanol: The selected fuel M90 consists of 90% methanol and 10% gasoline. The raw materials, processing energy, estimate on catalyst use, and emissions to air and water from process, plant infrastructure are included. The process describes the production of methanol from natural gas via steam reforming process to obtain syngas for the production of methanol. There is no CO_2 use and hydrogen is assumed as burned in the furnace. Raw materials, average transportation, emissions to air from tank storage, estimation for storage infrastructure are included for the distribution part where 40% of the methanol is assumed to be transported from overseas. Particulate emissions cover exhaust- and abrasions emissions.
- LPG: All processes on the refinery site excluding the emissions from combustion facilities, including waste water treatment, process emissions and direct discharges to rivers are considered. All flows of materials and energy due to the throughput of 1 kg crude oil in the refinery is accounted for. Refinery data include desalting, distillation (vacuum and atmospheric), and hydro treating operations. Particulate emissions cover exhaust- and abrasions emissions.

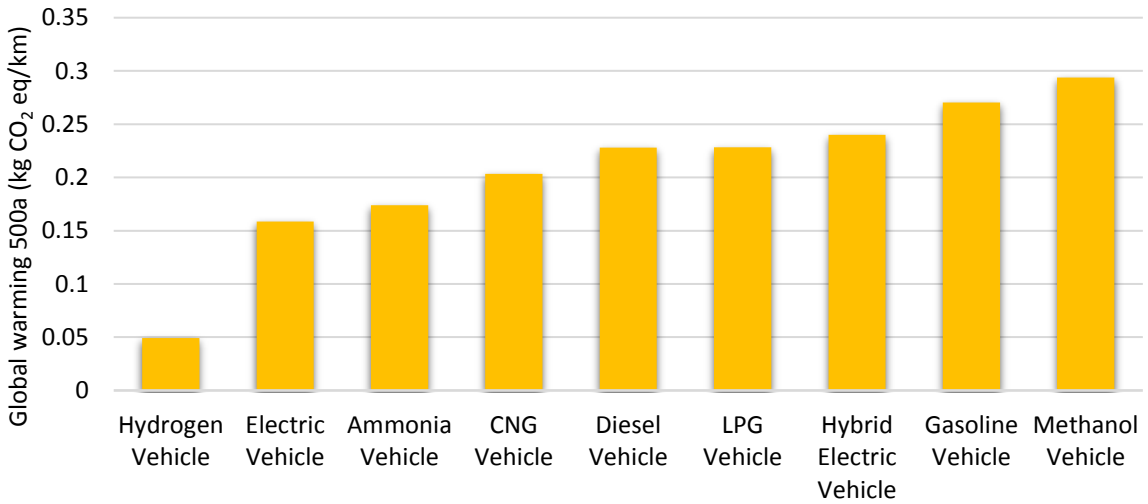

Figure 85 Life cycle comparison of global warming results for various vehicles

The global warming potentials of assessed vehicles are comparatively shown in Fig. 85. The lowest GHG emissions are observed in hydrogen, electric and ammonia vehicles corresponding to 0.049 kg CO_2 eq/km, 0.15 kg CO_2 eq/km and 0.17 kg CO_2 eq/km, respectively. Hydrogen consumption is quite lower than ammonia consumption in the passenger car because of higher energy density. It is an expectable result that EVs also yield lower global warming potential, however production pathway of electricity has a key role in GHG emissions. If electricity production can be realized by renewable sources such as solar, biomass, hydropower and wind energy, total emissions would decrease for both EVs and HEVs.

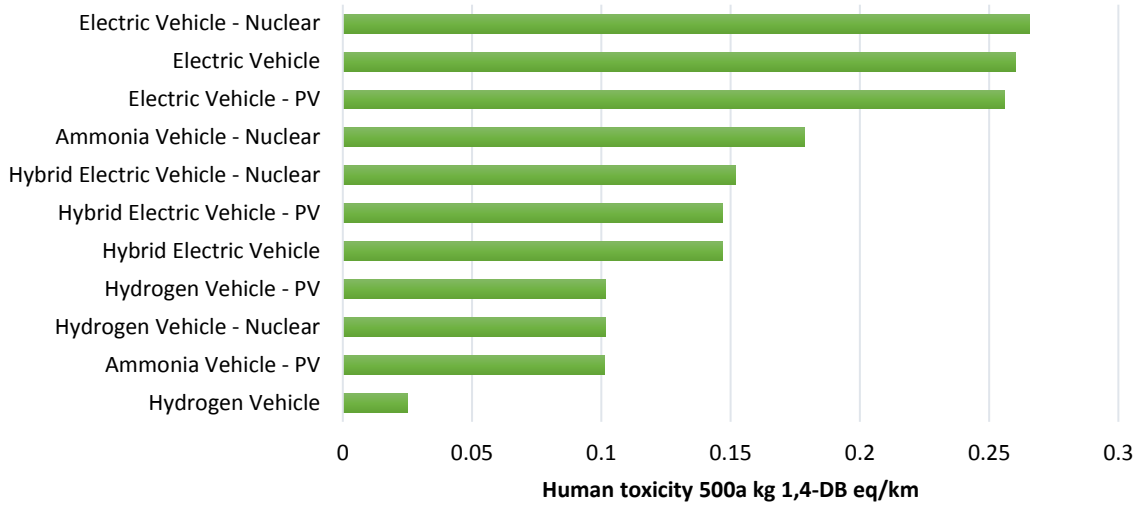

Figure 86 Life cycle comparison of human toxicity results for various vehicles from nuclear energy and solar PV routes

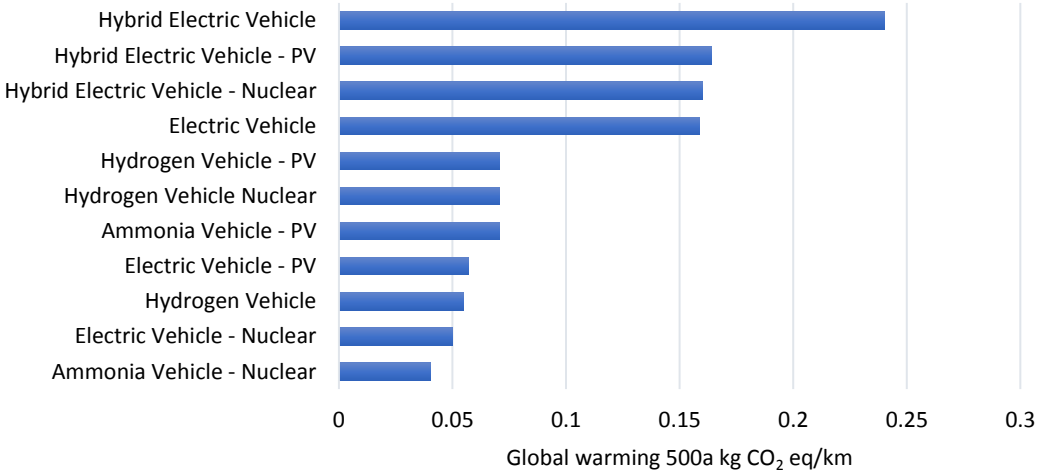

Figure 87 Life cycle comparison of global warming results for various vehicles from nuclear energy and solar PV routes

The electricity from nuclear (25%), biomass (25%), hydropower (25%) and solar PV (25%) are equally used only for the operation processes of the EVs and HEVs vehicles as renewable mix. Utilization of renewable electricity for EVs, HEVs, ammonia and hydrogen vehicles are comparatively shown for various impact categories. For human toxicity category, using solar and

nuclear energy does not cause significant reductions for EVs and HEVs as shown in Fig. 86. However, for global warming and abiotic depletion categories, both solar energy and nuclear energy routes lower the environmental impacts more than 50%.

Ammonia driven vehicle where the ammonia is produced from nuclear electrolysis method yield the lowest GHG emissions corresponding to about 0.04 kg CO_2 eq. per km as shown in Fig. 87. Hydrogen and EVs (from nuclear and PV) have quite similar greenhouse gas emissions in the range of 0.049-0.057 kg CO_2 eq. per km. In terms of abiotic depletion values, hydrogen vehicle still yields the lowest value whereas nuclear routes for ammonia and EVs further decrease the abiotic depletion impact as shown in Fig. 88.

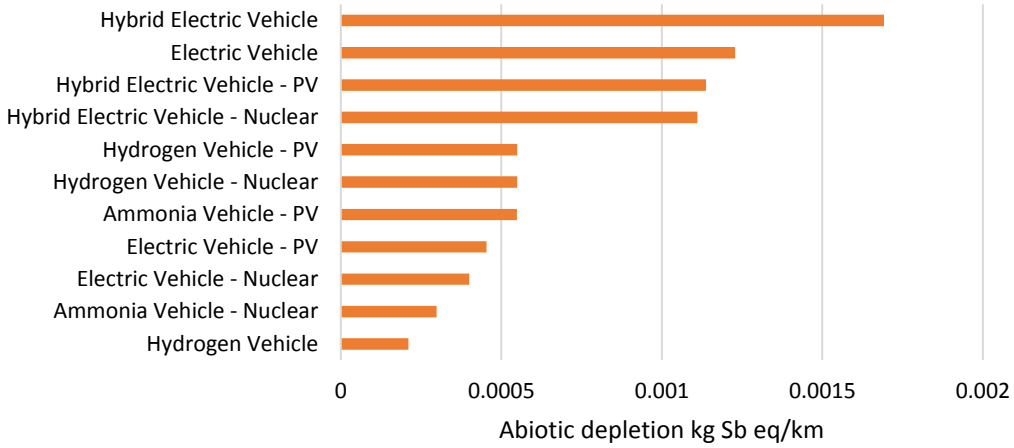

Figure 88 Life cycle comparison abiotic depletion for various vehicles from nuclear energy and solar PV routes

The results show that hydrogen and ammonia vehicles are the most environmentally benign ones in most of the environmental impact categories. Ammonia as a sustainable and clean fuel has lowest global warming potential after EVs and yield lower ozone layer depletion values than EVs. However, in case renewables are used both for ammonia vehicles and EVs, ammonia can suggest lower environmental impacts. Although EVs do not emit direct CO_2 during operation, the production and disposal processes of batteries bring some consequences which harm the environment in terms of acidification, eutrophication and human toxicity.

CHAPTER 8:ON-BOARD AMMONIA UTILIZATION

In this section, a comparative life cycle assessment of a hydrogen fueled car with on-board ammonia decomposition is conducted. Ammonia is used as the fuel source of hydrogen which is stored in anhydrous ammonia storage tank. Ammonia is decomposed into hydrogen and nitrogen on-board to fuel internal combustion engine of the car. Hydrogen production via ammonia decomposition is an endothermic process which is also a reversible chemical reaction. The storage and transportation of ammonia is similar to liquefied petroleum gas (LPG) which is commonly used for the current automobile industry. Ammonia can be produced by extracting nitrogen from air and hydrogen from water and combining them with the help of any type of energy source. The theoretical thermal efficiency under adiabatic conditions for a thermocatalytic reaction is about 85% as relative to the energy of the released hydrogen. If no other source of energy is available, at least 15% of the available hydrogen energy content will be sufficient to supply the necessary heat of hydrogen production reaction. In the present study, the life cycle environmental assessment of a hydrogen fueled car using on-board ammonia decomposition is carried out in which ammonia is synthesized via (i) steam methane reforming (SMR) , (ii) solar PV (iii) wind energy. SMR based ammonia production is the mostly used option in the world as of year 2016. In the analyses, manufacturing process starting with heavy fuel oil, natural gas, air and electricity is considered together with auxiliaries, energy, transportation, infrastructure and land use, as well as wastes and emissions into air and water. In addition, transport of the raw materials, auxiliaries and wastes is also included. Using the LCA methodology, the environmental impacts of using a hydrogen fueled internal combustion engine vehicle is comparatively identified and quantified from cradle to grave.

1. Life Cycle Assessment of On-Board Ammonia Cracking Vehicles

Ammonia can be decomposed thermo-catalytically to achieve hydrogen according to the following endothermic reaction [72]:

$$\frac{2}{3}\mathrm{NH_3} + 30.1\,\frac{\mathrm{kJ}}{\mathrm{mol}}\,\mathrm{H_2} \rightarrow \mathrm{H_2} + \frac{1}{3}\mathrm{N_2} \quad (7)$$

Here, the obligatory enthalpy signifies 10.6% of HHV or 12.5% of the lower heating value (LHV) of the generated hydrogen. The ammonia decomposition reaction does not need catalysis to be performed at high temperatures for example over 1,000 K; though, at inferior temperatures, the reaction rate is too little for practical applications such as hydrogen generation for energy conversion. At 400°C, the equilibrium conversion of NH_3 is very high at 99.1% [72] and at about 430°C, almost all ammonia is converted to hydrogen at equilibrium, below atmospheric pressure circumstances [72]. A schematic diagram of on-board ammonia usage is shown in Fig. 89.

There is a big array of catalysts appropriate to ammonia decomposition (e.g., Fe, Ni, Pt, Ir, Pd, and Rh), nonetheless ruthenium (Ru) seems to be the finest one when reinforced with carbon nanotubes, making hydrogen at additional than 60 kW equal power per kilogram of catalyst [72]. Over ruthenium catalysts, at temperatures lower than about 300°C, recombination of nitrogen atoms is rate limiting, while at temperatures higher than 550°C, the cleavage of ammonia's N–H bond is rate limiting. Though, the activation energy is greater at low temperature (180 kJ/mol) and inferior at higher temperatures (21 kJ/mol). The finest temperature range for ammonia decomposition over ruthenium catalysts may be 350°C to 525°C, which proposes that flue gasses from hydrogen ICEs, other hot exhausts from burning procedures, or electrochemical power conversion in high-temperature fuel cells can be used to drive ammonia decomposition [72,73].

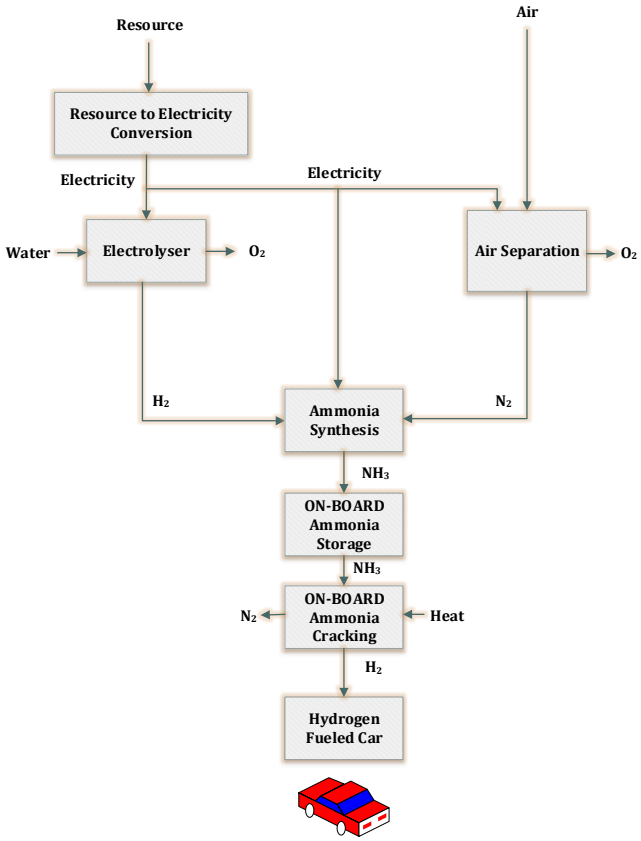

Figure 89 The complete process describing the production, storage and decomposition of ammonia for hydrogen driven vehicle

Here, the following hydrogen production routes required for ammonia synthesis are considered in LCA analyses:

- Steam methane reforming (SMR)
- Solar PV assisted water electrolysis
- Wind energy assisted water electrolysis

In LCA, ammonia synthesis process is Haber-Bosch. Catalyst is the ruthenium based catalyst for on-board ammonia cracking.

The following LCA phases are accounted for:

- manufacturing of the vehicle
- operation of the vehicle (including the fuel production)
- maintenance of the vehicle
- disposal of the vehicle

Considering all these processes, the environmental impact categories are defined and results are obtained as shown in Fig. 90 to Fig. 93 for ammonia cracking hydrogen vehicle. Here, ammonia is decomposed at elevated temperature thermo-catalytically. The abiotic depletion results of on-board ammonia cracking vehicles from various resources and gasoline vehicle are shown in Fig. 90. Gasoline vehicle has higher values than renewable based routes for ammonia cracking.

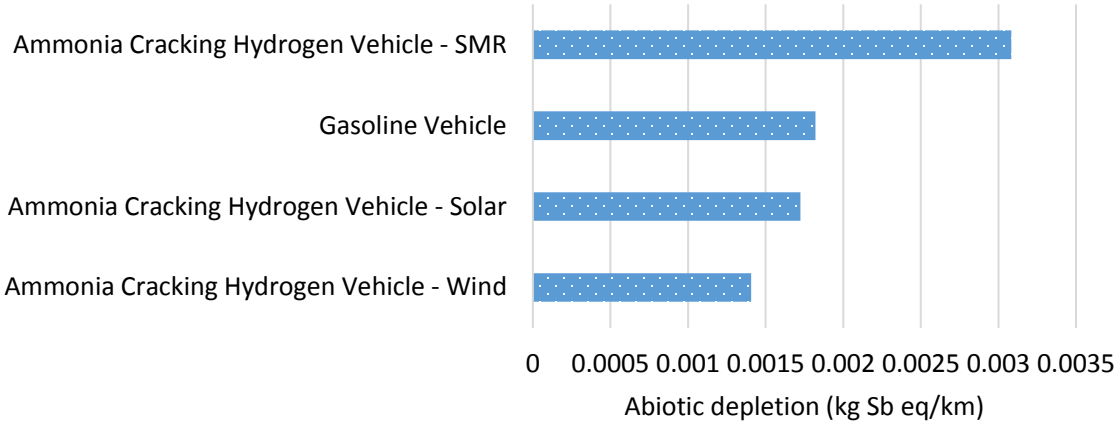

Figure 90 Abiotic depletion results of on-board ammonia cracking vehicles from various resources and gasoline vehicle

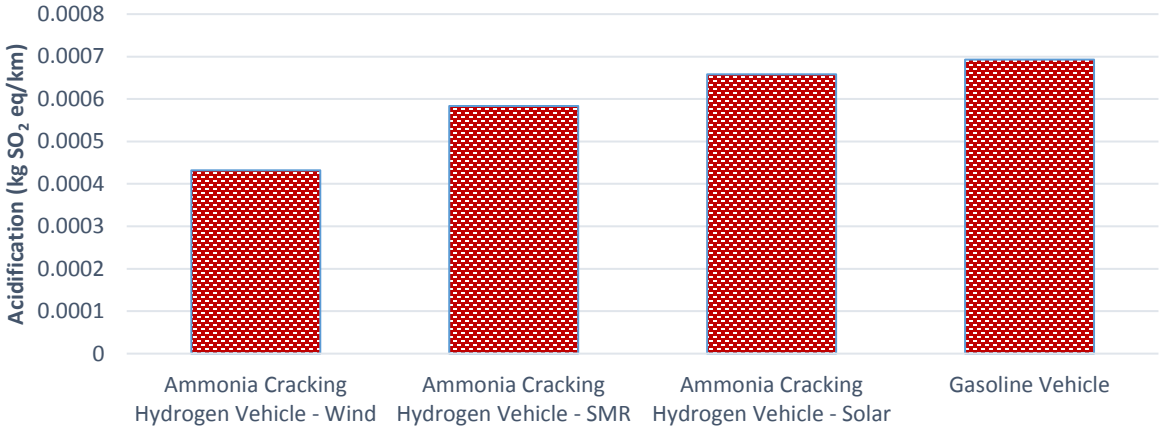

Figure 91 Acidification depletion results of on-board ammonia cracking vehicles from various resources and gasoline vehicle

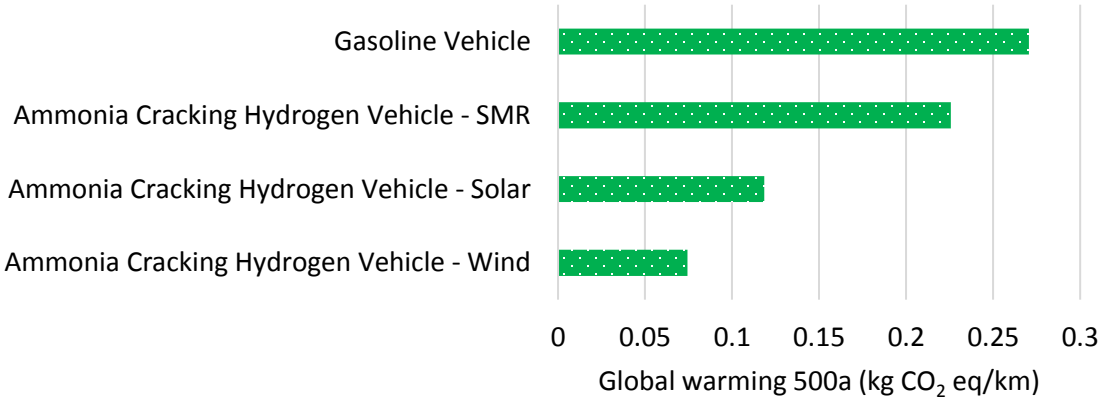

Figure 92 Global warming results of on-board ammonia cracking vehicles from various resources and gasoline vehicle

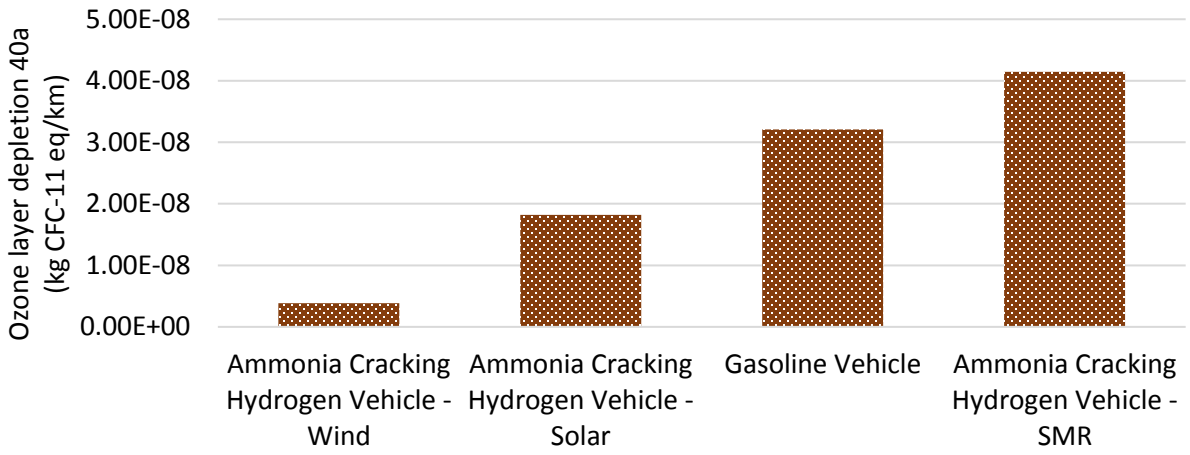

Figure 93 Ozone layer depletion results of on-board ammonia cracking vehicles from various resources and gasoline vehicle

The acidification depletion results of on-board ammonia cracking vehicles from various resources and gasoline vehicle are shown in Fig. 91. Gasoline vehicle has the highest acidification value in comparison with other ammonia cracking vehicles. Global warming potentials of ammonia cracking vehicles are quite better than conventional gasoline vehicles as shown in Fig. 92. Although ammonia is produced from SMR, the total GHG emissions are considerably lower. If ammonia is produced using wind energy and cracked on-board in the vehicle, the GHG emissions decrease down to 0.075 kg per every km considering the complete cycle. The ozone layer depletion results of on-board ammonia cracking vehicles from various resources and gasoline vehicle are shown in Fig. 93 where gasoline vehicle is higher than wind and solar based ammonia cracking vehicles.

2. Ammonia Decomposition

Ammonia decomposition (cracking) is simply the reverse of the synthesis reaction. NH_3 (g) → 1/2 N_2 (g) + 3/2 H_2 (g) ΔH = +46 kJ/mol Note that the reaction is endothermic. The temperature required for efficient cracking depends on the catalyst. There are a wide variety of materials that have been found to be effective, but some require temperatures above 1000°C. Others have high conversion efficiency at temperatures in the range of 650-700°C. As these temperatures are well above PEM fuel cell operating temperatures, some of the fuel or, perhaps, the fuel cell purge gas, would need to be burned to maintain an efficient reaction [74].

The theoretical adiabatic efficiency for the thermocatalytic reaction is about 85% relative to the energy (LHV) of the released hydrogen. If no other energy source were available, at least 15% of the available hydrogen energy content would have to be burned to supply the heat of reaction. Of course, additional energy would be required to overcome thermal losses in the cracking reactor. Since the reaction occurs at high temperature, this heat would likely come from the combustion of ammonia and/or hydrogen in onboard storage applications. In the forecourt, one would have the option of using other energy sources (electricity, natural gas, etc.) to supply the heat of reaction.

3. On-Board Ammonia

Table 25 shows the equilibrium conversion of ammonia, calculated using HSC10, as a function of temperature at reactor pressures of 1 and 10 bar. Actual decomposition conditions used in real-world operations involve tradeoffs between the costs of operations at higher temperatures and cost of removing unconverted ammonia. Since proton electrolyte membrane (PEM) fuel cells require ammonia concentrations below 0.1 ppm, significant purification will be necessary. Even at 900° C, the equilibrium calculations indicate 1500 ppm unconverted NH_3 at 10 bar.

Table 25 Ammonia conversion rates at equilibrium

Temperature (°C)	Unconverted Ammonia at 10 bar (%)	Unconverted Ammonia at 1 bar (%)
400	7.91	0.88
500	2.55	0.26
600	1	0.1
700	0.47	0.047
800	0.25	0.025
900	0.15	0.015

As the reactor temperature is increased, other problems emerge. In particular, it becomes more difficult for the reactor materials, such as the catalyst, its supports and the reactor container, to sustain exposure to this environment. Exposure of the container materials to stress corrosion cracking (SCC) and high temperature hydrogen embrittlement, for example, would have to be considered in the materials choices, particularly since the unit would be subjected to temperature swings from ambient temperatures (when not used) to the highest operating temperature. Furthermore, just from a strength and stability point of view, metal alloy choices become more limited (and generally more expensive) for high temperature applications. Although a stainless steel alloy might be used below 500°C, a Ni based or other alloy would be required at higher temperatures. A higher operating temperature would perhaps also require more insulation, increasing the weight and volume of the reactor. It could also increase the time required for the reactor to start producing hydrogen from a cold start, an important parameter for on-board vehicular applications [74].

A potential design for an ammonia cracking reactor is schematically shown in Fig. 94. Liquid ammonia would be pumped from a storage tank through a heat exchanger to capture waste heat from the hot gases exiting the cracking reactor. The preheated gases would then go through a furnace or catalytic combustor to heat them to the temperatures necessary for the reaction. The stream exiting the reaction would go to a separation system which would be optimized to produce a very pure stream of hydrogen while still leaving sufficient hydrogen with the nitrogen and unreacted ammonia to provide heat for the endothermic cracking reaction. This waste stream would be combusted to supply heat for the reaction and to remove unreacted ammonia.

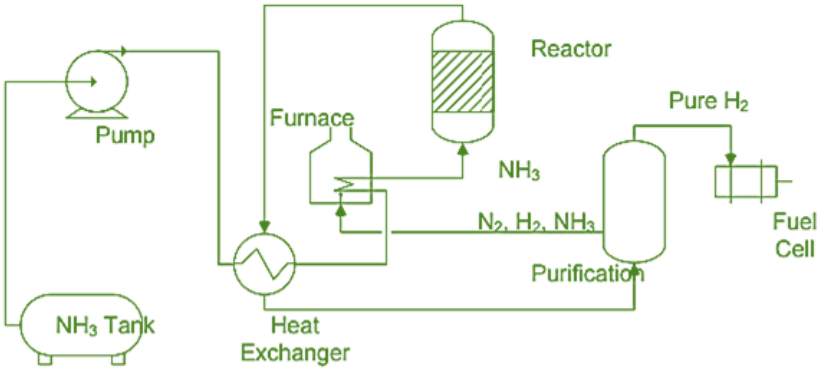

Figure 94 Ammonia fuel processing system (adapted from [74])

For onboard storage applications, the reactor would have to function over a very extensive dynamic range and with very fast response time to supply a fuel cell or ICE under all drive conditions. It would also have to be sized based on its ability to supply enough hydrogen for full power operation. For instance, the input hydrogen flow rate at full power for a 100 kW fuel cell (assuming a full power efficiency of about 45%) would be 2 g/s, or about 1,350 standard L/min of hydrogen. At 65% overall conversion efficiency, the cracking reactor would be consuming about 1.75 liters of liquid ammonia per minute and would need to process about 23 standard liters of ammonia per second [74]. Additional requirements on the cracking reactor component for on-board use would be to eliminate even trace amounts of ammonia in the outlet stream and to filter out the nitrogen. The ammonia removed from the outlet stream must be recycled into the inlet stream of the tank or used to supplement the inlet stream for source heat, since venting even small amounts of ammonia is not an option. Further details of ammonia cracking systems can be found in the literature, where a number of papers discuss the performance of different catalysts and other aspects of ammonia cracking. The system above is but one of many potential designs for an integrated reactor for ammonia cracking and purification. It does, however, serve to illustrate the complexity of practical reactor systems. An onboard system would likely be very different from a system designed for use in a forecourt application, but the basic components of reactor, heat recovery, waste stream recycling and highly effective purification will be vital parts of any successful system [74].

Advances in catalyst, high temperature materials, and separations will be necessary to produce an integrated reactor/separator that meets all the requirements. Metkemeijer et al. [75] compared the indirect use of both methanol (CH_3OH) and ammonia (NH_3) for the production of hydrogen to use in a fuel cell. Their findings extensively showed that the decomposition of ammonia was more attractive than methanol reforming from both thermodynamic and economic perspectives. They implied that the maximum specific energy produced from ammonia decomposition is 2.68 kWh_e/kg_f which is approximately 229% more than the 1.17 kWh_e/kg_f obtained from the reforming of methanol. They also assumed that both ammonia and methanol are both synthesized out of methane (CH_4) with a specific energy requirement of 8.05 $kWh/kg_{CH4}$for both cases. The researchers deduce that the overall efficiency with respect to the lower heating value of methane of the indirect ammonia and methanol approaches are 33.3% and 22.9%, respectively. According to Yin et al. [76] ruthenium catalyst supported on carbon nanotubes and promoted by potassium hydroxide was found to be the most effective catalyst for the thermal decomposition of ammonia. The researchers had discussed the kinetics of ammonia decomposition and had discovered that for temperatures less than 650.0 K the combinative desorption of nitrogen atoms was determined to be a rate limiting step. Chellappa et al. [77] examined the high

temperature decomposition of ammonia at near atmospheric pressures over a nickel catalyst. The researchers were prompted to conduct this study to further understand the kinetic mechanisms of ammonia decomposition and to verify the existence of a transitional region where the Tymken-Pyzhev mechanism changes to a Tamaru mechanism. Roy et al. [78] had extensively reviewed the catalytic decomposition over alumina supported nickel catalyst at temperatures ranging from 400°C – 600°C with two catalysts; 10.0% and 15.0% nickel content, respectively. The researchers had found that the partial pressure of hydrogen reduced the ammonia decomposition rate over the entire temperature range and the presence of nitrogen had negligible effect on ammonia decomposition. The comparison of various chemical reactions for thermal H_2 production are shown in Table 26.

Table 26 Various chemical reactions for thermal H_2 production.

Reaction	Chemical Equation	Standard Enthalpy of Reaction (kJ/mol)	Operating Temperatures (K)
Ammonia Decomposition	$2NH_3 \rightarrow 3H_2 + N_2$	92.8	673.0 – 873.0
Methanol Reforming	$CH_3OH + H_2O \rightarrow CO_2 + 3H_2$	131.70	400.0 – 570.0
Steam Methane Reforming	$CH_4 + 2H_2O \rightarrow CO_2 + 4H_2$	164.70	973.0 – 1173.0

Source: [79]

Anhydrous ammonia has very high gravimetric (about 17 wt.% or 5.8 kWh/kg) and volumetric (about 0.105 kg/liter or 3.6 kWh/L at 25° C) hydrogen energy densities and, hence, looks appealing for use as a potential hydrogen carrier for onboard storage. Also, compared to reforming hydrocarbon fuels, the dissociation, or cracking, of hydrogen from ammonia may require a less complex process. The byproduct of the hydrogen dissociation process, nitrogen, can be vented from the vehicle with no adverse environmental effects so there is no need for a recycling process, as in some other chemical hydride systems. However, ammonia has specific chemical and physical properties which require attention in the design and engineering of an onboard storage system. These issues are: high coefficient of thermal expansion, high vapor pressure at ambient conditions, propensity for reacting with water, reactivity with container materials and high toxicity of the vapor if released into the air. These will be discussed below. Importantly, PEM fuel cells cannot tolerate ammonia, even at very low ppm levels and, hence, an onboard storage system based on ammonia would require a cracking reactor with essentially no pass-through of undissociated ammonia and/or a very effective filtration system.

The onboard tank must also sustain a modest overpressure. At 60° C, the vapor pressure of anhydrous ammonia is about 365 psig (about 25 bar). With a safety factor of approximately 2 to 2.2, the tank should sustain a maximum pressure of about 800-900 psi. In order to maintain the high gravimetric density, lightweight tank fabrication would be desirable. Currently, fixed site ammonia tanks are often constructed of steel or ductile iron. Many polymers are compatible with ammonia, so it is likely that composite tanks or lightweight aluminum tanks with polymer liners could be used for onboard storage of ammonia. Filling the onboard tank from a forecourt source will require a demountable, leak-proof coupling. This is mainly due to the toxicity of ammonia, but also because of the high affinity of ammonia for water resulting in the formation of ammonium hydroxide. Humidity from the air leaking into the refueling tube or coupling would, over time,

lead to corrosion of the piping and tank by the hydroxide. The byproduct of the ammonia dissociation process, nitrogen, can be vented from the vehicle with no adverse environmental effects so there is no need for a recycling process, as in some other chemical hydride systems, Hydrogen production via ammonia decomposition is an endothermic process which is also a reversible chemical reaction. At 400°C, the equilibrium conversion of NH_3 is very high 99.1% [76]. Fe, Ni, Pt, Ir, Pd, Rh are a few of the possible catalysts whereas Ru and Ir appears to be more appropriate power per kg of catalyst. The waste heat could be supplied from sources such as: gas turbine, SOFC, or diesel power plants. All of these power plants have exhausts at temperatures of or greater than 600ºC and would be able to meet the thermal energy requirement of an NH_3 decomposition and separation reactor. For this scenario to be realized, an exhaust gas to reactor heat exchanger must be designed and built to facilitate efficient heat transfer to the reactor. A membrane reactor system to produce hydrogen by the thermal decomposition of ammonia could also take place in either large scale marine or rail applications. This is envisioned to be a process where a fraction of the hydrogen energy produced would be used to decompose additional ammonia for hydrogen. A major point of interest pertaining to this scenario would be the very high energy ratio of the ammonia decomposition reaction. Thermodynamically, the ammonia decomposition reaction only requires approximately 13.0% - 15.0% of the hydrogen's calorific value.

4. On-Board Ammonia Electrolysis

Ammonia stored in the tank of the vehicle can be electrolyzed to generate hydrogen and use in the fuel cell or engines. Ammonia electrolysis is a method by which ammonia is electrochemically oxidized on a suitable electrocatalyst to nitrogen and hydrogen. Based on thermodynamics, the energy required to produce hydrogen by ammonia electrolysis is 97% lower than that required by electrolyzing water [80].

The reactions for an ammonia electrolytic cell comprise of ammonia electro oxidation at the anode and alkaline water reduction at the cathode as shown in the following equations [80]:

Anode: $2NH_3 + 6OH^- \rightarrow N_2 + 6H_2O + 6e^-$, $E_0 = -0.770$ V vs SHE (8)

Cathode: $6H_2O + 6e^- \rightarrow 3H_2 + 6OH^-$, $E_0 = -0.828$ V vs SHE (9)

Overall: $2NH_3 \rightarrow N_2 + 3H_2$, $E_0 = 0.058$ V (10)

Therefore, thermodynamic values are much in favor of the production of hydrogen coupled to the oxidation of ammonia compared to hydrogen production by electrolysis of water, for which the theoretical cell voltage is 1.223V. The advantage of this process is its ease of integration with renewable energy (electricity) sources. Because the energy consumption is low, the cell could operate with renewable energy.

The theoretical energy consumption during ammonia electrolysis (assuming that there are not kinetics limitations for the reaction to take place at the thermodynamics conditions) can be calculated from the standard potential of the cell and is equal to 1.55Wh/g H_2 while the electrolysis of water requires at least 33 Wh/g H_2 at standard conditions; this means that theoretically the electrolysis of ammonia consumes 95% lower energy than a water electrolyzer [80]. The commercialization of the technology depends on the development of effective electrodes for the electro-oxidation of ammonia. The development of superior electrolytes and electrocatalysts for ammonia electrolysis are vital for the improvement of the electrolysis efficiency. Vitse et al. [81] stated that hydrogen produced from the electrolysis of ammonia costs 0.89 US$ /kg of H_2 opposed to 7.10 US$/kg of H_2 from water electrolysis. These numbers were based on an ammonia cost of 275 US$/ton and a solar energy cost of 0.214 US$/kWh. Thermodynamically for 1 g of H_2,

ammonia electrolysis consumes 1.55 Wh. For this same gram of H_2, a PEMFC, which is the reverse reaction of water electrolysis, generates 33 Wh. After sending 1.55 Wh back to the ammonia electrolysis cell (AEC) from the PEMFC, making the system self-sustaining, there is potential for a net energy of 31.45 Wh that can be used to recharge the batteries used for system start-up, to power a motor, or for any other applications. However, PEM fuel cells have efficiencies that range from 50 to 70% [82,83]. Additionally, ammonia is converted to hydrogen with 100% Faradaic efficiency, but kinetic problems creating large ammonia oxidation overpotentials exist. Boggs and Botte [84] integrated proton exchange membrane fuel cell with ammonia electrolyte cell (AEC), the electricity generated from the PEM fuel cell is utilized to feed the AEC with electricity. The study shows that using 203 L of aqueous ammonia will allow a hybrid fuel cell vehicle to travel 483 km before demanding another ammonia refill.

5. Case Study for Ammonia Electrolysis Vehicle

In this section, a case study is employed to show the practicability of the ammonia electrolysis vehicle for a 500 km driving range. Here, we follow the same procedure for AEC calculations as explained in the study by Boggs and Botte [84].The storage system costs, gravimetric, and volumetric capacities of an ammonia electrolysis vehicle are performed. A lightweight hydrogen fuel cell vehicle is considered. The driving range of the vehicle is taken as 500 km. A lightweight vehicle can consume about 5.3 km/L which is 2.5 less efficient than a hydrogen fuel cell vehicle. A gallon of gasoline is equivalent (gge) to a kg of hydrogen. Hence, the energy required for internal combustion engine (ICE) is found as 12.5 gal × 33.3 kWh/gal= 416.25 kWh [84].

Using this value, the amount of hydrogen is calculated as follows:

$$m_{H_2} = 416.25\ kWh/(2.5 \times 33\ kWh/kg) = 5\ kg \quad (11)$$

In order to travel about 500 km with this vehicle, about 5 kg of hydrogen is required. On average, if the vehicle is driven with the speed of 80 km/h, it will require refilling in every 6 hours. The nominal fuel cell power required to move a lightweight fuel cell vehicle is:

$$\dot{W}_{PEMFC} = \frac{416.25\ kWh}{(6h \times 2.5)} = 27.75\ kW \quad (12)$$

The generated electricity from the fuel cell is both used for vehicle propulsion and ammonia electrolysis. Therefore, the PEM fuel cell is required to be higher power rate. Ammonia electrolysis consumes about 60% of the energy. The increase of 60% in fuel cell cost, weight, and volume is considered as part the storage system.

To find the total PEM fuel cell power, the following calculation is used:

$$\dot{W}_{TOTAL,PEMFC} = \frac{27.75\ kW}{(1-0.6)} = 69.38\ kW \quad (13)$$

For the storage of the ammonia on-board, the ammonia storage vessel, Teflon tubing, centrifugal pump, start-up hydrogen drum, compressor, and controller are mostly common and commercially available devices. Based on the market, the estimated cost of ammonia storage unit is taken as US$ 3,633 (inflated to 2017) based on the study by Boggs and Botte [84]. The cost, weight, and volume of the ammonia electrolysis unit and PEM fuel cell modules are affected by many factors. Since there is an increase in power required from the PEM fuel cell, an increase in the amount of hydrogen is required between refueling.

$$m_{H_2} = \frac{69.375\ kW \times 6h}{(33\frac{kWh}{kg} \times 0.6)} = 21.2\ kg \quad (14)$$

In order to find the current required for ammonia electrolysis, under the assumption of 100% Faradaic efficiency, the Faraday law can be used:

$$I = 3500\,\frac{kg}{h} \times \frac{6e^-}{mol} \times \frac{26.8\frac{Ah}{e^-}}{3 \times 2\frac{g}{mol}} = 93,800\,A \quad (15)$$

Here, we assume a current density of 0.15 A/cm^2 in the cell and a corresponding cell area of 100 cm^2. This implies that about 15 A is needed for one cell. Hence, a total of about 6254 cells would be required to obtain 27.2 kW net energy for the motor.

The total catalyst (ruthenium is selected) required for the ammonia electrolysis can be calculated as follows [84]:

$$m_{catalyst} = 15\,\frac{mg}{cm^2} \times 2 \times 6254\,cells \times 100\,cm^2 = 18.762\,kg \quad (16)$$

Here, it is multiplied by 2 because of anode and cathode. Due to the expense of noble metals, the ammonia electrolysis cell cost is entirely dependent on the loading and catalyst costs.

We assume a ruthenium catalyst to be used in the ammonia electrolysis cell (AEC). The loading of the electrodes is kept at 15 mg/cm^2. In the open literature on catalysts for this reaction, loadings of up to 51 mg/cm^2 have been reported. The cost of ruthenium is US$1286 per kg in the market [85].

Therefore, the cost of ammonia electrolysis can be approximated as

$$Cost_{AEC,storage} = 18.762\,kg \times 1286\,\frac{US\$}{kg} = US\$\,24{,}128 \quad (17)$$

About 41.6 kW of the PEM fuel cell is required for storage calculations. Using the 35 US$/kW for fuel cells which was reported by DOE Boggs and Botte [84]:

$$Cost_{PEM,storage} = 35\,\frac{US\$}{kW} \times 41.6\,kW = US\$\,1456 \quad (18)$$

Counting the PEM fuel cell and ammonia electrolysis cell, the total system storage cost is found to be US$ 25,584. The DOE technical storage targets are summarized in the following Table 27. Capacities are defined as the usable quantity of hydrogen deliverable to the power plant divided by the total mass/volume of the complete storage system, including all stored hydrogen, media, reactants, and system components. Tank designs that are conformable and have the ability to be efficiently packaged onboard vehicles may be beneficial even if they do not meet the full volumetric capacity targets. Capacities must be met at end of service life. Hydrogen cost is independent of pathway and is defined as the untaxed cost of hydrogen produced, delivered, and dispensed to the vehicle.

Table 27 Technical targets for onboard hydrogen storage for light-duty vehicles

STORAGE PARAMETER	UNITS	2020	ULTIMATE
System Gravimetric Capacity			
Usable, specific-energy from H_2 (net useful energy/max system mass)	kWh/kg	1.8	2.5
	kg H_2/kg system	0.06	0.075
System Volumetric Capacity			
Usable energy density from H_2 (net useful energy/max system volume)	kWh/L	1.3	2.3
	kg H_2/L system	0.04	0.07
Storage System Cost			
System cost	$/kWh net	10	8
	$/kg H_2 stored	333	266
Fuel cost	$/gge at pump	2–4	2–4

Source: [86]

$$Cost_{per\ kg} = \frac{US\$\ 25{,}584}{21.2\ kg\ H_2} = 1206.8 \frac{US\$}{kg} \quad (19)$$

$$Cost_{per\ kWh} = \frac{US\$\ 25{,}584}{\frac{33 kWh}{kg} \times 60\% \times 21.2\ kg} = 60.95 \frac{US\$}{kWh} \quad (20)$$

The ammonia storage vessel, Teflon tubing, start-up drum, compressor, and process controller are estimated to weigh about 26.5 kg based on commercially available products. The weight of fuel, storage part of the fuel cell, and AEC are calculated.

The required ammonia mass can be found using molecular weight and percentage of hydrogen in ammonia:

$$m_{NH_3} = \frac{21.2\ kg\ H_2 \times 1\ kg\ NH_3}{0.177\ kg\ H_2} = 119.8\ kg \quad (21)$$

According to Satyapal et al. [87], the target power density for PEM fuel cell is 2000 W/kg. As a result, the storage part of the fuel cell would weigh about $\frac{41.6\ kW}{2\frac{kW}{kg}} = 20.8\ kg$. It is assumed that the ammonia electrolysis unit is twice as heavy as the fuel cell that means 69.4 kg.

$$m_{AEC} = \frac{2 \times 69.4\ kW}{2\frac{kW}{kg}} = 69.4\ kg \quad (22)$$

The total gravimetric capacity is determined using the total estimated storage system weight, which is 249.9 kg.

$$Capacity_{Gravimetric\ (per\ kg\ system)} = \frac{21.2\ kg}{249.9\ kg} = 0.0.084 \quad (23)$$

$$Capacity_{Gravimetric\left(\frac{kWh}{kg}\right)} = 21.2\ kg \times 33 \frac{kWh}{kg} \times \frac{60\%}{249.9\ kg} = 1.68 \frac{kWh}{kg} \quad (24)$$

Similarly, the volumes of the tubing, start-up drum, compressor, and process control are estimated to occupy about 100 L. Using the fact that 119.8 kg of ammonia is required and considering a density of 682 kg/m^3, the storage vessel volume is 174 L. The targeted power/volume density for PEM fuel cell is 2000 W/L according to the DOE. Based on the 41.6 kW of fuel cell power that is used for storage, the storage part of the PEM fuel cell requires 20.8 L. Using the 2 times relation for ammonia : PEM fuel cell for volume and weight, the AEC occupies:

$$V_{AEC} = \frac{2 \times 69.4\ kW}{2\frac{kW}{L}} = 69.4\ L \quad (25)$$

Total storage system volume required is calculated to be 364.2 L. The volumetric storage parameters are as follows:

$$Capacity_{Volumetric\left(\mathrm{kg}_{\frac{\mathrm{H_2}}{\mathrm{L\ system}}}\right)} = \frac{21.2\ kg}{364.2\ L} = 0.058 \frac{kg}{L} \quad (26)$$

$$Capacity_{Volumetric\ \left(\frac{\mathrm{kWh}}{\mathrm{L}}\right)} = 21.2\ kg \times 33 \frac{kWh}{kg} \times \frac{60\%}{364.2\ L} = 1.15 \frac{kWh}{L} \quad (27)$$

6. Thermodynamic Analyses of On-Board Ammonia Electrolysis

The theoretical electrolysis voltage of liquid NH_3 at any temperature is evaluated from Nernst's equation as follows [88]:

$$E_{r,AEC} = -\frac{\Delta G}{3\ F} + \frac{R\ T_{operation}}{3\ F} \ln(P_{N_2}^{0.5} P_{H_2}^{1.5}) \quad (28)$$

where, P_{H_2} is the partial pressure of H_2, and P_{N_2} is the partial pressure of N_2.

To obtain the required practical cell voltage, it is necessary to add all the cell losses (activation, concentration, ohmic overpotentials) to reversible cell voltage as below:

$$E_{actual} = E_{open} + E_{act} + E_{ohm} + E_{conc} \quad (29)$$

The ohmic overpotential is identified as

$$E_{ohm,i} = \rho_i \, \delta_i \, J \quad (30)$$

where ρ is the material resistivity, i represents the component and δ is the element thickness. The ohmic overpotential for each component of the cell can be calculated and added.

The activation polarization is given in terms of current density and exchange current density by Butler-Volmer equation:

$$J = J_0 \left\{ \exp\left(\frac{\alpha_a n F E_{act,a}}{RT}\right) - \exp\left(-\frac{\alpha_c n F E_{act,c}}{RT}\right) \right\} \quad (31)$$

where J_0 is the exchange current density, α_a and α_c are the electron transfer coefficients for anode and cathode, respectively, n is number of transferred electrons, and $E_{act,a}$ and $E_{act,c}$ are the activation overpotentials related with anode, and cathode respectively.

The total activation overpotential is the summation of each electrode:

$$E_{act} = E_{act,c} + E_{act,a} \quad (32)$$

The concentration polarizations are derived for each electrode:

$$E_{conc,c} = -\frac{RT}{nF} \ln\left(1 - \frac{J}{J_{L,c}}\right) \quad (33)$$

$$E_{conc,a} = -\frac{RT}{nF} \ln\left(1 - \frac{J}{J_{L,a}}\right) \quad (34)$$

Here, $J_{L,a}$ and $J_{L,c}$ are the limiting current densities for anode and cathode, respectively.

The values for different parameters used in the analyses of AEC unit are shown in Table 28.

Table 28 Data used in the analyses for ammonia electrolysis

Parameter	Range or value
Current density	0.15 A/cm^2
Exchange current density	0.037 mA/cm^2
Cell operating temperature	30°C
Cell operating pressure	10 bar
No of cells	6254
Anode thickness	0.0020 cm
Cathode thickness	0.0020 cm
Electrolyte thickness	0.0040 cm
Liquefied ammonia temperature	20°C
Liquefied ammonia pressure	10 bar

Source: [80,89]

The energy and exergy efficiencies of the ammonia electrolysis cell can be defined as follows:

$$\eta_{en,AEC} = \frac{LHV_{Hydrogen} \, \dot{m}_{H_2}}{LHV_{ammonia} \, \dot{m}_{NH_3} + J \, E_{actual} \, A_{cell}} \quad (35)$$

$$\eta_{ex,AEC} = \frac{ex_{Hydrogen} \, \dot{m}_{H_2}}{ex_{ammonia} \, \dot{m}_{NH_3} + J \, E_{actual} \, A_{cell}} \quad (36)$$

where ex represents the total exergy counting chemical and physical components.

The open cell voltage is found to be 0.078 V whereas the actual cell voltage counting the overpotentials is calculated to be 0.29 V. In total, 6254 cells are used to obtain the required power of 27.2 kW for the ammonia electrolysis. Under these conditions, the exergy destruction rate 28.93 kW. The inlet mass flow rate of ammonia is 220.8 g/min which yields 39.2 g/min hydrogen. The energy and exergy efficiencies of the AEC are found to be 82.03% and 79.51%, respectively as shown in Fig. 95.

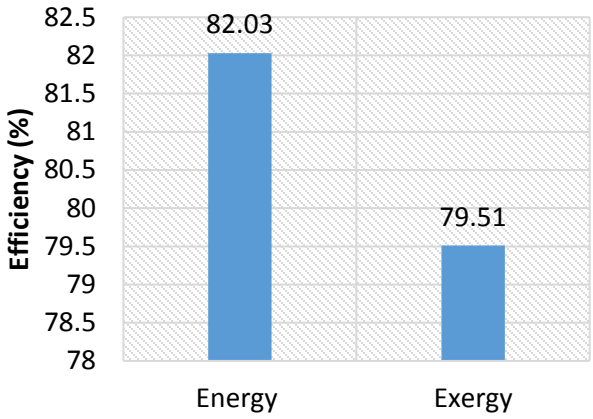

Figure 95 Energy and exergy efficiencies of the ammonia electrolysis cell unit

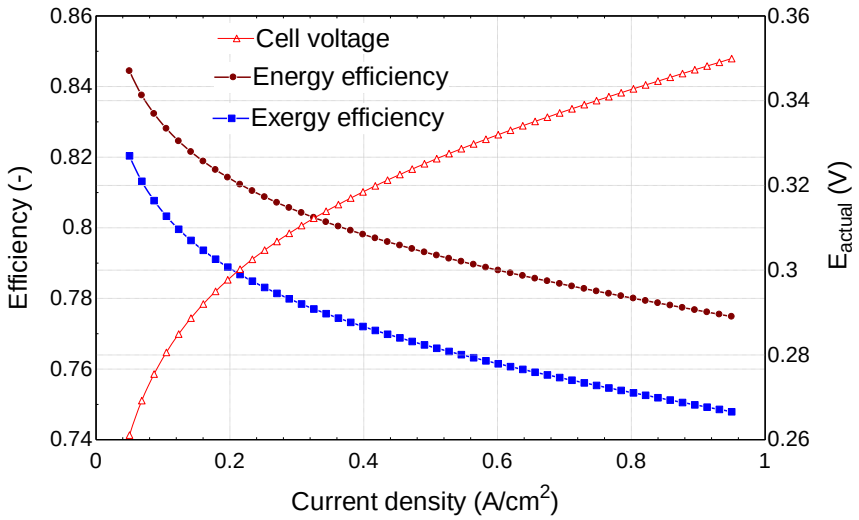

Figure 96 Effect of changing AEC current density on electrolysis voltage and overall AEC energy and exergy efficiencies

The overpotentials and actual cell voltage in the AEC are listed in Table 29.

Table 29 The overpotentials and actual cell voltage in the AEC

Activation overpotential (V)	0.2102
Concentration overpotential (V)	0.0008567
Ohmic overpotential (V)	0.001134
Actual cell potential (V)	0.2902

In Fig. 96, the effect of changing the AEC current density on the AEC electrolysis voltage, energy and exergy efficiencies of the AEC unit are illustrated. The electrolysis voltage required to separate the ammonia increased from 0.26 V to 0.35 V due to the increase of the AEC current density from 0.05 A/cm^2 to 0.95 A/cm^2. However, the same range of change of the AEC current density leads to a drop in energy and exergy efficiency of the AEC unit from 84.44% to 77.49% and from 82.04% to 74.79% respectively.

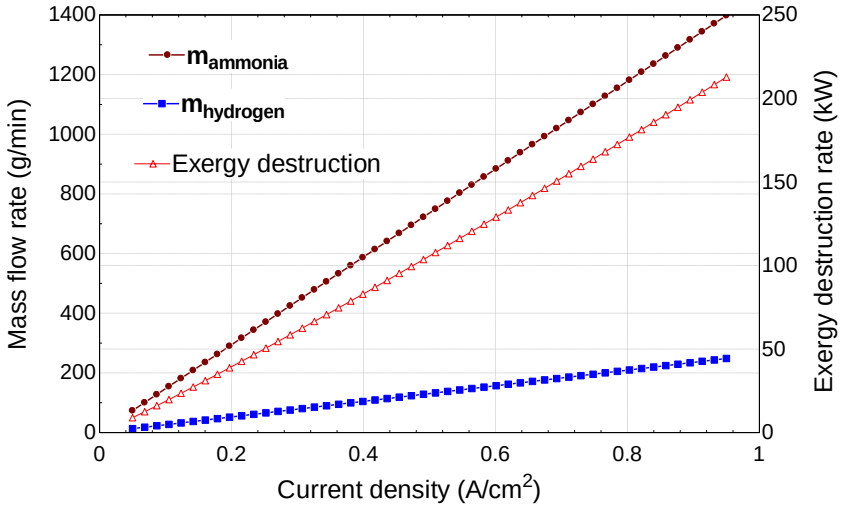

Figure 97 Effect of changing AEC current density on AEC exergy destruction, ammonia amount required for electrolysis and hydrogen produced by AEC

The increase in the electrolysis voltage and the decrease in the energy and exergy efficiency of the AEC unit can be interpreted by the growth in the AEC voltage losses. As it increase directly proportional to the increase in the current density, which leads to an increase in the exergy destruction rate and eventually a drop in the AEC efficiency. Fig. 97 shows the relation between applied current density and yielding mass flow rate of the chemicals. When the current density is 4 A/cm^2, then the required ammonia flow rate is about 600 g/min to produce about 100 g/min hydrogen. The exergy destruction also increases by rising current density. The effects of changing AEC operating temperature on exergy destruction and overall AEC energy and exergy efficiencies are shown in Fig. 98. Although operating at higher temperature decreases the exergy destruction in the AEC, the efficiencies slightly lowers at higher temperatures.

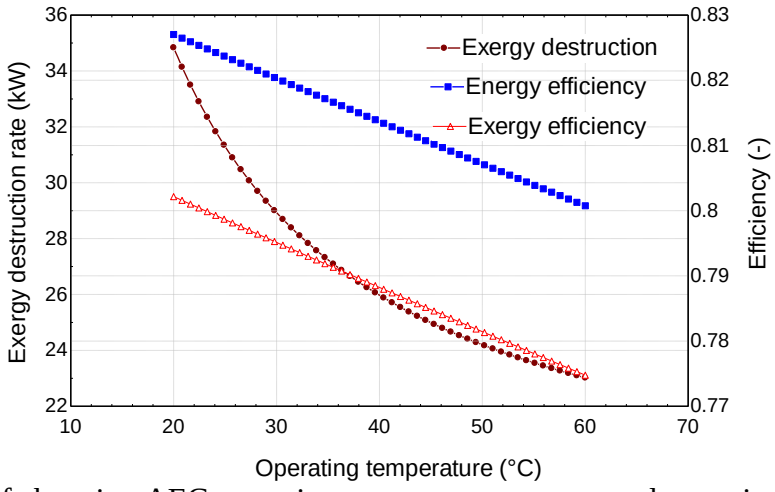

Figure 98 Effect of changing AEC operating temperature on exergy destruction and overall AEC energy and exergy efficiencies

Operating pressure is also important for the system performance as shown in Fig. 99. At higher pressure, the required potential increases causing a higher power requirements in the AEC for

hydrogen production from ammonia. In Fig. 100, the effects of ambient temperature are illustrated. At higher ambient temperatures, the total exergy destruction rate is higher.

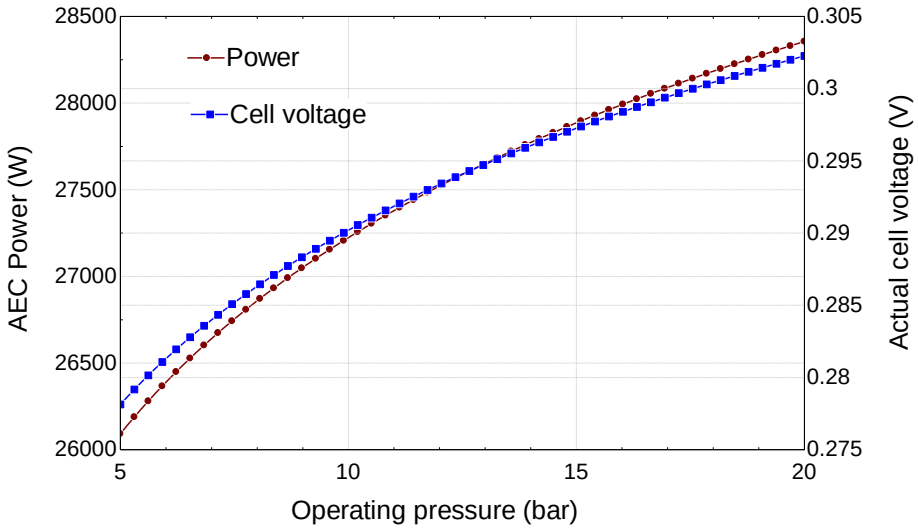

Figure 99 Effect of changing AEC operating pressure on AEC cell voltage and required power

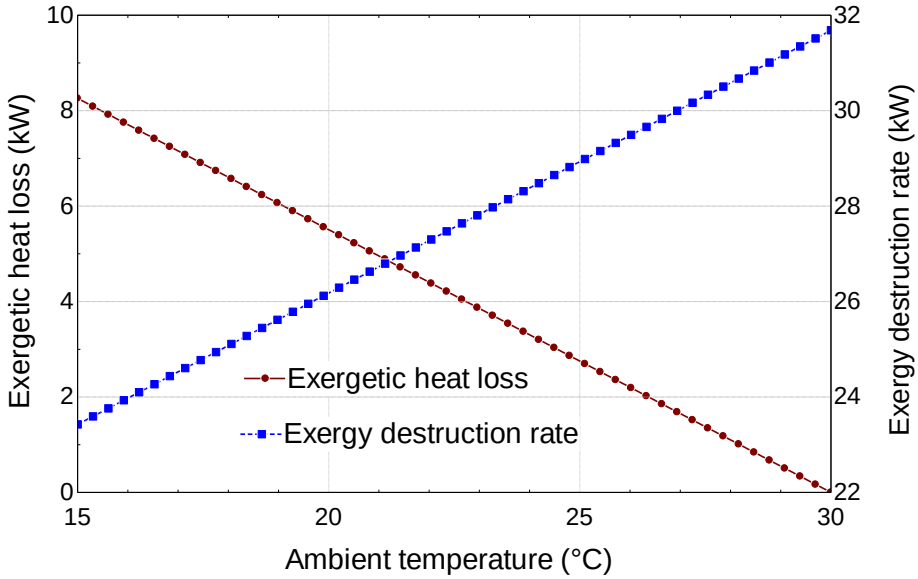

Figure 100 The effects of ambient temperature on the total exergy destruction rate and heat loss of the AEC

One of the key parameters is the mass flow rate of ammonia entering the AEC unit as shown in Fig. 101. Increasing the mass flow rate causes a decrease in efficiency which is mainly caused by the definition of efficiency.

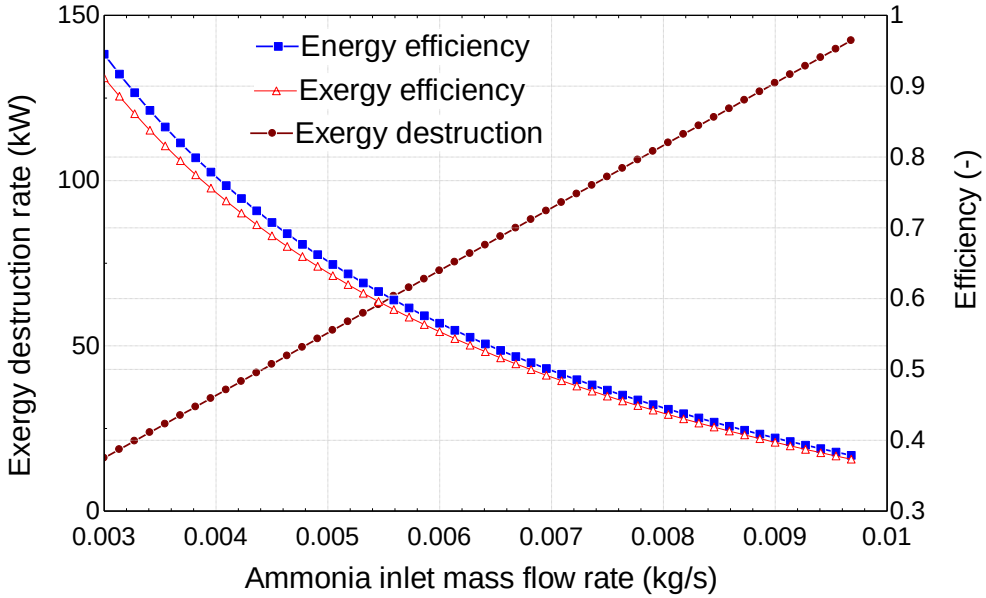

Figure 101 The effects of ammonia inlet mass flow rate on exergy destruction and efficiencies of AEC

CHAPTER 9:ECONOMIC ANALYSES OF SOLAR ENERGY BASED AMMONIA PRODUCTION

In this section, the exergoeconomic analyses of the experimental systems are performed. The purchased costs of the experimental systems in this study are presented in the following tables. The experimental systems are divided into three main sub-systems;

- Photoelectrochemical hydrogen production reactor
- Electrochemical ammonia production reactor
- Integrated system comprising of solar light concentrator and splitter, PV cell and support mechanism.

The purchased costs of the materials used in the PEC reactor are listed in Table 30.

Table 30 The cost of materials used in the PEC hydrogen production reactor

Material	Quantity	Unit Price ($)	Total Price ($)
Reactor casing (HDPE)	2	$130	$260
Stainless steel electrodes	2	$200	$400
Nafion membrane	1	$2,000	$2,000
Chemicals for electrodeposition	3	$150	$450
Washers, bolt nuts	50	$1	$50
Acrylic or polycarbonate reactor window	1	$100	$100
Piping (plastic)	4	$25	$100
Rubber gasket	6	$10	$60
Machining (for casing and electrodes)	1	$450	$450
Others (adhesive, silicon etc.)	1	$120	$120
TOTAL			$3,990

The reactor casing is chosen as HDPE for the reactor because of the advantages explained in the experimental apparatus. The machining is easier and requires low cost. For higher solar concentration ratios, the temperature levels on the PEC reactor body may rise more than material specification. It is similar for the viewing panel of the reactor which is made of acrylic.

Table 31 The cost of materials used in the electrochemical ammonia production reactor

Material	Price ($)
Nickel wiring	$40
Nickel electrodes	$160
Reactor casing alumina crucible (Alumina Al_2O_3)	$140
Reactor lids (Stainless steel 316 Alloy)	$120
Bolt Nuts and Washers	$55
Reactor tubes (Alumina Al_2O_3)	$160
Piping (plastic)	$50
Heating tape	$110
Gaskets	$25
Others (adhesive, insulation etc.)	$65
TOTAL	$925

Therefore, the temperature levels on the PEC reactor surface need to be checked before deciding the materials selection. In total, the cost of the PEC reactor in the experimental setup is calculated to be 3990$. The purchased costs of the materials used in the electrochemical ammonia production reactor are listed in Table 31. The ammonia reactor casing has 500 mL capacity. The tubes for the gas inlet and outlet the reactor are also made of Alumina (Al_2O_3) which is non-corrosive. After the gasses exit the reactor, plastic pipes are used. The heating tape used in the experiments are for sustaining the reaction temperature. That is an additional equipment to the reactor construction. The total cost of ammonia reactor is found to be 925$. The PEC hydrogen production reactor is used under concentrated and split spectrum. Therefore, the solar concentrator, dielectric mirrors and PVs are included in the integrated system costs as shown in Table 32. These two sub-systems for hydrogen and ammonia production are integrated in the experimental setup which yield the total system capital cost.

Table 32 The cost of materials used in the integrated system for PEC hydrogen based electrochemical ammonia production system

Photovoltaic cell, multicrystalline silicon	$80
Fresnel lens	$75
Dielectric mirrors (6 in total) (Borosilicate glass)	$672
PEC hydrogen production reactor	$3,990
Ammonia production reactor	$925
Support structure (wood)	$45
Metal support mechanism including nuts and bolts	$75
TOTAL	$5,862

The support mechanism used in the integrated system consists of wood and metal parts. The highest cost is for the PEC hydrogen production reactor which corresponds to about 68% of total cost as show in Fig. 102.

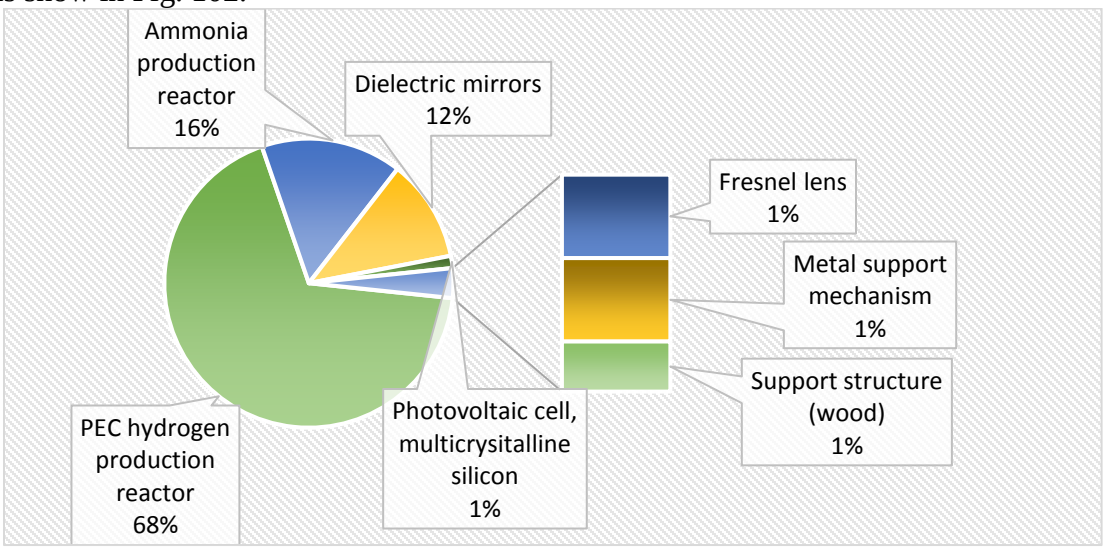

Figure 102 Cost breakdown of the integrated system for hydrogen and ammonia production

The exergoeconomic analysis requires that a specific cost is put on the exergy streams in an exergy balance on a component. On top of putting costs on the exergy streams, capital and running costs

are taken into account in order to get a complete cost analysis. The exergoeconomic analyses are performed for the experimental integrated system. The capital costs are taken from the experimental setup costs as listed above. Exergy cost for the streams in any cost rate balance is given as [90,91]

$$\dot{C} = c\,\dot{Ex} \tag{37}$$

Here, c is in given in \$/kWh and $\dot{Ex}$ is given in W. The capital costs of the components is given as $\dot{Z}$ in \$/h.

Typical cost rate balance for a component is given below [92,93]:

$$\sum \dot{C}_{in} + \dot{W}\, c_{in} + \dot{Z} = \sum \dot{C}_{out} + \dot{W}\, c_{out} \tag{38}$$

CRF refers to capital recovery factor and depends on the interest rate and equipment life time, and is determined here as follows:

$$CRF = \frac{i\,(1+i)^n}{(1+i)^n - 1} \tag{39}$$

Here, i denotes the interest rate and n the total operating period of the system in years. Total costs for each of the components in the system are needed in \$/h in order to use them in cost rate balance equations. The capital cost and the operating and maintenance costs are added. The total costs are then divided by the number of hours in a year to get a cost in \$/h. Operating and maintenance costs are assumed to be a ratio of the capital costs as

$$OM = CC\ \ OM_{ratio} \tag{40}$$

where OM_{ratio} depends on the type of application and material.

The capital costs of the equipment are calculated based on the experimental setup costs as explained in the previous tables. The total cost balance is written as follows:

$$TCC = CRF\ (CC + OM) \tag{41}$$

The annual investment cost rate of any component, $\dot{Z}$ is calculated for the components of the experimental integrated system. It is the summation of the annual capital investment cost rate and the annual O&M cost rate and defined as follows:

$$\dot{Z} = \frac{TCC}{t_{operation}} \tag{42}$$

where $t_{operation}$ is the total operational hours in a year.

The cost rate of exergy destruction for each component is expressed as [92,93]

$$\dot{C}_D = c\,\dot{E}x_d \tag{43}$$

Summation of additional cost caused by exergy destruction, $\dot{C}_D$ and final capital and operating cost rate $\dot{Z}$ gives a critical parameter named as total cost rate $\dot{C}_D + \dot{Z}$:

$$\dot{C}_{total} = \dot{C}_D + \dot{Z} \tag{44}$$

Total cost rates of the system consists of the total investment cost and cost of exergy destruction. In general, the smaller the sum of this parameter, it means that the component is more cost effective. Therefore, this parameters is taken as optimization function in the optimization analyses.

The exergoeconomic factor, which is a measure of system effectiveness in terms of cost, obtained through exergoeconomic analysis is given as

$$f = \frac{\dot{Z}}{\dot{Z} + \dot{C}_D} \tag{45}$$

The exergoeconomic variables $\dot{Z}$ and $\dot{C}_D$ provide the significance of component in the system optimization, whereas the variable f exergoeconomic factor is a relative measure of the component cost effectiveness.

The obtained results in the exergoeconomic analysis of the streams for each of the sub-systems in the experimental setup are presented in results and discussion chapter. The following financial parameters shown in Table 33 are used in the exergoeconomic analysis.

Table 33 The financial and operation parameters used in the exergoeconomic analyses

Parameter	Value
Interest rate	7%
Lifetime of all components	10 years
Calculated capital recovery factor	0.1424
Calculated hydrogen cost	3.24 $/kg
Calculated ammonia cost	0.73 $/kg
Cost of electricity	0.06 $/kWh
Cost of thermal energy	0.02 $/kWh
O&M percentage of capital cost	2.2%
System annual operation hours	2500 hours

The main findings of the exergoeconomic assessment is based on stream exergy rates and corresponding exergy destruction ratios. Thus, exergy destruction rates of the system components is illustrated in Fig. 103. In the Fresnel lens and dielectric mirror, only light interactions occur. Therefore, the exergy destruction rates are quite higher than other components. In addition, inlet irradiance is about 946 W/m^2 and it is concentrated about 6 to 10 times. The concentration and light splitting processes destruct more exergy than PV and PEC processes.

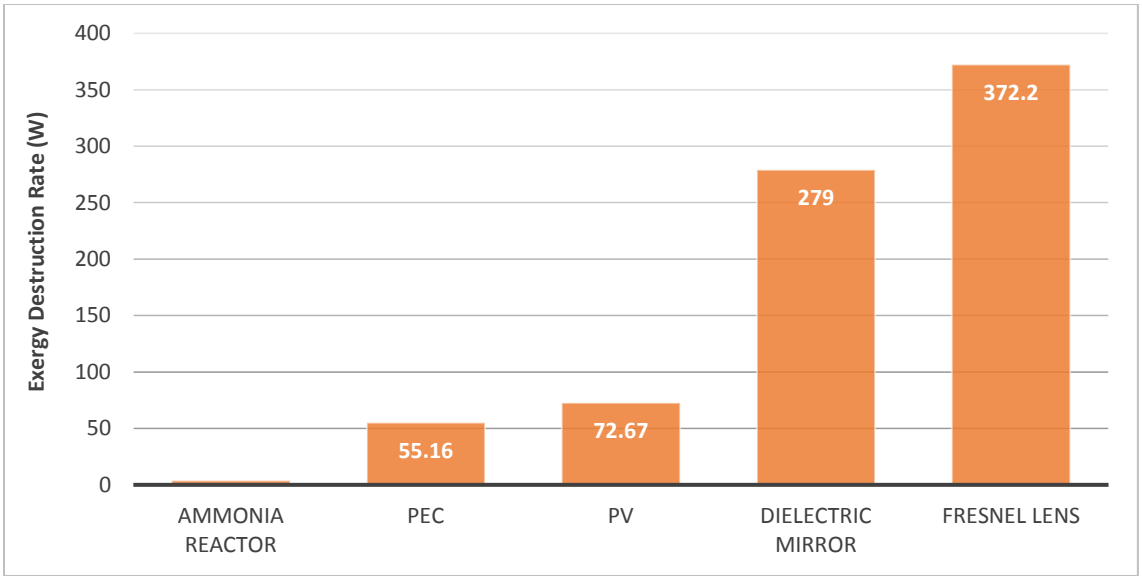

Figure 103 The exergy destruction rates of the integrated system components

The cost rates and costs of exergy destructions for each component are tabulated in Table 34. The highest capital cost is observed in PEC reactor because of high purchased cost and electricity input. Secondly, ammonia reactor has highest cost rate as shown in Fig. 104. These two reactors are the only electricity consuming devices resulting in a larger cost rates. Furthermore, since PV generates electricity, the total cost rate is quite lower than other components.

Table 34 The exergoeconomic results of the components in the integrated system

Component	Cost Rate of Exergy Destruction - $\dot{C}_D$ ($/h)	Exergoeconomic Factor - f (%)	Total Cost Rate - $\dot{C}_{total}$ ($/h)	Annual Investment Cost Rate - $\dot{Z}$ ($/h)
Ammonia reactor	0.07295	42.46	0.1268	0.05384
Fresnel Lens	0.004365	50	0.008731	0.004365
Dielectric Mirror	0.03911	50	0.07823	0.03911
PEC	0.1596	59.27	0.3918	0.2322
PV	0.003902	54.4	0.008559	0.004656
TOTAL	0.2799	54.42	0.6141	0.3342

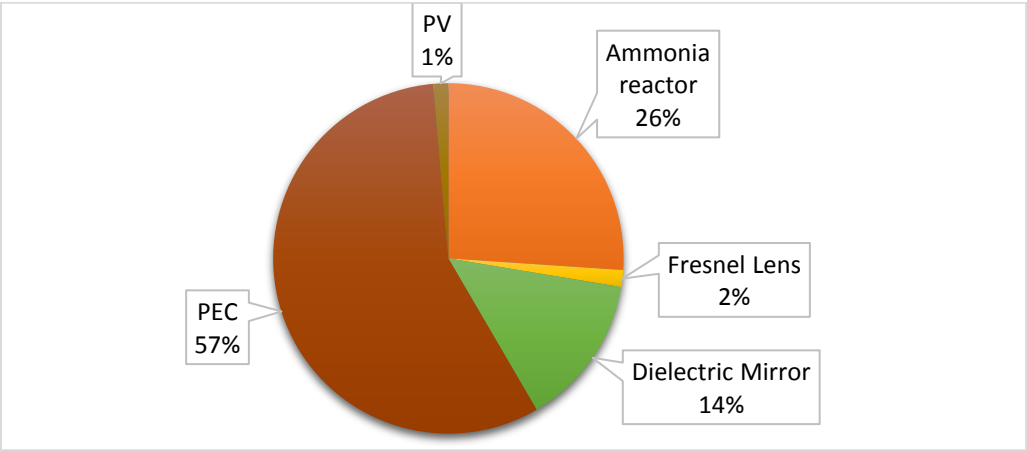

Figure 104 The cost rate of exergy destruction in each component of the integrated system

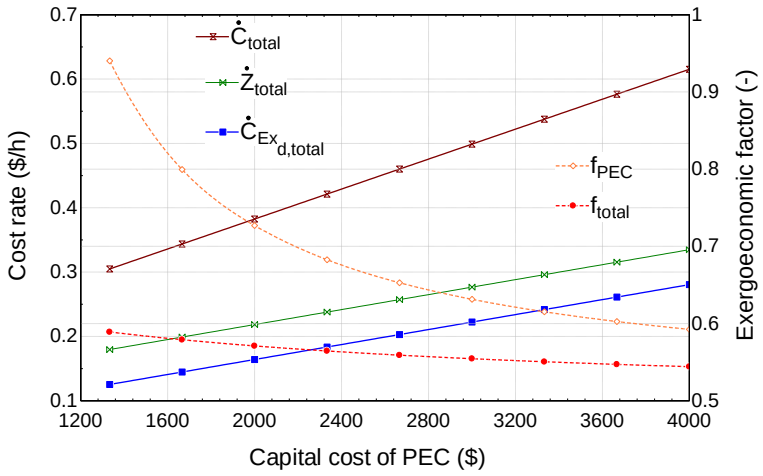

Figure 105 The effects of PEC reactor capital cost on the system cost rates and exergoeconomic factors

Since the PEC reactor capital cost is the highest contributor to the system cost, a parametric study is conducted to investigate the effect on the total cost rates as shown in Fig 105. In case the PEC reactor can be built in a more cost effective way corresponding to about 2000$, the total exergy destruction cost rate decreases to 0.1641 $/h whereas total exergoeconomic factor increases to 57.1%. Also, the exergoeconomic factor of PEC reactor component increases to 72.7 % from 54.41%.

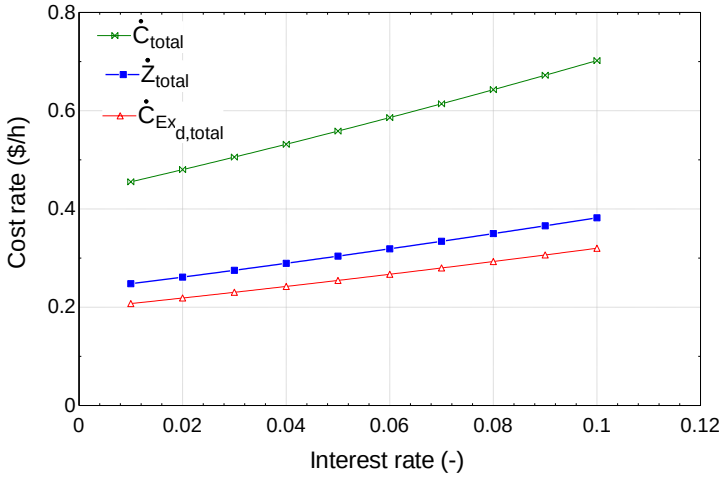

Figure 106 The effects of increasing interest rate on the total system cost rates

Fig 106 clearly shows that interest rate has a negative impact on the system cost rates. Although the total cost rate of the system is 0.4801 $/h at 2% interest rate, it rises to 0.702 $/h at 10% interest. The lifetime of the system and components has also important role in the total cost rate as shown in Fig. 107. Each component can have different lifetime periods. For example, the PEC electrodes may need to be replaced in two years whereas the solar concentrator may have up to ten years operation. In the base case, the system lifetime is taken to be 10 years for the experimental system that is about 0.6141 $/h total cost rate. However, in case the lifetime can be increased up to 40 years, the total cost rate can be decreased down to 0.3233 $/h.

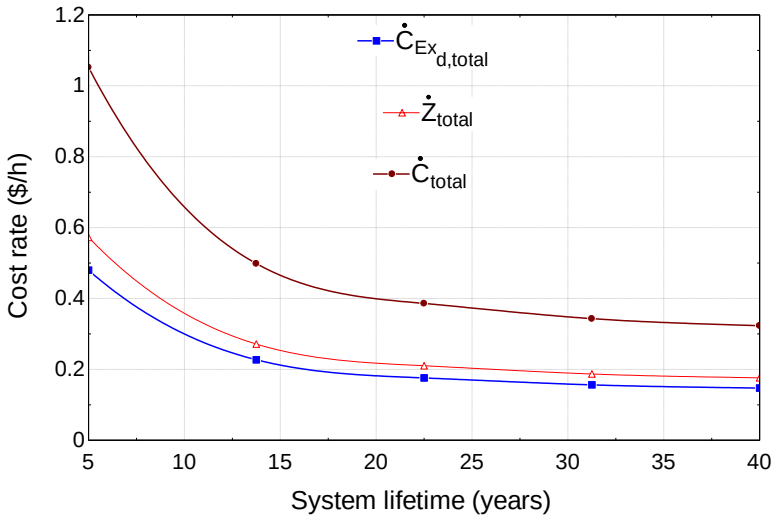

Figure 107 The effects of system total lifetime on the system cost rates

Annual operation time of the systems are also critical for the solar energy applications. The intermittency of the solar energy decreases the total annual operation time. The availability of the sunshine depends on the season and location. This is also named as capacity factor. In general, the capacity factor of the solar energy applications range between 10-30% corresponding to about 876 to 2628 hours annually. In the base case of the system, the operation time is set to 2500 hours. However, if the operation time diminishes to 1000 hours, the total cost rate rises to about 1 $/h as shown in Fig. 108.

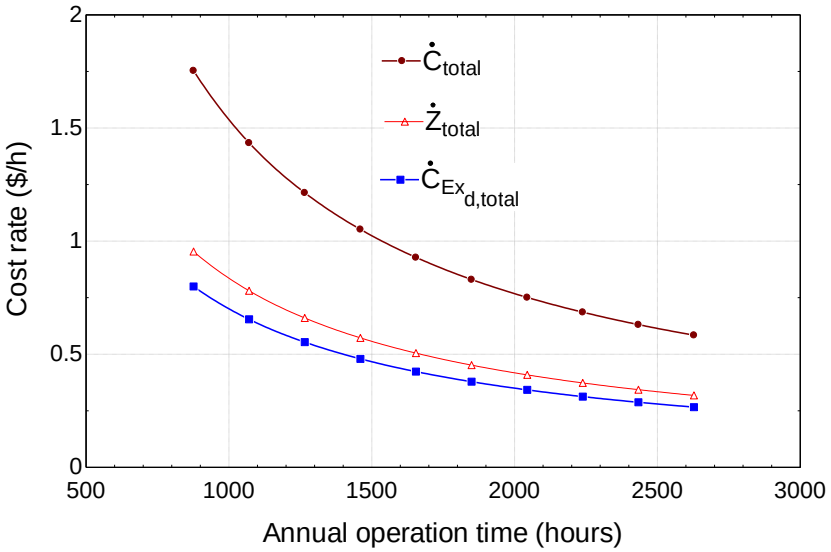

Figure 108 The effects of system total lifetime on the system cost rates

CHAPTER 10: SCALE-UP ANALYSES FOR SOLAR ENERGY BASED AMMONIA PRODUCTION

In case of larger production scales, the mass manufacturing of these equipment will be considerably lower. In order to analyze the cost of hydrogen and ammonia at larger production capacities such as 1000 kg/day, the scale up analyses are conducted as explained in the following paragraphs. PEC systems use solar photons to generate a voltage in an electrolysis cell sufficient to electrolyze water, producing H_2 and O_2 gases. For the economic analyses of the photoelectrochemical hydrogen production system, the Hydrogen Analysis (H2A) production model [94] is used which is developed by U.S. DOE Hydrogen & Fuel Cells Program. The H2A Production Model analyzes the technical and economic aspects of central and forecourt hydrogen production systems. Using a standard discounted cash flow rate of return methodology, it determines the minimum hydrogen levelized cost, including a specified after-tax internal rate of return from the production technology. The employed scenario models a PEC solar concentrator system using reflectors to focus the solar flux with a concentration ratio of 10 intensity ratio onto multi-junction PEC cell receivers immersed in an electrolyte reservoir and pressurized to 300 psi. The PEC cells are in electrical contact with a small electrolyte reservoir and produce oxygen gas on the anode side and hydrogen gas on the cathode side. The start-up year of the plant is taken as 2020. The Chemical Engineering Plant Cost Index (CEPCI) is used to adjust the capital cost of the H_2 Production facility from the basis year to the current year. The Consumer Price Inflator (CPI) is used to deflate all dollars from the current year to the Reference Year. The available model is quite similar to the designed and tested concentrated PEC system except for the solar light splitting part. Hence, the solar splitting mechanism is not considered in the scaled-up cost assessment. A solar tracking system is employed to make best use of direct radiation capture. Solar concentrators, which can use reflectors or lenses to concentrate the solar energy, considerably lessen the cost influence of the PV component of the system, but add the costs of the concentrators and directing systems. For the concentrator PEC system, the water reservoir and the H_2 and O_2 collected are pressurized by the inlet water pump at relatively low added cost. Pressurization to 300 psi avoids the need for a separate compressor, minimizes water vapor loss by the reactor, and reduces O_2 gas bubble size, which minimizes potential bubble scattering of incident photons at the anode face.

The H2A Costing Model [94] delivers an organized layout to enter factors which impact cash inflows and outflows associated with the construction and operation of a hydrogen production plant. The system practices a solar concentrator reflector to focus solar direct radiation onto the PEC cell. A PEC concentrator system can possibly use a concentration ratio of 10-50 suns; nonetheless, since the experimentally tested system uses about a concentration ratio of 6 to 10, the scale-up analyses are considered for 10 suns. Plant control arrangements perform many duties including local and remote monitoring, alarming and controlling of plant equipment and functions. The model comprises the control and instrumentation mechanisms including the functionality and safety. In the scaled up analyses for hydrogen production, the capacity factor and plant outputs are listed in Table 35. The main financial parameters used in the cost analyses are shown in Table 36. Industrial electricity prices are taken in the calculations as \$0.06/kWh [95]. The overall solar-to-hydrogen conversion efficiency of the concentrated PEC hydrogen production system is taken as 16% which is the expected efficiency by 2020 as mentioned in the literature review section. It is assumed that the average solar irradiance is 6.55 kWh/m^2/day.

Table 35 The capacity and hydrogen production plant output

Operating Capacity Factor (%)	85.0%
Plant Design Capacity (kg of H_2/day)	1,000
Plant Output (kg/day)	850
Plant Output (kg/year)	310,250

Table 36 The financial input parameters used to calculate the unit hydrogen production cost

Reference year	2009
Assumed start-up year	2020
Basis year	2009
Length of Construction Period (years)	2
% of Capital Spent in 1st Year of Construction	20%
% of Capital Spent in 2nd Year of Construction	80%
Start-up Time (years)	0.4
Plant life (years)	40
Analysis period (years)	40
Depreciation Schedule Length (years)	20
Decommissioning costs (% of depreciable capital investment)	10%
Salvage value (% of total capital investment)	5%
Inflation rate (%)	1.1%

Source: [94]

Engineering & design and up-Front permitting costs are assumed to be 7.5% of the direct capital cost whereas process contingency cost is assumed to be 10% of direct capital cost. Furthermore, the land cost in Ontario, Canada is taken as $6,500 per acre for rural area. The costs are expressed in U.S dollar. The total required land area is calculated based on the solar-to-hydrogen efficiency and light absorption efficiencies. The basis year costs (2009) are inflated to 2017 dollars using inflation tool [96].

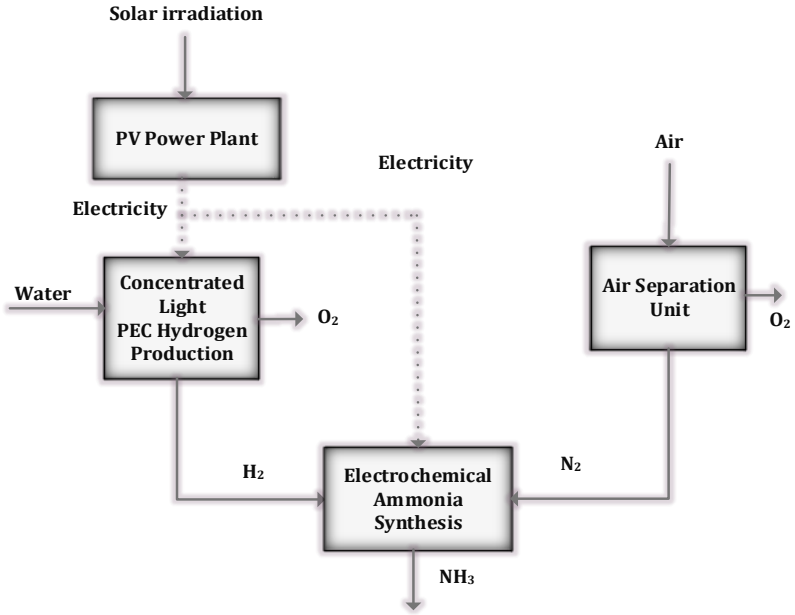

Figure 109 Illustration of large scale electrochemical ammonia production plant

The cost of production for the ammonia facility is of principal importance: a great portion of the complete costs will come from acquiring electricity, presumed to be the utility cost. The cost of production is the summation of waste disposal, labor costs, utilities, general expenses, raw materials, taxes, maintenance expenses as well as other minor costs. Cryogenic air separation methods are frequently used in medium to large scale facilities to yield nitrogen, oxygen, and argon as gases or liquid products. Cryogenic air separation is generally favored technology for generating very high purity oxygen and nitrogen. The plants producing only nitrogen are less complex and need less power to function than an oxygen-only plant making the same amount of product. Producing these products in liquid form necessitates additional apparatus and more power required per unit of delivered product. The average cost of ammonia production from the electrolysis-based systems are approximately 20-40% of hydrogen production cost as previously given in [97] for various ammonia production methods such as PV electrolysis. 17.8% of ammonia is hydrogen in weight, and around 3% of ammonia production cost comes from air separation based nitrogen production [98]. The schematic diagram of the large scale electrochemical ammonia production plant using photoelectrochemical hydrogen is depicted in Fig 109. In Haber-Bosch ammonia synthesis plants, there are two main compressors to compress the feed gases into the Haber-Bosch reactor. These compressors consume most of the electricity in the synthesis loop. The synthesis loop requires about 5.5% of the total power requirements in an electrolyzer based Haber-Bosch plant [98]. On the other hand, in the tested electrochemical ammonia synthesis, the gases are in atmospheric pressure in the reaction. Hence, compression costs are eliminated. However, currently electrochemical ammonia synthesis requires more electricity than Haber-Bosch process per unit kg of product because of the strong chemical bonds. Considering these conditions, a conversion factor is calculated for ammonia cost determination based on the hydrogen cost. Therefore, ammonia production costs are calculated as the 26% of hydrogen production cost. The prices are production prices for hydrogen and ammonia which means that the transportation to the final end user or storage processes are not included. The economic analyses results scale-up study are presented in this section. The plant is scaled-up to 1000 kg/day. The capital costs, operation/maintenance costs etc. are considered in the analyses. Table 37 shows the total capital costs of the hydrogen production plant with cost breakdown of indirect and direct capital costs. The total capital cost of the concentrated light PEC hydrogen production plant is calculated as $6,428,852.03. Total Variable Operating Costs per year is estimated as $4,800 because of unpredicted Replacement Capital Cost. The fixed operating costs are tabulated in Table 38.

Table 37 The direct and indirect depreciable capital costs

Indirect Depreciable Capital Costs	**2017$**
Site Preparation ($)	$98,690.81
Engineering & design ($)	$370,089.69
Project contingency ($)	$493,452.92
Up-Front Permitting Costs ($)	$370,089.69
Total Depreciable Capital Costs (Including direct capital costs)	$6,266,851.18
Cost of land ($/acre)	$7,256.69
Land required (acres)	22.32
Land Cost ($)	$162,001.32
Total Non-Depreciable Capital Costs	$162,000.85
Total Capital Costs	$6,428,852.03

Table 38 The fixed operating costs of the PEC hydrogen production plant

Fixed Operating Costs	**2017$**
Burdened labor cost, including overhead ($/man-hour)	$45.20
Labor cost ($/year)	$24,444.16
General and administrative expense ($/year)	$4,888.38
Licensing, Permits and Fees ($/year)	$589.11
Property tax and insurance rate (% of total capital investment per year) (In Ontario)	1.45%
Property taxes and insurance ($/year)	$93,218.22
Production Maintenance and Repairs ($/year)	$19,973.88
Total Fixed Operating Costs	$143,114.50

Production maintenance and repair costs are predicted to 4% of the overall cost excluding the replacement parts which are mainly electrodes and lens. The state, federal taxes and after-tax real rate of return are taken as 6.0%, 35.0% and 1%, respectively in the cost analysis. The after-tax real rate of return affects the cost considerably which would increase the cost of hydrogen. The after-tax real rate of return is the actual financial benefit of an investment after accounting for inflation and taxes. The calculations include the replacement of the PEC reactor electrodes every two years and replacement of the PEC cells including the Fresnel lens solar concentrator every ten years as tabulated for 40 year operation in Table 39. The other components are allocated for 20 years.

Table 39 The cost of material replacements of the system components

Operations Year	Total Yearly Replacement Costs (2017$)	Replacement
1	$35,061	
2	$632,966	Replacement of PEC electrodes every 2 years.
3	$35,061	
4	$632,966	Replacement of PEC electrodes every 2 years.
5	$35,061	
6	$632,966	Replacement of PEC electrodes every 2 years.
7	$35,061	
8	$632,966	Replacement of PEC electrodes every 2 years.
9	$35,061	
10	$4,997,679	Replacement of PEC electrodes every 2 years and replacement of PEC cell including solar concentrator, windows and sealing every 10 years plus installation
11	$35,061	
12	$632,966	Replacement of PEC electrodes every 2 years.
13	$35,061	
14	$632,966	Replacement of PEC electrodes every 2 years.
15	$35,061	
16	$632,966	Replacement of PEC electrodes every 2 years.
17	$35,061	
18	$632,966	Replacement of PEC electrodes every 2 years.

19	$35,061	
20	$4,997,679	Replacement of PEC electrodes every 2 years and replacement of PEC cell including solar concentrator, windows and sealing every 10 years plus installation
21	$35,061	
22	$632,966	Replacement of PEC electrodes every 2 years.
23	$35,061	
24	$632,966	Replacement of PEC electrodes every 2 years.
25	$35,061	
26	$632,966	Replacement of PEC electrodes every 2 years.
27	$35,061	
28	$632,966	Replacement of PEC electrodes every 2 years.
29	$35,061	
30	$4,997,679	Replacement of PEC electrodes every 2 years and replacement of PEC cell including solar concentrator, windows and sealing every 10 years plus installation
31	$35,061	
32	$632,966	Replacement of PEC electrodes every 2 years.
33	$35,061	
34	$632,966	Replacement of PEC electrodes every 2 years.
35	$35,061	
36	$632,966	Replacement of PEC electrodes every 2 years.
37	$35,061	
38	$632,966	Replacement of PEC electrodes every 2 years.
39	$35,061	
40	$35,061	

The capital cost of the system components including the control unit, PEC cell, pumps and other components are shown in Table 40.

Table 40 The direct capital costs of the components in 1000 kg/day PEC concentrated light hydrogen production plant

Major components/systems	**Installed Costs (2017$)**
PEC cell body, concentrating and containment system	$ 3,139,192
PEC Electrodes	$ 506,321
Make-up Water Pump	$ 237
Manifold Piping	$ 18,062
Collection Piping	$ 4,475
Column Collection Piping	$ 2,111
Final Collection Piping	$ 481
Condenser	$ 7,924
Manifold Piping (diameter)	$ 18,062
Collection Piping (diameter)	$ 4,475
Column Collection Piping (diameter)	$ 2,111
Final Collection Piping (diameter)	$ 481
PLC	$ 3,349

Control Room building	$ 19,567
Control Room Wiring Panel	$ 3,349
Computer and Monitor	$ 1,675
LabVIEW Software	$ 4,799
Water Level Controllers	$ 78,902
Pressure Sensors	$ 6,933
Hydrogen Area Sensors	$ 152,725
Hydrogen Flow Meter	$ 6,140
Instrument Wiring	$ 453
Power Wiring	$ 227
Conduit	$ 6,771
Piping Installation	$ 8,870
Reactor Foundation & Erection	$ 556,953
Reactor feed install	$ 71
Gas processing Subassembly install	$ 2,377
Control System Install	$ 85,467
TOTAL DIRECT CAPITAL COST	$ 4,675,618

Here, the PEC cell reactor body cost is taken as $145.23/m^2 including the concentrating and containment system. In addition, the PEC electrodes are taken as $234.24/m^2 unit cost. For a 1 ton/day hydrogen production plant, an overall solar capturing area of 21,615 m^2 and electrode area of about 2162 m^2 are required. The highest cost is the PEC cell with the concentrators which is followed by the PEC electrodes.

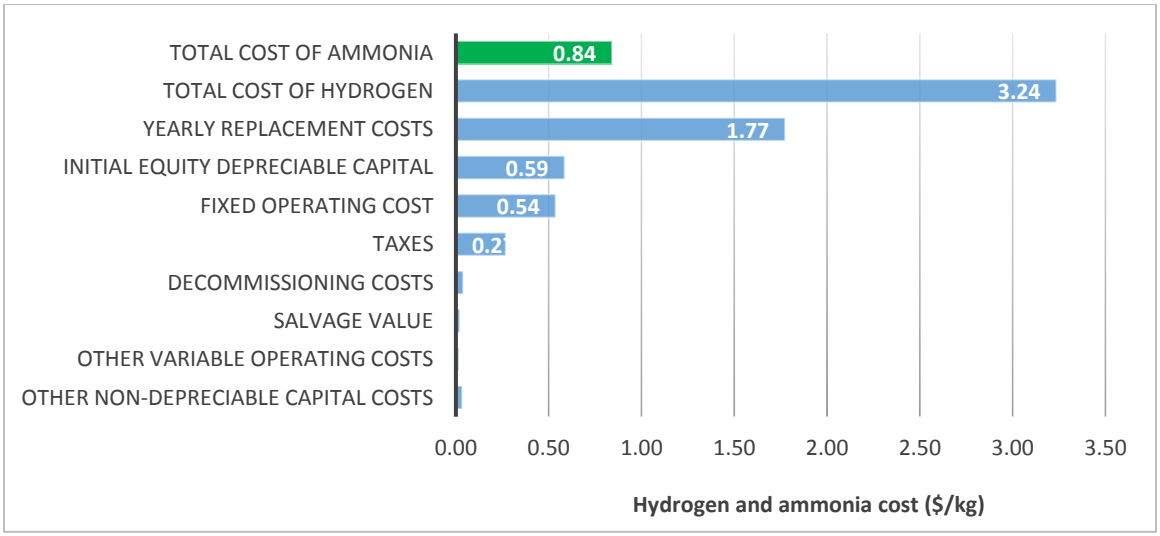

Figure 110 The calculated cost of hydrogen and ammonia with contributing factors for a 1000 kg/day concentrated PEC hydrogen production plant

The hydrogen and ammonia costs calculated based on the model are shown in Fig. 110. Moreover, the breakdown of the hydrogen cost are illustrated. Yearly replacement costs are about 1.77 $/kg hydrogen. This implies that if the durability and stability of the PEC electrodes and solar concentrators can be improved, the unit cost of hydrogen would decrease considerably. The

hydrogen cost per kg is calculated to be 3.24 $/kg. The cost of ammonia is found to be 0.84 $/kg. The fixed operation and maintenance costs represent about 14% of the overall hydrogen cost whereas the capital cost of the plant has about 84% share as shown in Fig. 111

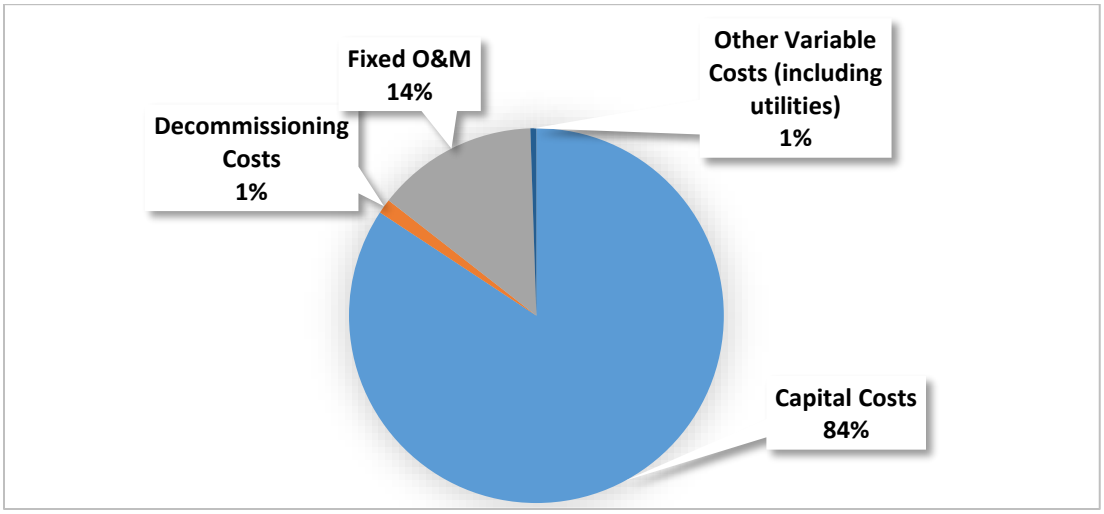

Figure 111 The cost breakdown of hydrogen production plant

The cost of hydrogen is expected to decrease with higher concentration ratio. The bars within the tornado chart in Fig. 112 show the range of minimum hydrogen cost values obtained by entering a base value for each specified variable, a reducing value, and an increasing value while holding all other variables constant at their base values.

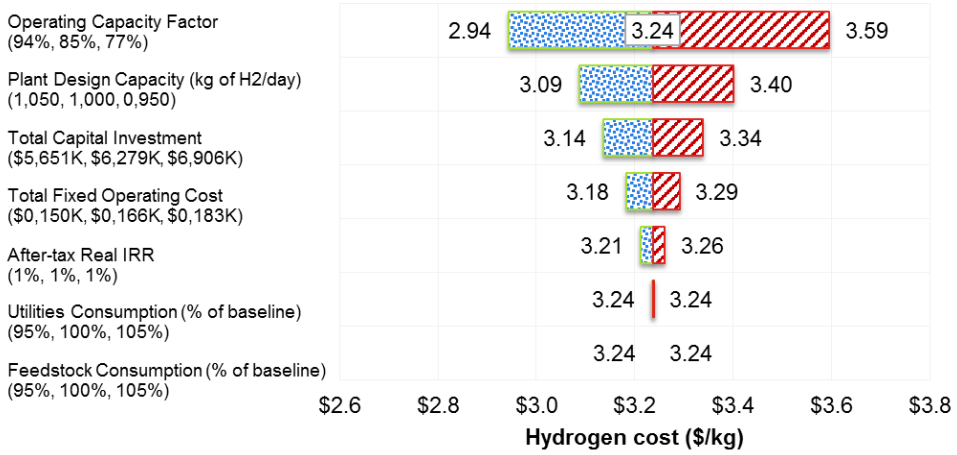

Figure 112 The sensitivity of the hydrogen cost based on different parameters

The operating capacity is chosen as 85% in the base case. As shown in Fig. 113, when operating capacity is increased to 94%, the cost of hydrogen can decrease down to 2.94 $/kg.

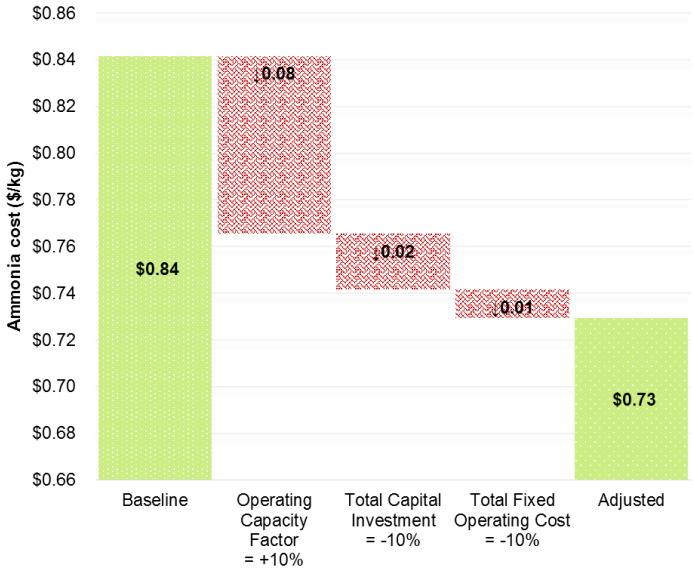

Figure 113 Waterfall diagram for ammonia cost considering better plant operating capacity and lower capital, operating costs

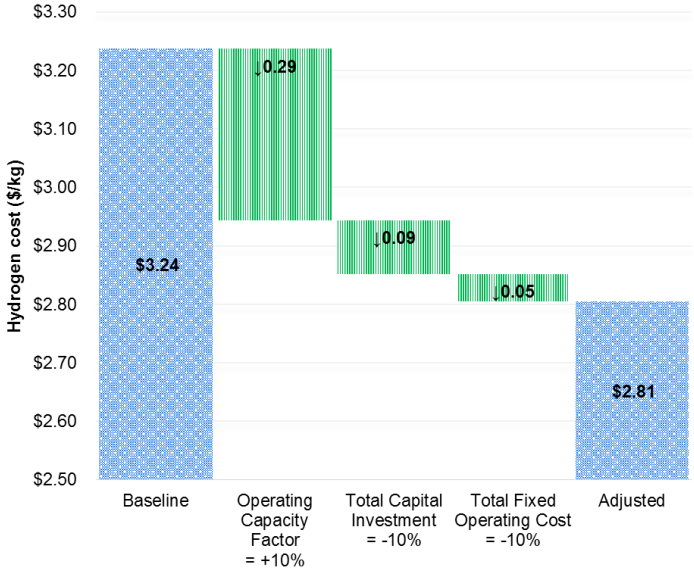

Figure 114 Waterfall diagram for hydrogen cost considering better plant operating capacity and lower capital, operating costs

On the other hand, if there is 10% lower capital investment, the cost of hydrogen can drop by 0.1 $/kg. The plant capacity factor is increased 10%, the capital investment and fixed operating costs are lowered 10% and utilities consumption is decreased by 5%. Under these conditions, the adjusted hydrogen cost can decrease down to 2.82 $/kg and ammonia cost in this case is found to be 0.73$/kg. The waterfall diagram of the hydrogen cost by increasing the operating conditions is shown in Fig. 114 where multiple improvements are considered.

7. Case Study for Ontario

In this section, the total cost of ammonia under different production pathways is calculated. The hydrogen production costs for wind and hydropower routes are calculated using H2A Central

Hydrogen Production Model, Version 3.1 of U.S. DOE [94] whereas the cost for photoelectrochemical hydrogen is previously calculated in scale-up analyses. The cost of electricity considered in the calculations is shown in Table 41. The land transportation is assumed to be for 800 km where 0.025 US$/kg is considered by truck transportation to the port in Quebec. The overseas transport is realized by the ocean tankers similar to LPG tankers in which the unit cost is taken as 0.1097 US$/kg of liquid ammonia.

Table 41 Cost of electricity considered in the analyses

Method	Cost of Electricity (US$/kWh)
Hydropower	0.0275
Wind	0.045
SMR	0.05
Solar	0.06

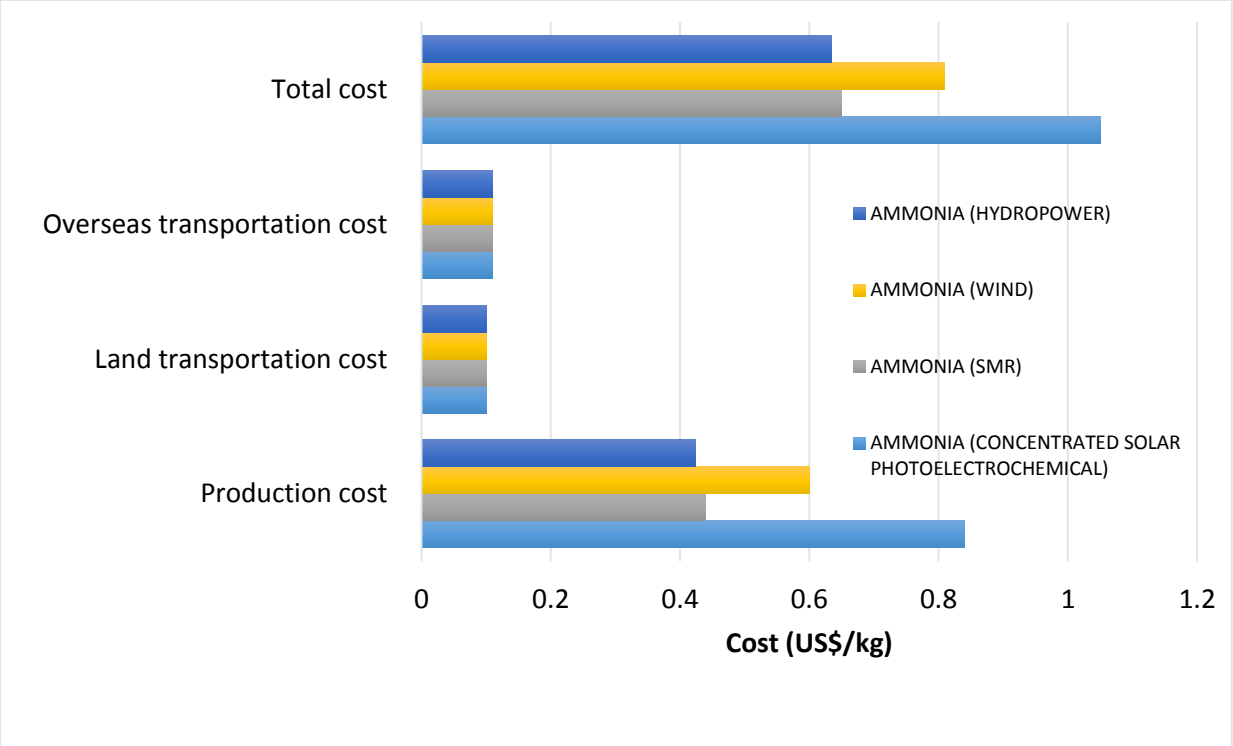

Figure 115 Comparison of ammonia costs using different production routes in Ontario

The required hydrogen for ammonia is produced using electrolysis of water except for the SMR method. The low-cost hydropower yields slightly lower total cost compared to SMR method as shown in Fig. 115. Since the solar energy route employs electrochemical ammonia synthesis rather than Haber-Bosch plant, the production cost is higher than other methods. The electrochemical ammonia synthesis route is in development phase and the costs will decrease by improving technology. However, Haber-Bosch process is a mature and saturated technology in which cost reduction is less likely to happen.

CHAPTER 11: CONCLUDING REMARKS

Ammonia is a carbon-free fuel suitable for use in transportation sector. It has a well-established production and distribution infrastructure, and has zero global warming potential during operation. In addition to its attractive qualities as a fuel, ammonia is widely used as a NOx reducing agent for combustion exhaust gases using selective catalytic reduction (SCR), and its capacity as a refrigerant can be applied to recover and further utilize engine heat that would otherwise be lost. Renewable ammonia (NH_3), which is a carbon-free fuel, refrigerant and working fluid; and storage media of hydrogen, are unique solutions to Canada's energy and environmental challenges. Renewable ammonia and hydrogen can serve almost all economic sectors, ranging from transportation to residential, industrial to commercial, public to utility, and agricultural to chemical. Ammonia as a potential fuel for vehicles or power generation can also be economically produced using conventional hydrocarbons in a cleaner manner by implying current technologies and developments. Ammonia can be produced using fossil fuels, or any renewable energy source using heat and/or electricity. Ammonia and hydrogen applications have been developed for sectors including but not limited to: transportation, industrial, commercial, utility, agricultural, and the chemical industries.

High-efficiency ammonia/urea plants using natural gas and other hydrocarbon feed stocks can be built beside natural gas power plants and oil sand extraction sites. Utilizing the waste, low-grade heat and excess oxygen results in a significant reduction of costs and emissions. The 200 million metric tonnes of ammonia produced globally each year comes from combining nitrogen from air with the hydrogen in coal and natural gas. The carbon in these hydrocarbons is usually emitted as carbon dioxide (CO_2), but about 40 per cent of the ammonia produced is combined with CO_2 sequestered in the a well-known Haber-Bosch synthesis process to make urea.

Dissociation of hydrocarbons such as methane and oil sand bitumen into hydrogen which can be then converted to ammonia is a promising option for oil sand and natural gas reserves in Western Canada and stranded gas reserves in Newfoundland and Labrador. Ammonia has significant environmental advantages. Even if ammonia is produced from hydrocarbons, it has similar greenhouse gas emissions with a solar energy based route.

In terms of environmental sustainability, ammonia can be produced using either fossil fuels, or any renewable energy source, using heat and/or electricity, which allows for evolution of ammonia production methods and technologies in parallel with sustainable development. Ammonia as a sustainable fuel can be used in all types of combustion engines, gas turbines, burners with only small modifications and directly in fuel cells which is a very significant advantage compared to another type of fuels. Reducing the total greenhouse gas emissions from marine transportation is possible by using ammonia which is carbon-free fuel. When ammonia is produced using renewable energy such as wind (versus conventional unleaded gasoline), a further 30 per cent greenhouse gas reduction is possible. When compared to propane, greenhouse gas emissions decrease about 18 per cent. An ammonia-driven passenger vehicle emits less greenhouse gas than compressed natural gas (CNG), liquefied petroleum gas (LPG), diesel, gasoline, and even hybrid electric vehicles. They can be utilized for maritime ship engines directly as supplementary fuels or individual fuels. Ammonia fueled ships yield considerably lower global warming impact during operation. Ammonia as a sustainable and clean fuel in road vehicles yield also the lowest global warming potential after electric and hydrogen vehicles. As a result, ammonia usage in the communities for transportation sector will bring significant cost and environmental benefits together with public satisfaction.

REFERENCES

1. Yara Fertilizer Industry Handbook. 2017.
2. Weekly Fertilizer Review [Internet]. Ammonia prices. [cited 2017 Jan 7]. Available from: http://www.farmfutures.com/story-weekly-fertilizer-review-0-30765
3. U.S., Mexico to source 50% of electricity from clean energy by 2025 - Politics - CBC News [Internet]. [cited 2017 Mar 24]. Available from: http://www.cbc.ca/news/politics/three-amigos-summit-climate-policies-1.3654166
4. Muradov NZ, Veziroğlu TN. From hydrocarbon to hydrogen–carbon to hydrogen economy. Int J Hydrogen Energy. 2005;30(3):225–37.
5. Muradov N. Hydrogen via methane decomposition: an application for decarbonization of fossil fuels. Int J Hydrogen Energy. 2001;26(11):1165–75.
6. Muradov NZ. How to produce hydrogen from fossil fuels without CO2 emission. Int J Hydrogen Energy. 1993;18(3):211–5.
7. Brohi EA. Ammonia as fuel for internal combustion engines ? An evaluation of the feasibility of using nitrogen-based fuels in ICE. CHALMERS UNIVERSITY OF TECHNOLOGY; 2014.
8. Iki N, Kurata O, Matsunuma T, Inoue T, Suzuki M, Tsujimura T, et al. Micro Gas Turbine Firing Kerosene and Ammonia. In: ASME Turbo Expo 2015: Turbine Technical Conference and Exposition. American Society of Mechanical Engineers; 2015. p. V008T23A023-V008T23A023.
9. Haputhanthri SO, Maxwell TT, Fleming J, Austin C. Ammonia and Gasoline Fuel Blends for Spark Ignited Internal Combustion Engines. J Energy Resour Technol. 2015;137(6):62201.
10. Nozari H, Karabeyoğlu A. Numerical study of combustion characteristics of ammonia as a renewable fuel and establishment of reduced reaction mechanisms. Fuel. 2015;159:223–33.
11. Reiter AJ, Kong S-C. Combustion and emissions characteristics of compression-ignition engine using dual ammonia-diesel fuel. Fuel. 2011;90(1):87–97.
12. Ryu K, Zacharakis-Jutz GE, Kong S-C. Performance enhancement of ammonia-fueled engine by using dissociation catalyst for hydrogen generation. Int J Hydrogen Energy. 2014;39(5):2390–8.
13. Zamfirescu C, Dincer I. Using ammonia as a sustainable fuel. J Power Sources. 2008;185(1):459–65.
14. Zamfirescu C, Dincer I. Ammonia as a green fuel and hydrogen source for vehicular applications. Fuel Process Technol. 2009;90(5):729–37.
15. Hinnemann B, Nørskov JK. Catalysis by Enzymes: The Biological Ammonia Synthesis. Top Catal. 2006 Mar;37(1):55–70.
16. Lan R, Irvine JTS, Tao S. Synthesis of ammonia directly from air and water at ambient temperature and pressure. Sci Rep. 2013;3:1145.
17. Li F-F, Licht S. Advances in Understanding the Mechanism and Improved Stability of the Synthesis of Ammonia from Air and Water in Hydroxide Suspensions of Nanoscale Fe2O3. Inorg Chem. 2014;53(19):10042–4.
18. Licht S, Cui B, Wang B, Li F-F, Lau J, Liu S. Ammonia synthesis by N2 and steam electrolysis in molten hydroxide suspensions of nanoscale Fe2O3. Science (80-). 2014;345(6197):637–40.
19. Paschkewitz TM. Ammonia Production at Ambient Temperature and Pressure: An

Electrochemical and Biological Approach. PhD (Doctor of Philosophy) thesis. University of Iowa; 2012.
20. Skodra A, Stoukides M. Electrocatalytic synthesis of ammonia from steam and nitrogen at atmospheric pressure. Solid State Ionics. 2009;180(23–25):1332–6.
21. Kordali V, Kyriacou G, Lambrou C. Electrochemical synthesis of ammonia at atmospheric pressure and low temperature in a solid polymer electrolyte cell. Chem Commun. 2000;(17):1673–4.
22. Ganley JC. An intermediate-temperature direct ammonia fuel cell with a molten alkaline hydroxide electrolyte. J Power Sources. 2008;178(1):44–7.
23. Serizawa N, Miyashiro H, Takei K, Ikezumi T, Nishikiori T, Ito Y. Dissolution Behavior of Ammonia Electrosynthesized in Molten LiCl–KCl–CsCl System. J Electrochem Soc. 2012;159(4):E87–91.
24. Amar I, Lan R, Petit CG, Tao S. Solid-state electrochemical synthesis of ammonia: a review. J Solid State Electrochem. 2011;15(9):1845–60.
25. Murakami T, Nohira T, Ogata YH, Ito Y. Electrolytic Ammonia Synthesis in Molten Salts under Atmospheric Pressure Using Methane as a Hydrogen Source. Electrochem Solid-State Lett. 2005;8(4):D12–4.
26. Yiokari CG, Pitselis GE, Polydoros DG, Katsaounis AD, Vayenas CG. High-Pressure Electrochemical Promotion of Ammonia Synthesis over an Industrial Iron Catalyst. J Phys Chem A. 2000;104(46):10600–2.
27. Marnellos G, Stoukides M. Ammonia Synthesis at Atmospheric Pressure. Science (80-). 1998;282(5386):98–100.
28. Zhang Z, Zhong Z, Liu R. Cathode catalysis performance of SmBaCuMO5+δ (M=Fe, Co, Ni) in ammonia synthesis. J Rare Earths. 2010;28(4):556–9.
29. Wang WB, Cao XB, Gao WJ, Zhang F, Wang HT, Ma GL. Ammonia synthesis at atmospheric pressure using a reactor with thin solid electrolyte BaCe0.85Y0.15O3−α membrane. J Memb Sci. 2010;360(1–2):397–403.
30. Marnellos G, Zisekas S, Stoukides M. Synthesis of Ammonia at Atmospheric Pressure with the Use of Solid State Proton Conductors. J Catal. 2000;193(1):80–7.
31. Goto T, Ito Y. Electrochemical reduction of nitrogen gas in a molten chloride system. Electrochim Acta. 1998;43(21–22):3379–84.
32. Kugler K, Luhn M, Schramm JA, Rahimi K, Wessling M. Galvanic deposition of Rh and Ru on randomly structured Ti felts for the electrochemical NH3 synthesis. Phys Chem Chem Phys. 2015;17(5):3768–82.
33. Yun DS, Joo JH, Yu JH, Yoon HC, Kim J-N, Yoo C-Y. Electrochemical ammonia synthesis from steam and nitrogen using proton conducting yttrium doped barium zirconate electrolyte with silver, platinum, and lanthanum strontium cobalt ferrite electrocatalyst. J Power Sources. 2015;284:245–51.
34. Xu G, Liu R, Wang J. Electrochemical synthesis of ammonia using a cell with a Nafion membrane and SmFe0. 7Cu0. 3− xNixO3 (x= 0− 0.3) cathode at atmospheric pressure and lower temperature. Sci China Ser B Chem. 2009;52(8):1171–5.
35. Garagounis I, Kyriakou V, Skodra A, Vasileiou E, Stoukides M. Electrochemical Synthesis of Ammonia in Solid Electrolyte Cells. Front Energy Res. 2014;2.
36. Skodras G, Kaldis S, Topis S, Koutsonikolas D, Grammelis P, Sakellaropoulos G. NH3 decomposition and simultaneous H 2 separation with a commercial Pd-Cu-Ag/V membrane. In: Proceedings of the Second International Green Energy Conference June.

2006. p. 25–9.
37. Norby T. Solid-state protonic conductors: principles, properties, progress and prospects. Solid State Ionics. 1999;125(1–4):1–11.
38. Iwahara H, Esaka T, Uchida H, Maeda N. Proton conduction in sintered oxides and its application to steam electrolysis for hydrogen production. Solid State Ionics. 1981;3:359–63.
39. Zhai Y, Ye C, Xiao J, Dai L. A microwave-induced solution-polymerization synthesis of doped LaGaO3 powders. J Power Sources. 2006;163(1):316–22.
40. Nowick AS, Du Y, Liang KC. Some factors that determine proton conductivity in nonstoichiometric complex perovskites. Solid State Ionics. 1999;125(1–4):303–11.
41. Giddey S, Badwal SPS, Kulkarni A. Review of electrochemical ammonia production technologies and materials. Int J Hydrogen Energy. 2013;38(34):14576–94.
42. Kyriakou V, Garagounis I, Vasileiou E, Vourros A, Stoukides M. Progress in the Electrochemical Synthesis of Ammonia. Catal Today.
43. Shipman MA, Symes MD. Recent progress towards the electrosynthesis of ammonia from sustainable resources. Catal Today.
44. Muradov NZ, Veziroğlu TN. "Green" path from fossil-based to hydrogen economy: An overview of carbon-neutral technologies. Int J Hydrogen Energy. 2008;33(23):6804–39.
45. Transportation of liquefied natural gas - Energy Education [Internet]. [cited 2017 Mar 23]. Available from: http://energyeducation.ca/encyclopedia/Transportation_of_liquefied_natural_gas
46. Jefferies LLC. LNG & LPG Shipping Fundamentals. 2013.
47. WHOLESALE GAS PRICE SURVEY 2016 EDITION. 2016.
48. U.S. Department of Energy. Potential Roles of Ammonia in a Hydrogen Economy.
49. Resources / Nitrogen / Production Cost Profile and Operational Capability [Internet]. [cited 2017 Mar 25]. Available from: http://www.potashcorp.com/overview/resources/nitrogen/production-cost-profile-operational-capability#
50. Nutrients / Nitrogen / Overview / Nitrogen Production Cash Costs [Internet]. [cited 2017 Mar 25]. Available from: http://www.potashcorp.com/overview/nutrients/nitrogen/overview/nitrogen-production-cash-costs
51. Advantages / Nitrogen / US Midwest Delivered Ammonia Cost [Internet]. [cited 2017 Mar 25]. Available from: http://www.potashcorp.com/overview/advantages/nitrogen/us-midwest-delivered-ammonia-cost
52. Alternative Fuels Data Center– Fuel Properties Comparison.
53. Barton R. Estimation of Costs of Heavy Vehicle Use Per Vehicle-Kilometre. 2006.
54. Johnson AP, LO CM, FARJO SF. Microwave-assisted bitumen extraction with vacuum-assisted sediment filtration. Google Patents; 2016.
55. Bosisio RG, Cambon JL, Chavarie C, Klvana D. Exprimental Result on the Hesting of Athabasca Tar Sand Samples with Microwave Power. J Microw Power. 1977 Jan 17;12(4):301–7.
56. Pringle FG. Microwave-based recovery of hydrocarbons and fossil fuels. Google Patents; 2009.
57. Renouf G, Scoular RJ, Soveran D. Treating Heavy Slop Oil With Variable Frequency Microwaves. In: Canadian International Petroleum Conference. Petroleum Society of

Canada; 2003.
58. Process for the recovery of shale oil, heavy oil, kerogen or tar from their natural sources. 1981.
59. Mutyala S, Fairbridge C, Paré JRJ, Bélanger JMR, Ng S, Hawkins R. Microwave applications to oil sands and petroleum: A review. Fuel Process Technol. 2010;91(2):127–35.
60. Consultants P. SimaPro Life Cycle Analysis version 7.2 (software).
61. GREET 2016. IL 60439-4844 USA: Argonne National Laboratory; 2016.
62. Facts and FIGURES - Air Transport Action Group (ATAG) [Internet]. [cited 2017 Mar 25]. Available from: http://www.atag.org/facts-and-figures.html
63. Koroneos C, Dompros A, Roumbas G, Moussiopoulos N. Advantages of the use of hydrogen fuel as compared to kerosene. Resour Conserv Recycl. 2005;44(2):99–113.
64. Contreras A, Yiğit S, Özay K, Veziroğlu TN. Hydrogen as aviation fuel: A comparison with hydrocarbon fuels. Int J Hydrogen Energy. 1997;22(10–11):1053–60.
65. A Full Fuel-Cycle Analysis of Energy and Emissions Impacts of Transportation Fuels Produced from Natural Gas.
66. Alternative Jet Fuels, Addendum 1 to Aviation Fuels Technical Review (FTR-3/A1).
67. Hileman JI, Stratton RW. Alternative jet fuel feasibility. Transp Policy. 2014;34:52–62.
68. Turner D, Xu H, Cracknell RF, Natarajan V, Chen X. Combustion performance of bio-ethanol at various blend ratios in a gasoline direct injection engine. Fuel. 2011;90(5):1999–2006.
69. Kong S-C. Combustion Efficiency and Exhaust Emissions of Ammonia Combustion in Diesel Engines. In: 2008 Annual NH3 Fuel Conference. MINNEAPOLIS: NH3 Fuel Association; 2008. p. SEPTEMBER 29-30.
70. Dincer I, Zamfirescu C. Apparatus for using ammonia as a sustainable fuel, refrigerant and NOx reduction agent. Google Patents; 2012.
71. GREET 2015. IL 60439-4844 USA: Argonne National Laboratory; 2015.
72. Appl M. Ammonia: principles and industrial practice. Vch Verlagsgesellschaft Mbh; 1999.
73. Dincer I, Zamfirescu C. Ammonia as a Potential Substance. In: Sustainable Energy Systems and Applications. Boston, MA: Springer US; 2011. p. 203–32.
74. Thomas G, Parks G. Potential roles of ammonia in a hydrogen economy: a study of issues related to the use ammonia for on-board vehicular hydrogen storage. US Dep Energy. 2006;23.
75. Metkemeijer R, Achard P. Ammonia as a feedstock for a hydrogen fuel cell; reformer and fuel cell behaviour. J Power Sources. 1994;49(1):271–82.
76. Yin SF, Xu BQ, Zhou XP, Au CT. A mini-review on ammonia decomposition catalysts for on-site generation of hydrogen for fuel cell applications. Appl Catal A Gen. 2004;277(1):1–9.
77. Chellappa AS, Fischer CM, Thomson WJ. Ammonia decomposition kinetics over Ni-Pt/Al 2 O 3 for PEM fuel cell applications. Appl Catal A Gen. 2002;227(1):231–40.
78. Roy SK, Ray N, Mukheriee D. Kinetics and mechanism of ammonia decomposition over alumina supported nickel catalysts. Plan Dev Div. 1975;41:48.
79. Chorkendorff I, Niemantsverdriet JW. Concepts of modern catalysis and kinetics. John Wiley & Sons; 2006.
80. Palaniappan R. Improving the efficiency of ammonia electrolysis for hydrogen production. Ohio University; 2013.

81. Vitse F, Cooper M, Botte GG. On the use of ammonia electrolysis for hydrogen production. J Power Sources. 2005;142(1):18–26.
82. Barbir F. PEM fuel cells : theory and practice. Academic Press; 2013. 518 p.
83. Barbir F. PEM electrolysis for production of hydrogen from renewable energy sources. Sol Energy. 2005;78(5):661–9.
84. Boggs BK, Botte GG. On-board hydrogen storage and production: An application of ammonia electrolysis. J Power Sources. 2009 Jul 15;192(2):573–81.
85. 1 Month Ruthenium Prices and Ruthenium Price Charts - InvestmentMine [Internet]. [cited 2017 Mar 22]. Available from: http://www.infomine.com/investment/metal-prices/ruthenium/1-month/
86. DOE Technical Targets for Hydrogen Storage Systems for Material Handling Equipment | Department of Energy [Internet]. [cited 2017 Mar 22]. Available from: https://energy.gov/eere/fuelcells/doe-technical-targets-hydrogen-storage-systems-material-handling-equipment
87. Satyapal S, Petrovic J, Read C, Thomas G, Ordaz G. The U.S. Department of Energy's National Hydrogen Storage Project: Progress towards meeting hydrogen-powered vehicle requirements. Catal Today. 2007 Feb 28;120(3–4):246–56.
88. Dong B-X, Tian H, Wu Y-C, Bu F-Y, Liu W-L, Teng Y-L, et al. Improved electrolysis of liquid ammonia for hydrogen generation via ammonium salt electrolyte and Pt/Rh/Ir electrocatalysts. Int J Hydrogen Energy. 2016 Sep;41(33):14507–18.
89. Mulder FM. Electrolytic cell for the production of ammonia. Google Patents; 2016.
90. Tsatsaronis G. Thermoeconomic analysis and optimization of energy systems. Prog Energy Combust Sci. 1993;19(3):227–57.
91. Dincer I, Zamfirescu C. Sustainable hydrogen production. 2016;494.
92. Bejan A, Tsatsaronis G (George), Moran MJ. Thermal design and optimization. Wiley; 1996. 542 p.
93. Lazzaretto A, Tsatsaronis G. SPECO: A systematic and general methodology for calculating efficiencies and costs in thermal systems. Energy. 2006 Jul;31(8–9):1257–89.
94. DOE Hydrogen and Fuel Cells Program: DOE H2A Production Analysis [Internet]. H2A Central Hydrogen Production Model, Version 3.1. [cited 2017 Jan 7]. Available from: https://www.hydrogen.energy.gov/h2a_production.html
95. Comparison of Electricity Prices in Major North American Cities | Publications | Hydro-Québec [Internet]. [cited 2017 Jan 7]. Available from: http://www.hydroquebec.com/publications/en/corporate-documents/comparaison-electricity-prices.html
96. Inflation Calculator | Find US Dollar's Value from 1913-2017 [Internet]. [cited 2017 Mar 3]. Available from: http://www.usinflationcalculator.com/
97. Bartels J. A feasibility study of implementing an Ammonia Economy. Graduate Theses and Dissertations. Iowa State University; 2008.
98. Morgan E. Techno-Economic Feasibility Study of Ammonia Plants Powered by Offshore Wind. Dissertations. University of Massachusetts - Amherst; 2013.